APPENDIX E
P-21-049 ATLAS CAR POST TEST ANALYSIS REPORT (FORMERLY P-21-042)

ATLAS CAR POST TEST ANALYSIS REPORT

P-21-049

(formerly P-21-042)

Prepared for United States Department of Energy

October 26, 2022
Revised December 6, 2022

PROPRIETARY REPORT

TTCI
TRANSPORTATION TECHNOLOGY CENTER, INC.

ATLAS CAR POST TEST ANALYSIS REPORT

Prepared for United States Department of Energy

P-21-049
(formerly P-21-042)

Prepared by
Russell Walker
Michael Craft
MaryClara Jones
Matt DeGeorge

Transportation Technology Center, Inc.
A subsidiary of the Association of American Railroads
Pueblo, Colorado USA

October 26, 2022
Revised December 6, 2022

ERRATA STATEMENT

Report: P-21-049

Errata refer to the correction of errors introduced to the article by the publisher. The following errors have been found and corrected since this report was originally submitted.

In MxV Rail report, P-21-042, "Cask Car Post-Test Analysis (S-2043 Section 8.0) and Final Report," two inadvertent typographical errors were present. The corrected text is as follows.

- **Cover and inside cover:** As listed in the committee approved letter dated April 29, 2022 (File 209.240), the report number was erroneously listed as P-21-042. The corrected report number is P-21-049.
- **Executive Summary**, p. ii, fourth column of table, information corrected: "Wheel load at 43% during 3" drop condition." Corrected to "Wheel load at 24% during 3" drop condition."

Standard S-2043 Section	Met/Not Met		
	Preliminary Simulations CSM 58 pads	Revised Simulations CSM 58 pads	Test Result and Details if Not Met
5.2 Nonstructural Static Tests			
4.2.1/5.2.1 Truck Twist Equalization	Met	Not Simulated	Not Met with CSM 58 pads **Minimum Test Load:** Wheel load at 50% during 2" drop condition. Wheel load at 24% during 3" drop condition. **Maximum Test Load:** Wheel load at 43% during 2" drop condition. Wheel load at 29% during 3" drop condition.

- Section 8.0 Conclusions, Table 65, p. 90, information corrected. Sentence "Wheel load at 43% during 3" drop condition." Corrected to "Wheel load at 24% during 3" drop condition."

Standard S-2043 Section	Met/Not Met		
	Preliminary Simulations	Revised Simulations CSM 58 pads	Test Result and Details if Not Met
5.2 Nonstructural Static Tests			
4.2.1/5.2.1 Truck Twist Equalization	Met	Not Simulated	Not Met with CSM 58 pads – **Minimum Test Load:** Wheel load at 50% during 2" drop condition. Wheel load at 24% during 3" drop condition. **Maximum Test Load:** Wheel load at 43% during 2" drop condition. Wheel load at 29% during 3" drop condition.

For questions or comments on this document, contact **Russell_Walker@aar.com.**

Disclaimer: This report was prepared for the United States Department of Energy (DOE) by Transportation Technology Center, Inc. (TTCI), a subsidiary of the Association of American Railroads, Pueblo, Colorado. It is based on investigations and tests conducted by TTCI with the direct participation of DOE to criteria approved by them. The contents of this report imply no endorsements whatsoever by TTCI of products, services, or procedures, nor are they intended to suggest the applicability of the test results under circumstances other than those described in this report. The results and findings contained in this report are the sole property of DOE. They may not be released by anyone to any party other than DOE without the written permission of DOE. TTCI is not a source of information with respect to these tests, nor is it a source of copies of this report. TTCI makes no representations or warranties, either expressed or implied, with respect to this report or its contents. TTCI assumes no liability to anyone for special, collateral, exemplary, indirect, incidental, consequential, or any other kind of damages resulting from the use or application of this report or its contents.

Executive Summary

Transportation Technology Center, Inc., (TTCI) a subsidiary of the Association of American Railroads (AAR), performed certification testing and modeling on the United States Department of Energy's (DOE) 12-axle cask car (Atlas car). The Atlas car has been developed as part of the DOE's Atlas railcar Design Project that is intended to meet the need for future large-scale transport of spent nuclear fuel and high-level radioactive waste. Tests and modeling were performed according to the AAR's *Manual of Standards and Recommended Practices* (MSRP), Standard S-2043, "Performance Specification for Trains Used to Carry High-Level Radioactive Material," revised 2017.[1]

The objective of this report is to demonstrate acceptable railcar performance. This objective was accomplished by comparing the test results to the modeling predictions as part of the structural and dynamic analysis of the DOE Atlas car. Where necessary, the revised simulation predictions are presented.

The preliminary simulations were performed according to Standard S-2043, Paragraph 4.3 as part of the railcar design phase before the prototype car was built. The results of the preliminary simulation were submitted to the AAR as part of the preliminary design review package. The test results have been compared to the preliminary dynamic analysis predictions and revised model predictions in this report to verify that the model accurately represents the vehicle as required in Standard S-2043, Paragraph 8.

As originally equipped with chlorosulfonated polyethylene (CSM) 58 primary pads, the Atlas railcar with a minimum test load did not meet the Standard S-2043 single-car dynamic test requirement for hunting (Standard S-2043, Paragraph 5.5.7). The hunting tests were the first tests to be performed, and the testing process was paused to solve this problem. During troubleshooting tests the railcar met the hunting requirements with stiffer CSM 70 primary suspension pads, and all the remaining dynamic tests were completed with these pads. With the stiffer pads, the performance met the hunting requirements but not all the curving requirements. After reviewing the available data with the AAR Equipment Engineering Committee (EEC), TTCI performed additional troubleshooting and found that the CSM 58 pads provided the best balance between the curving and the hunting performance results.

The testing data was used to revise the preliminary multi-body vehicle dynamics models that had used CSM 58 pads and to modify this revised model into one that used the CSM 70 primary pads. Both revised models showed good alignment with most relevant testing data, such as wheel loads, although some variation between the predicted behavior and the tested behavior was observed. Regimes with existing CSM 70 pad test data were re-modeled using CSM 70 pads to demonstrate the model was validated. These regimes were also modeled with CSM 58 pads to show the change in performance with the final pad. Numerous other simulations, (in addition to creating and solving models to replicate the conducted tests), were performed to estimate the car's behavior in conditions that are not easily tested, such as buff and draft curving, rail lubrication, and the effect of worn components.

Like the earliest tests, the revised model of the car equipped with CSM 58 pads did not meet the criterion for the standard deviation of lateral carbody acceleration in the hunting regime. In addition, the model revealed other simulation-only regimes, including curving with single rail perturbation simulation regimes with 3-inch amplitude and curving with various lubrication conditions, where the requirements were not met. However, in most circumstances, the model was more conservative than the test results and is indicative of the actual performance.

The following table shows a summary of the test results and the model predictions for the Atlas railcar:

Standard S-2043 Section	Met/Not Met		
	Preliminary Simulations CSM 58 pads	**Revised Simulations CSM 58 pads**	**Test Result and Details if Not Met**
5.2 Nonstructural Static Tests			
4.2.1/5.2.1 Truck Twist Equalization	Met	Not Simulated	Not Met with CSM 58 pads **Minimum Test Load:** Wheel load at 50% during 2″ drop condition. Wheel load at 24% during 3″ drop condition. **Maximum Test Load:** Wheel load at 43% during 2″ drop condition. Wheel load at 29% during 3″ drop condition.
4.2.2/5.2.2 Carbody Twist Equalization	Met	Not Simulated	Met with CSM 58 pads
4.2.3/5.2.3 Static Curve Stability	Met	Not Simulated	Met with CSM 58 pads
4.2.4/5.2.4 Horizontal Curve Negotiation	Met	Not Simulated	Met with CSM 58 pads
5.4 Structural Tests			
5.4.2 Squeeze (Compressive End) Load	Met	Not Simulated	Met with CSM 58 pads
5.4.3 Coupler Vertical Loads	Met	Not Simulated	Met with CSM 58 pads
5.4.4 Jacking	Met	Not Simulated	Met with CSM 58 pads
5.4.5 Twist	Met	Not Simulated	Met with CSM 58 pads
5.4.6 Impact	Met	Not Simulated	Met with CSM 58 pads
5.5 Dynamic Tests			
4.3.11.3/5.5.7 Hunting	Met	Not Met At Minimum Test Load: Car unstable at speeds greater than 65 mph with KR wheel profiles Meets with Maximum Test Load	Not Met with CSM 58 pads At Minimum Test Load: Car unstable at speeds greater than 65 mph with KR wheel profiles Meets with Maximum Test Load

Standard S-2043 Section	Met/Not Met		
	Preliminary Simulations CSM 58 pads	**Revised Simulations CSM 58 pads**	**Test Result and Details if Not Met**
4.3.9.6/5.5.8 Twist and Roll	Met	Met	Not tested with CSM 58 pads – Met with CSM 70 pads
5.5.9 Yaw and Sway	Met	Met	Not tested with CSM 58 pads – Met with CSM 70 pads
5.5.10 Dynamic Curving	Not Met Max. Test Load Wheel L/V 0.88, Limit=0.8, A-end and B-end lead, 39-ft. input	Met	Met with CSM 58 pads – Not met with CSM 70 pads (0.81 Wheel L/V)
4.3.9.7/5.5.11 Pitch and Bounce (Chapter 11)	Met	Met	Not tested with CSM 58 pads – Met with CSM 70 pads
4.3.9.7/5.5.12 Pitch and Bounce (Special)	Met	Not Simulated	Not tested
		Truck center spacing close to Chapter 11 wavelength	
4.3.10.1/5.5.13 Single Bump Test	Met	Met	Not tested with CSM 58 pads – Met with CSM 70 pads
4.3.11.6/5.5.14 Curve Entry/Exit	Met	Met	Not tested with CSM 58 pads – Met with CSM 70 pads
4.3.10.25.5.15 Curving with Single Rail Perturbation	Not met **Empty with Ballast Load:** Wheel L/V 0.96, Limit=0.8 Truck Side L/V 0.52, Limit=0.5 **Loaded** 5.0-degree roll angle, Limit=4.0	Not met **Minimum Test Load** Carbody roll angle =4.2, limit=4.0 **Maximum Test Load** Carbody roll angle =4.7, limit=4.0	Minimum Test Load: Not met with CSM 70 pads (Wheel L/V = 0.88, Truck L/V = 0.50), not tested with CSM 58 pads
4.3.11.4/5.5.16 Standard Chapter 11 Constant Curving	Met	Met	Not tested with CSM 58 pads – Not Met with CSM 70 pads: **Minimum Test Load:** Wheel L/V ratio = 0.86 95% Wheel L/V ratio = 0.66 **Maximum Test Load:** 95% Wheel L/V ratio = 0.63
4.3.11.7/5.5.17 Special Trackwork, No 7 Crossovers	Not Met **Loaded:** Truck side L/V Ratio=0.52, Limit=0.5	Met	Not tested with CSM 58 pads – Met with CSM 70 pads on a No 10 crossover

Standard S-2043 Section	Met/Not Met		
	Preliminary Simulations CSM 58 pads	**Revised Simulations CSM 58 pads**	**Test Result and Details if Not Met**
4.3.11.5 Curving with Various Lubrication Conditions	Not Met **Min Test Load with new profiles:** 95% Wheel L/V = 0.62 (Case 2), Limit=0.6 95% Wheel L/V = 0.66 (Case 4), Limit=0.6 **Min Test Load with worn profiles:** Truck Side L/V = 0.56 (Case 1), 0.62 (Case 2), 0.61 (Case 4), Limit=0.5 95% Wheel L/V = 0.68 (Case 2), 0.61 (Case 4), Limit=0.6 **Max Test Load with worn profiles:** Truck Side L/V = 0.56 (Case 1), 0.62 (Case 2), 0.61 (Case 4), Limit=0.5 95% Wheel L/V = 0.68 (Case 2), 0.61 (Case 4), Limit=0.6	Not Met in following cases **Min Test Load with new profiles:** 95% Wheel L/V = 0.62 (Case 4), Limit=0.6 **Min Test Load with worn profiles:** Truck Side L/V = 0.53 (Case 1), 0.61 (Case 2), 0.58 (Case 4), Limit=0.5 95% Wheel L/V = 0.64 (Case 2), Limit=0.6 **Max Test Load with worn profiles:** Truck Side L/V = 0.52 (Case 1), 0.60 (Case 2), 0.58 (Case 4), Limit=0.5 95% Wheel L/V = 0.66 (Case 2), 0.61 (Case 4), Limit=0.6	Not required
4.3.12 Ride Quality	Met	Not Simulated	Not required
4.3.13 Buff and Draft Curving	Not Met When coupled between other Atlas cars under buff load Truck side L/V Ratio=0.51, Limit=0.50	Met	Not required
4.3.14 Braking Effects on Steering	Met	Not Simulated	Not required
4.3.15 Worn Component Simulations	Not Met Numerous criteria not met in dynamic curving and hunting regimes with several worn components. See reference 2 for details	Not Met in following cases: **Hunting stability, maximum lateral acceleration standard deviation:** Worn CCSB low preload: 0.17 Worn primary pads, soft: 0.19 Worn primary pads, stiff: 0.20	Not required

Table of Contents

1.0 Introduction 1
2.0 Atlas Railcar Description 1
2.1 Variations in Components During Testing 4
3.0 Objective 5
4.0 Refining the FEA 5
4.1 Loading Conditions for Structural Tests 6
4.1.1 Test Loads 6
4.1.2 Measured Stresses from Test Loads 6
4.2 Squeeze (Compressive End) Load 9
4.3 Coupler Vertical Loads 12
4.4 Jacking 14
4.5 Twist 16
4.5.1 Suspension Twist 16
4.5.2 Carbody Twist 19
4.6 Impact 21
5.0 New FEA Predictions 23
6.0 Refining the Dynamic Model 23
7.0 New Dynamic Predictions 27
7.1 Twist and Roll 29
7.1.1 Minimum Test Load 29
7.1.2 Maximum Test Load 30
7.2 Pitch and Bounce (Chapter 11) 32
7.2.1 Minimum Test Load 32
7.2.2 Maximum Test Load 33
7.3 Yaw and Sway 35
7.4 Dynamic Curving 37
7.4.1 Minimum Test Load 37
7.4.2 Maximum Test Load 40
7.4.3 Other Various Load Conditions 41
7.5 Single Bump Test 43
7.5.1 Minimum Test Load 44
7.5.2 Maximum Test Load 45
7.6 Curving with Single Rail Perturbation 47
7.6.1 Minimum Test Load 47
7.6.2 Maximum Test Load 50
7.7 Hunting 53
7.7.1 Minimum Test Load 53
7.7.2 Maximum Test Load 55
7.8 Constant Curving 57
7.8.1 Minimum Test Load 58
7.8.2 Maximum Test Load 59
7.9 Curving with Various Lubrication Conditions 61
7.9.1 Minimum Test Load 62
(1) New Profiles 62

(2) Worn Profiles 62
7.9.2 Maximum Test Load 66
(1) New Profiles 66
(2) Worn Profiles 67
7.10 Limiting Spiral Negotiation 71
7.10.1 Minimum Test Load 71
7.10.2 Maximum Test Load 73
7.11 Special Trackwork: Turnouts and Crossovers (S-2043, Paragraph 4.3.11.7) 74
7.11.1 Minimum Test Load – Turnouts and Crossovers 75
7.11.2 Maximum Test Load – Turnouts and Crossovers 76
7.12 Buff and Draft Curving 77
7.13 Worn Component Simulations 79
7.13.1 Worn Constant Contact Side Bearings 80
7.13.2 Centerplate 82
7.13.3 Primary Pad 84
7.13.4 Friction Wedges 86
7.13.5 Broken Spring 88
8.0 Conclusions 89
References 94

List of Figures

Figure 1. IDOX 010001 during Testing with Minimum Test Load 2
Figure 2. Exploded view of Swing Motion® truck 3
Figure 3. Roller Bearing Adapter Pad 3
Figure 4. Axle and side naming convention 4
Figure 5. Measurement locations reported in Table 4 and Table 5 8
Figure 6. Measurement locations reported in Table 6, and Table 7 12
Figure 7. Measurement locations reported in Table 8 12
Figure 8. Measurement locations with highest stresses during jacking test 14
Figure 9. Suspension twist locations 19
Figure 10. Measurement locations with highest stresses during carbody twist test 21
Figure 11. Measurement locations with highest stresses during impact test 23
Figure 12. Results of the second interaxle stiffness test with CSM 58 and CSM 70 primary pads 27
Figure 13. Twist-and-roll test results and simulation predictions of maximum peak-to-peak carbody roll angle with minimum test load 30
Figure 14. Twist-and-roll test results and simulation predictions of maximum peak-to-peak carbody roll angle with maximum test load using CSM 70 pads 31
Figure 15. Twist-and-roll pre-test and refined model simulation predictions of maximum peak-to-peak carbody roll angle with maximum test load using CSM 70 pads 32
Figure 16. Simulation predictions of maximum vertical carbody acceleration in the pitch and bounce regime with minimum test load 33
Figure 17. Pitch and bounce test results and simulation predictions of maximum vertical acceleration with CSM 70 Pads at maximum test load 34
Figure 18. Pitch and bounce simulation predictions of maximum vertical acceleration with CSM 58 Pads at maximum test load 35
Figure 19. Simulation predictions and test results of maximum truck side L/V ratio in the yaw-and-sway regime with CSM 70 pads and the maximum test load 36
Figure 20. Simulation predictions of maximum truck side L/V ratio in the yaw-and-sway regime with CSM 58 pads and the maximum test load 37
Figure 21. Simulation prediction and test results of maximum wheel L/V ratio in the dynamic curving regime with minimum test load and CSM 70 pads 38
Figure 22. Simulation prediction and test results of maximum wheel L/V ratio in the dynamic curving regime with minimum test load and CSM 58 pads 39

Figure 23. Distance plot of axle 5 lead left wheel L/V ratio during 12 mph run counterclockwise (CCW) through dynamic curve with B-End leading using CSM 70 primary pads 39
Figure 24. Simulation prediction and test results of maximum wheel L/V ratio in the dynamic curving regime with maximum test load using CSM 70 pads 41
Figure 25. Simulation predictions of maximum wheel L/V ratio in the dynamic curving regime with maximum test load using CSM 70 and CSM 58 pads 41
Figure 26. Simulation prediction and test results of minimum vertical wheel load in the single bump regime with minimum test load 45
Figure 27. Simulation prediction and test results of maximum vertical carbody acceleration in the single bump test regime with maximum test load using CSM 70 pads..... 46
Figure 28. Original (2017) and revised simulation predictions of maximum vertical carbody acceleration in the single bump test regime with maximum test load using CSM 58 pads 47
Figure 29. Simulation predictions and test results using CSM 70 primary pads of maximum wheel L/V ratio in the curve with single dip regime with minimum test load..... 48
Figure 30. Simulation predictions using CSM 70 and CSM 58 primary pads of maximum wheel L/V ratio in the curve with single dip regime with minimum test load 49
Figure 31. Simulation prediction and test results of maximum wheel L/V ratio in the curving with single rail perturbation dip regime with maximum test load using CSM 70 and CSM 58 pads 51
Figure 32. Simulation prediction and test results of the standard deviation of carbody lateral acceleration over 2,000 feet with minimum test load using CSM 70 pads and KR profile wheels 54
Figure 33. Simulation prediction and test results of the standard deviation of carbody lateral acceleration over 2,000 feet with minimum test load using CSM 58 pads and KR profile wheels 55
Figure 34. Simulation prediction and test results of maximum wheel L/V ratio in the dynamic curving regime with maximum test load using CSM 70 pads 57
Figure 35. Simulation predictions of maximum wheel L/V ratio in the dynamic curving regime with maximum test load using CSM 70 and CSM 58 pads 57
Figure 36. Test Results and Simulation Predictions of the 95 Percentile Wheel L/V Ratio in the 12-degree Constant Curve with CSM 70 and CSM 58 Primary Pads for Minimum Test Load 59
Figure 37. Test Results and Simulation Predictions of the 95 Percentile Wheel L/V Ratio in the 12-degree Constant Curve with CSM 70 Primary Pads for Maximum Test Load 60

Figure 38. Original (20170 and Revised Simulation Predictions of the 95 Percentile Wheel L/V Ratio in the 12-degree Constant Curve with CSM 58 Primary Pads for Maximum Test Load 61
Figure 39. Worn Wheel Profiles on the Ground Rail Profiles (The Wheelset is Shifted to the High Rail in the Position it Would be in a Left-Hand Curve) 62
Figure 40. Plot of Wheel L/V Ratio versus distance for Case 2 friction with worn profiles, CCW, A-leading. Plot shows data for the lead axle of the trailing span bolster. 64
Figure 41. Plot of Truck Side L/V Ratio versus distance for Case 2 friction with worn profiles, CCW, B-leading. Plot shows data for the high rail of the middle truck on the lead span bolster. 64
Figure 42. Atlas car with minimum test load 95-Percent Wheel L/V Ratio for curving with Case 2 lubrication and worn wheel and rail profiles 65
Figure 43. Minimum Test Load Truck Side L/V Ratio for curving with Case 2 lubrication and worn wheel and rail profiles 65
Figure 44. Predictions of Wheel L/V Ratio for multiple lubrication cases with new wheel and rail profiles (most severe results shown) 66
Figure 45. Predictions of Truck Side L/V Ratio for Case 2 lubrication with worn wheel and rail profiles for both directions of travel, with most severe results shown, at maximum and minimum test load 68
Figure 46. Predictions of 95% Wheel L/V Ratio for Case 2 lubrication with worn wheel and rail profiles for both directions of travel, with most severe results shown, at maximum and minimum test loads 68
Figure 47. Predictions of Truck Side L/V Ratio for Case 4 lubrication with worn wheel and rail profiles for both directions of travel, with most severe results shown, at maximum and minimum test loads 69
Figure 48. Plot of Truck Side L/V Ratio versus distance for Case 2 friction with worn wheel and rail profiles. The plot shows data for the high rail of the middle truck on the lead span bolster 69
Figure 49. Worst-case predictions for Truck Side L/V Ratio at all lubrication cases of worn wheel and rail profiles, at maximum test load 70
Figure 50. Worst-case predictions for 95 percentile Wheel L/V Ratio at all lubrication cases of worn wheel and rail profiles, at maximum test load 70
Figure 51. Simulation prediction and test results of maximum wheel L/V ratio in the limiting spiral regime with minimum test load using CSM 70 pads 72

Figure 52. Simulation prediction and test results of maximum wheel L/V ratio in the limiting spiral regime with minimum test load using CSM 58 pads 72
Figure 53. Simulation prediction and test results of maximum wheel L/V ratio in the dynamic curving regime with maximum test load using CSM 70 pads 74
Figure 54. Simulation predictions of maximum wheel L/V ratio in the dynamic curving regime with maximum test load using CSM 70 and CSM 58 pads 74
Figure 55. Simulation Predictions of Truck side L/V Ratio on No. 7 Crossovers for Original Simulations of Atlas Car with Minimum Test Load 76
Figure 56. Simulation Predictions of Truck Side L/V Ratio on No. 7 Crossover. Original Simulations (a) and revised simulations (b) at maximum load 77
Figure 57. Truck Side L/V Ratio for Curving Simulations Under 250,000 Pounds Draft Force for Revised Simulations with the Minimum Test Load 78
Figure 58. Truck Side L/V Ratio for Curving Simulations Under 250,000 Pounds Buff Force for Revised Simulations with the Minimum Test Load 79
Figure 59. Single Wheel L/V Ratio for Worn CCSB Cases 81
Figure 60. Maximum Carbody Lateral Acceleration for CCSB Wear Cases Plotted Against Speed 82
Figure 61. Hunting stability, considering centerplate wear 84
Figure 62. Hunting stability, considering primary pad deterioration 86

List of Tables

Table 1. Car Dimensions 2
Table 2. Car Configuration 4
Table 3. Summary of structural tests and load condition 6
Table 4. Comparison of highest measured stresses with predicted stresses for Atlas car loaded to the maximum test load condition with no additional applied forces 7
Table 5. Comparison of highest measured stresses with predicted stresses for Atlas car loaded to the minimum test load condition with no additional applied forces 8
Table 6. Comparison of highest total stresses with predicted stresses for squeeze (compressive end) load test in the maximum test load condition 10
Table 7. Comparison of total stresses and stresses from applied load with predicted stresses for squeeze (compressive end) load test in the minimum test load condition 11
Table 8. Comparison of highest measured stresses with predicted stresses for coupler vertical load test 13
Table 9. Comparison of selected measured stresses with predicted stresses for jacking test 15
Table 10. Comparison of selected measured stresses with predicted stresses for suspension twist test with the A-end LH corner lifted 3 inches 17
Table 11. Comparison of selected measured stresses with predicted stresses for suspension twist test with the A-end RH corner lifted 3 inches 17
Table 12. Comparison of selected measured stresses with predicted stresses for suspension twist test with the B-end LH corner lifted 3 inches 18
Table 13. Comparison of selected measured stresses with predicted stresses for suspension twist test with the B-end RH corner lifted 3 inches 18
Table 14. Comparison of selected measured stresses with predicted stresses for carbody twist test 20
Table 15. Comparison of selected measured stresses with predicted stresses for impact test 22
Table 16. Comparison of values used in preliminary modeling and values measured during characterization 24
Table 17. Twist-and-roll test results and simulation predictions using minimum test load 29
Table 18. Twist-and-roll test results and simulation predictions with maximum test load 31
Table 19. Pitch and bounce test results and simulation predictions 33
Table 20. Test results and simulations predictions for Pitch and Bounce with maximum test load 34
Table 21. Yaw-and-sway test results and simulation predictions 36

Table 22. Dynamic curving test results and simulation predictions 38
Table 23. Dynamic curving test results and simulation predictions with maximum test load 40
Table 24. Dynamic Curving with Various Loads (Part 1 of 3) 42
Table 25. Dynamic Curving with Various Loads (Part 2 of 3) 43
Table 26. Dynamic Curving with Various Loads (Part 3 of 3) 43
Table 27. Single bump test results and simulation predictions with minimum test load 44
Table 28. Single bump test results and simulation predictions with maximum test load 46
Table 29. Curving with 2-inch rail dip test results and simulation predictions using measured track inputs with minimum test load 48
Table 30. Simulation prediction for curve with single rail perturbation bump section at varying amplitudes with minimum test load 49
Table 31. Simulation prediction for curve with single rail perturbation dip section at varying amplitudes with minimum test load 50
Table 32. Curving with 2-inch rail dip test results and simulation predictions using measured track inputs with maximum test load 51
Table 33. Simulation prediction for curve with single rail perturbation bump section at varying amplitudes with maximum test load 52
Table 34. Simulation prediction for curve with single rail perturbation dip section at varying amplitudes with maximum test load 53
Table 35. Hunting test results and simulation predictions with minimum test load 54
Table 36. Hunting test results and simulation predictions with maximum test load 56
Table 37. Constant curving test results and simulation predictions with minimum test load 58
Table 38. Constant curving test results and simulation predictions with maximum test load 60
Table 39. Wheel/rail Coefficients of Friction for the Curving with Various Lubrication Conditions Regime 61
Table 40. Simulation Results for Curving with Rail Lubrication Cases 1-4 and New Wheels and Rails, with Minimum Test Load 62
Table 41. Simulation Predictions for Curving with Rail Lubrication Cases 1-4 and Hollow Worn Wheels and Ground Rails, with Minimum Test Load 63
Table 42. Simulation predictions for Curving with Rail Lubrication Cases 1–4 and New Wheels and Rails, Car Loaded with the Maximum Test Load 66
Table 43. Simulation predictions for Curving with Rail Lubrication Cases 1–4 and Hollow Worn Wheels and Ground Rails, Car Loaded with the Maximum Test Load 67
Table 44. Limiting spiral test results and simulation predictions with minimum test load 71
Table 45. Dynamic curving test results and simulation predictions with maximum test load 73

Table 46. Crossover Simulation Predictions with Minimum Test Load 75
Table 47. Crossover Simulation Predictions, Car Loaded at Maximum Load 76
Table 48. Revised Simulation Predictions for 250,000 Draft Force, Minimum Test Load 78
Table 49. Revised Simulation Predictions for 250,000 Buff Force, Minimum Test Load 79
Table 50. Simulation Predictions of the Atlas Cask Car with Worn CCSB in Dynamic Curving..... 80
Table 51. Simulation Predictions of the Atlas Cask Car with Worn CCSB in Hunting..... 81
Table 52. Simulation Predictions of the Atlas Cask Car with Worn CCSB in Twist and Roll 82
Table 53. Simulation Predictions of the Atlas Cask Car with Worn Centerplate in Constant Curving 83
Table 54. Simulation Predictions of the Atlas Cask Car with Worn Centerplate in Dynamic Curving..... 83
Table 55. Simulation Predictions of the Atlas Cask Car with Worn Centerplate in Hunting 84
Table 56. Simulation Predictions of the Atlas Cask Car with Worn Primary Pads in Constant Curving 85
Table 57. Simulation Predictions of the Atlas Cask Car with Worn Primary Pads in Dynamic Curving..... 85
Table 58. Simulation Predictions of the Atlas Cask Car with Worn Primary Pads in Hunting 86
Table 59. Simulation Predictions of the Atlas Cask Car with Worn Friction Wedges in Dynamic Curving..... 87
Table 60. Simulation Predictions of the Atlas Cask Car with Worn Friction Wedges in Pitch and Bounce..... 87
Table 61. Simulation Predictions of the Atlas Cask Car with Worn Friction Wedges in Twist and Roll..... 88
Table 62. Simulation Predictions of the Atlas Cask Car with a Broken Spring in Dynamic Curving..... 88
Table 63. Simulation Predictions of the Atlas Cask Car with a Broken Spring in Pitch and Bounce..... 89
Table 64. Simulation Predictions of the Atlas Cask car with a Broken Spring in Twist and Roll..... 89
Table 65. Summary of Dynamic Modeling and Test Results 90

1.0 INTRODUCTION

The United States Department of Energy (DOE) contracted with the Transportation Technology Center, Inc. (TTCI) to perform dynamic modeling and certification testing on its Atlas railcar. The Atlas railcar has been developed as part of the DOE's Atlas Railcar Design Project that is intended to meet the need for future large-scale transport of high-level radioactive material (HLRM) as defined in AAR Standard S-2043 that includes spent nuclear fuel and high-level waste.

All tests and analyses were performed according to the Association of American Railroads' (AAR) *Manual of Standards and Recommended Practices* (MSRP), Standard S-2043, "Performance Specification for Trains used to carry High-level Radioactive Material," Section 5.0 – Single Car Tests.[1] Single-car testing of the Atlas railcar was conducted at the United States Department of Transportation's Transportation Technology Center (TTC) near Pueblo, Colorado between April 2019 and August 2021. Static brake testing was conducted per relevant requirements of AAR Standards S-401 and S-486 at the manufacturer's facility prior to delivery.

Standard S-2043 requires that both a structural and a dynamic analysis be performed during the car design process. Kasgro Rail Corporation (Kasgro) designed the car and performed the structural analysis, and TTCI performed the dynamic analysis. In this report, the predictions from these analyses are compared to the single car test results. The single-car tests were described in TTCI report P-21-037.[2] The pretest dynamic analysis was described in TTCI report P-17-021.[3]

2.0 ATLAS RAILCAR DESCRIPTION

The Atlas railcar is a 12-axle span bolster car with fittings to accommodate various cradles and end stops designed so the car can carry various casks used for transportation of spent nuclear fuel and/or high-level waste. The car deck is supported on two span bolsters. Each span bolster rested on three 2-axle trucks. Figure 1 shows the car with a test load installed. Table 1 shows the car dimensions.

Kasgro manufactured the Atlas railcar along with two prototype buffer railcars in 2018. The car delivered for testing was numbered IDOX 010001.

Figure 1. IDOX 010001 during Testing with Minimum Test Load

Table 1. Car Dimensions

Dimension	Value
Length over pulling faces	78 feet 1 1/4 inches
Length over strikers	73 feet 5 1/4 inches
Span bolster spacing	38 feet 6 inches
Axle spacing on trucks	72 inches
Distance between adjacent trucks	10 feet 6 inches

The car uses six Swing Motion® trucks (Figure 2). Each truck uses two wheelsets having AAR Class K-axles and AAR1B narrow flange wheels. Narrow flange wheels are specified for this car because the increased gage clearance allows more lateral movement for better performance. The trucks are designed to use a polymer element between the bearing adapter and side frame. This gives the truck a passive steering capability. Figure 3 shows the bearing adapter pad. Table 2 shows the truck configuration used for testing. The secondary suspension is made up of non-AAR-standard springs.

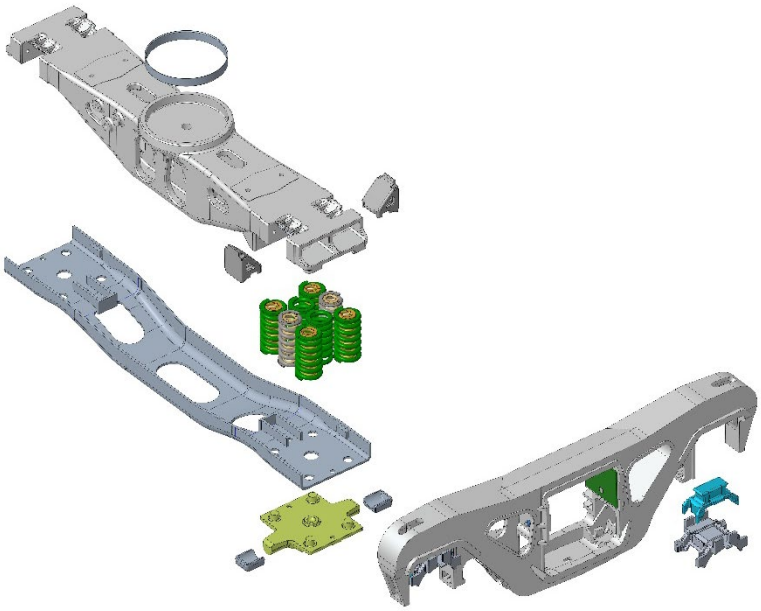

Figure 2. Exploded view of Swing Motion® truck

Figure 3. Roller Bearing Adapter Pad

Table 2. Car Configuration

Component	Description	
Secondary Suspension Springs at End Trucks (A,B,D,E)	(2) 1-94, (2) 1-95, (2) 1-96, (4) 1-97, (4) 1-92, (4) 1-99	
Secondary Suspension Springs at Middle Trucks (C,F)	(2) 1-88, (2) 1-89, (2) 1-90, (4) 1-91, (4) 1-92, (2) 1-93, (4) 1-99	
Primary suspension	12A Adapter Plus pads, ASF-Keystone part number 10522A	
Side Frames	F9N-10FH-UB	
Bolsters	B9N-71 EJFZ on A, F, and C-trucks B9N-71 HN-FX on B, D, and E-trucks	
Side Bearings	Miner TCC-III 60LT	
Friction Wedge, composition faced (four per truck)	ASF-Keystone Part number 48446	
Bearings and Adapters	AAR Class K 6 1/2 × 9 bearings with 6 1/2 × 9 Special Adapter ASF-Keystone Part number 10523A	
Center Bowl Plate	Metal Horizontal Liner	
	End Truck Average	Middle Truck Average
Minimum Test Load Spring Nest Height	8.97 inches	9.13 inches
Maximum Test Load Spring Nest Height	8.20 inches	8.17 inches

The convention for wheel and truck identification is shown in Figure 4. The B-end of a railroad freight car is normally the end with the handbrake, but because the Atlas car has two handbrakes, the car manufacturer designated and stenciled the B-end. The right and left sides of the car are designated when standing at the B-end of the car and looking toward the A-end of the car. Axles are numbered starting from the B-end. For axle numbers greater than nine, the locations are stenciled with letters descending from Z.

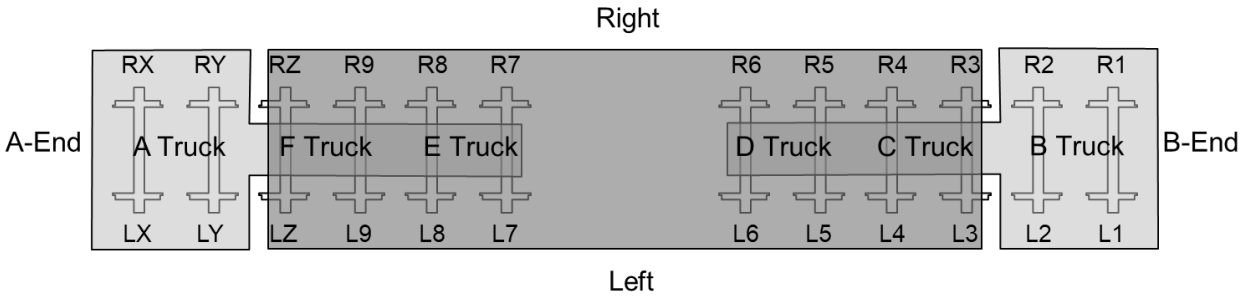

Figure 4. Axle and side naming convention

2.1 Variations in Components During Testing

During initial tests the Atlas car, loaded with the minimum test load, showed some hunting instability at speeds above 65 mph. The Atlas car was stable to 75 mph when loaded with the maximum test load. TTCI tested different side bearings, centerplate liners, and primary pads to address the hunting instability with the minimum test load. The stiffer primary pads (prototype

chlorosulfonated polyethylene or CSM 70 pads) were the only change that improved the hunting performance. After the change to stiffer pads resulted in improved hunting stability performance, all Standard S-2043 prescribed dynamic test regimes were completed with the CSM 70 pads. However, using these stiffer pads, car performance did not meet Standard S-2043 criteria in Dynamic Curving or Curve with Single Rail Perturbation regimes.

On October 15, 2020, TTCI reviewed the results with the AAR Equipment Engineering Committee (EEC). The EEC directed TTCI to re-test the car with softer primary pads with minimum test load in the Dynamic Curving regime. Because the car would be limited to less than 50 mph by AAR Operating Transportation (OT) circular OT-55 when in high-level radioactive material (HLRM) service, the EEC noted that curving performance was more important than high speed stability performance.

During the testing program, TTCI tested the car with a total of four primary suspension pad models. The pads are made from CSM and are categorized by the Shore D durometer hardness value. The production pads the car arrived with were CSM 58 pads. TTCI also tested the car with prototype pad types CSM 70, CSM 68, and CSM 65. The 58 in the model name "CSM 58" pads indicates the minimum hardness value, while the numbers in the names of other pads indicate the target hardness value.

The hunting regime was tested with CSM 58 pads in both the minimum and maximum test load conditions. The dynamic curving regime was tested with CSM 58 pads in the minimum test load condition. All other dynamic tests were completed with CSM 70 pads. Considering the results of curving and hunting tests, the production CSM 58 pads provide the best performance overall, when compared to the alternative pad materials that were tested.

After updating Nucars models with characterization data, the regimes with recorded test data using CSM 70 pads were again simulated with CSM 70 pads to demonstrate the model was validated. These regimes were modeled again with CSM 58 pads to show the change in performance with the final pad as directed by EEC.

3.0 OBJECTIVE

The objective of this report is to demonstrate acceptable railcar performance and it was accomplished by comparing the test results to the modeling predictions as part of the structural and dynamic analysis of the DOE Atlas car. Revised simulation predictions are presented where necessary.

4.0 REFINING THE FINITE ELEMENT ANALYSIS (FEA)

Structural test results are compared to FEA predictions in this section. The FEA results were examined to determine the normal stress in the active direction at the location of the strain gages for comparison to test results. Paragraph 8.1 of Standard S-2043 requires the following:

> *"If any measured stress exceeding 75% of allowable varies from its predicted value by more than 15%, then the model must be refined to provide more accurate predictions. If the designer feels that unique or unforeseen test conditions caused the discrepancy, then adequate*

explanation must be provided so that useful conclusions can be made about the model predictions and the test results."

The results presented in this report show that none of the measured stresses exceed 75 percent of the allowable stress.

4.1 Loading Conditions for Structural Tests

4.1.1 Test Loads

The physical test loads (masses) from Orano Federal Services were designed and fabricated to simulate both the weight and the center of gravity (CG) of the lightest and heaviest payloads the DOE Atlas railcar is designed to transport. The minimum condition test load assembly was designed to simulate the empty MP-197 cask, and the maximum condition test load assembly was designed to simulate the heaviest package (HI-STAR 190XL).[4] Based on actual weights from measurements conducted prior to shipment to TTCI, the maximum test load along with the associated cradle and end stops weighed 479,827 pounds, and the minimum test load and cradle weighed 196,107 pounds.[5]

Table 3 shows the structural tests conducted and the associated load condition(s).

Table 3. Summary of structural tests and load condition

Test Name	Maximum	Minimum
Squeeze (compressive end) load	x	x
Coupler vertical loads	x	
Jacking	x	
Twist	x	
Impact	x	

4.1.2 Measured Stresses Due to Test Loads only

Table 4 shows a summary of stresses from static measurements of the Atlas car, after loading the maximum test load (but without any additional applied force), for the locations with highest measured stress. The maximum measured stress was 38 percent of yield. Table 5 shows summary of stresses from static measurements, after loading the minimum test load (but without any additional applied force), for the locations with highest measured stress. The maximum measured stress was 15 percent of yield. The locations for both the minimum and maximum test loads are highlighted in Figure 5.

Table 4. Comparison of highest measured stresses with predicted stresses for Atlas car loaded to the maximum test load condition with no additional applied forces

Channel Name	Approximate Location	Normal Stress in the Active Direction of the Strain Gage				
		Measured Stress (ksi)	Yield Stress (ksi)	Measured Stress as percent of Yield	Predicted Stress (ksi)	Percent Difference Test vs Predicted
SGBF26	Center of LH side sill bottom flange, 74 1/8 inches from B end body bolster toward center of car	27	72	38%	26	NA*
SGDP45	Top of deck plate, above LH side sill web, 66 3/8 inches from line across centermost edges of B-end end stop pin blocks toward center of car	-21	60	35%	-18	NA*
SGDP48	Top of deck plate, above RH side sill web, 66 3/8 inches from line across centermost edges of B-end end stop pin blocks toward center of car	-20	60	33%	-18	NA*
SGBF15	Center of RH side sill bottom flange, 74 1/8 inches from B end body bolster toward center of car	18	72	25%	26	NA*

*Not required because measured stress does not exceed 75% of allowable

Table 5. Comparison of highest measured stresses with predicted stresses for Atlas car loaded to the minimum test load condition with no additional applied forces

Channel Name	Approximate Location	Normal Stress in the Active Direction of the Strain Gage				
		Measured Stress (ksi)	Yield Stress (ksi)	Measured Stress as percent of Yield	Measured Stress (ksi)	Percent Difference Test vs Predicted
SGBF26	Center of LH side sill bottom flange, 74 1/8 inches from B end body bolster toward center of car.	11	72	15%	10	NA*
SGBF15	Center of RH side sill bottom flange, 74 1/8 inches from B end body bolster toward center of car	9.4	72	13%	10	NA*
SGDP52	Top of deck plate, above LH center sill web, 66 3/8 inches from line across centermost edges of A-end stop pin blocks toward center of car	-8.8	60	15%	-8	NA*
SGDP45	Top of deck plate, above LH side sill web, 66 3/8 inches from across centermost edges of B-end end stop pin blocks toward center of car	-8.7	60	15%	-8	NA*

*Not required because measured stress does not exceed 75% of allowable

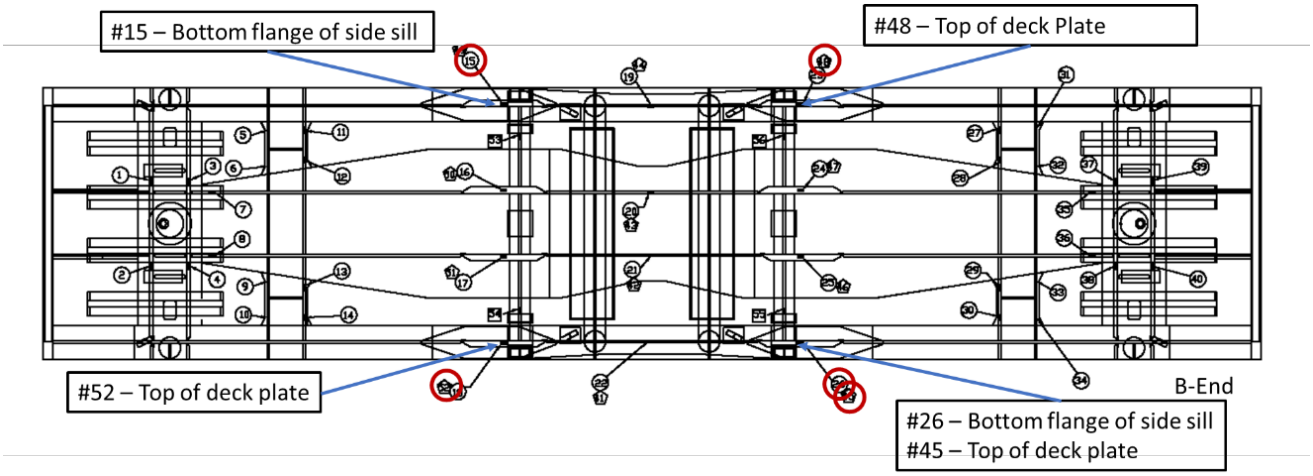

Figure 5. Measurement locations reported in Table 4 and Table 5

4.2 Squeeze (Compressive End) Load

The compressive end-load test was conducted in both the minimum and maximum test load conditions. In both cases, the strain gauges were zeroed before application of the one-million-pound compressive force. The stresses measured from the applied force were then combined with the stresses measured from the applicable test load to calculate the total stress.

Table 6 shows the summary results from the compressive end load test with the maximum test load for the locations with highest total stress. The stress from the applied force is small compared to the tension stress (in the bottom fibers of the car's sills) from the bending imparted by the maximum test load. In these cases, the applied compressive force opposed the tension force and reduced the total stress. The maximum total stress was 35 percent of the material yield.

Table 7 shows the summary results from the compressive end load test using the minimum test load for the locations with the highest stress from the applied force. The maximum total stress was 16 percent of the material yield. The locations are highlighted in Figure 6.

Table 6. Comparison of highest total stresses with predicted stresses for squeeze (compressive end) load test in the maximum test load condition

Channel Name	Approximate Location	Normal Stress in the Active Direction of the Strain Gage						
		Measured Stress from Max Test Load (ksi)	Measured Stress from Applied Force (ksi)	Total Stress (ksi)	Yield Stress (ksi)	Total Stress as percent of Yield	Predicted Total Stress (ksi)	Percent Difference Test vs Predicted
Highest total stress								
SGBF26	Center of LH side sill bottom flange, approx. 74 1/8 inches from B end body bolster toward center of car.	27	-4.1	23	72	32%	19	NA*
SGDP45	Top of deck plate, above LH side sill web, 66 3/8 inches from line across centermost edges of pin blocks toward center of car (directly above SBGF 26)	-21	0.12	-21	60	35%	-18	NA*
Highest stress from applied load								
SGBF36	LH side of bottom flange of center sill 5 3/16 inches from B-end body bolster toward center of car - aligns with center sill web	3.4	-8.9	-5.5	60	9%	-6	NA*
SGBF35	RH side of bottom flange of center sill – 5 3/16 inches from B-end body bolster toward center of car - aligns with center sill web	3.6	-8.5	-4.9	60	8%	-6	NA*

* Not required because measured stress does not exceed 75% of allowable

Table 7. Comparison of total stresses and stresses from applied load with predicted stresses for squeeze (compressive end) load test in the minimum test load condition

Channel Name	Approximate Location	Normal Stress in the Active Direction of the Strain Gage						
		Measured Stress from Min Test Load (ksi)	Measured Stress from Applied Force (ksi)	Total Stress (ksi)	Yield Stress (ksi)	Total Stress as percent of Yield	Predicted Stress (ksi)	Percent Difference Test vs Predicted
Highest total stress (also highest stresses from applied load)								
SGBF35	RH side of bottom flange of center sill – 5 3/16 inches from B-end body bolster toward center of car - aligns with center sill web	0.29	-9.9	-9.6	60	16%	-10	NA*
SGBF7	RH side of bottom flange of center sill - 5 3/16 inches from A-end body bolster toward center of car - aligns with center sill web	1.2	-10	-8.8	60	15%	-10	NA*
SGBF36	LH side of bottom flange of center sill – 5 3/16 inches from B-end body bolster toward center of car - aligns with center sill web	1.1	-9.8	-8.6	60	14%	-10	NA*
SGBF8	LH side of bottom flange of center sill - 5 3/16 inches from A-end body bolster toward center of car - aligns with center sill web	1.3	-9.7	-8.4	60	14%	-10	NA*

* Not required because measured stress does not exceed 75% of allowable

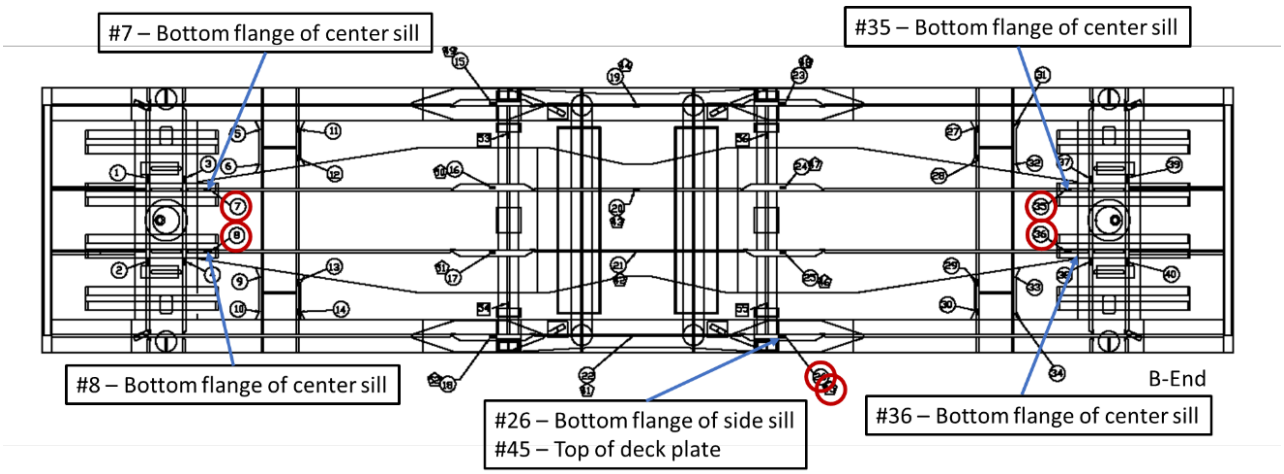

Figure 6. Measurement locations reported in Table 6, and Table 7

4.3 Coupler Vertical Loads

Table 8 shows the summary results from the coupler vertical load test for the locations with highest measured stress. These locations are highlighted in Figure 7. Measurement locations reported in Table 8. The maximum measured stress was 5 percent of the material yield.

The Atlas car couplers are connected to the span bolsters. All the strain gages are applied to the carbody. The forces applied to the couplers may be reacted either from the span bolster into the ground via the trucks or from the span bolster into the carbody via the carbody centerplate. The FEA model used by the car builder to predict stresses in the car body was not capable of modeling the complex contact conditions necessary to simulate this test.

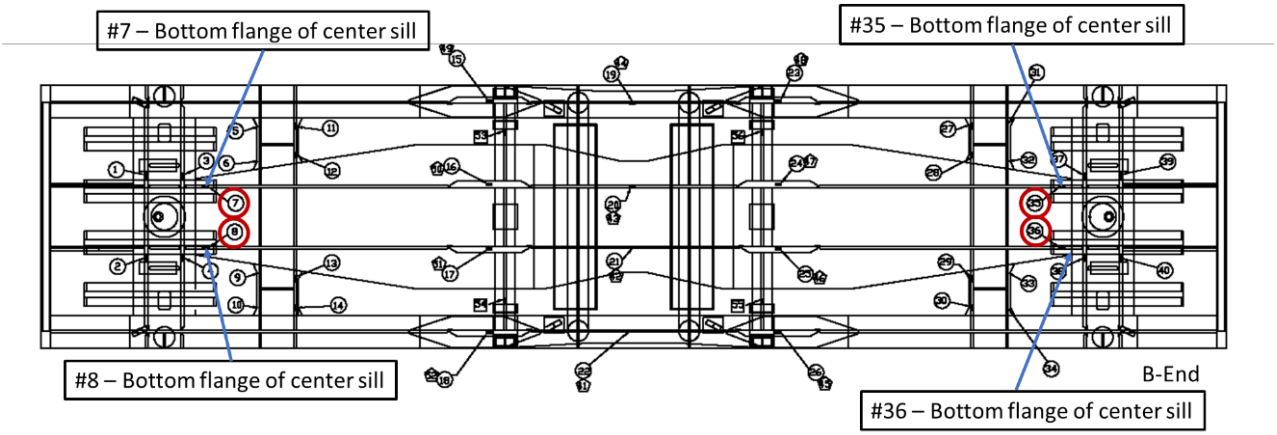

Figure 7. Measurement locations reported in Table 8

Table 8. Comparison of highest measured stresses with predicted stresses for coupler vertical load test

Channel Name	Approximate Location	Normal Stress in the Active Direction of the Strain Gage						
		Measured Stress from Min Test Load (ksi)	Measured Stress from Applied Force (ksi)	Total Stress (ksi)	Yield Stress (ksi)	Total Stress as percent of Yield	Predicted Stress (ksi)	Percent Difference Test vs Predicted
Downward Direction								
SGBF35	RH side of bottom flange of center sill – 5 3/16 inches from B-end body bolster toward center of car - aligns with center sill web	3.7	-1.0	2.6	60	4%	NP**	NA*
SGBF36	LH side of bottom flange of center sill – 5 3/16 inches from B-end body bolster toward center of car - aligns with center sill web	3.4	-.98	2.4	60	4%	NP**	NA*
Upward Direction								
SGBF7	RH side of bottom flange of center sill - 5 3/16 inches from A-end body bolster toward center of car - aligns with center sill web	2.3	.89	3.2	60	5%	NP**	NA*
SGBF8	LH side of bottom flange of center sill - 5 3/16 inches from A-end body bolster toward center of car - aligns with center sill web	2.3	.86	3.2	60	5%	NP**	NA*

*Not required because measured stress does not exceed 75% of allowable

**FEA prediction could not be completed for this test due to the coupler being connected to the span bolster and not the carbody

4.4 Jacking

Table 9 shows the summary results from the jacking test for the locations with the highest measured stress. These locations are highlighted in Figure 8. The maximum measured stress was 8 percent of the material yield.

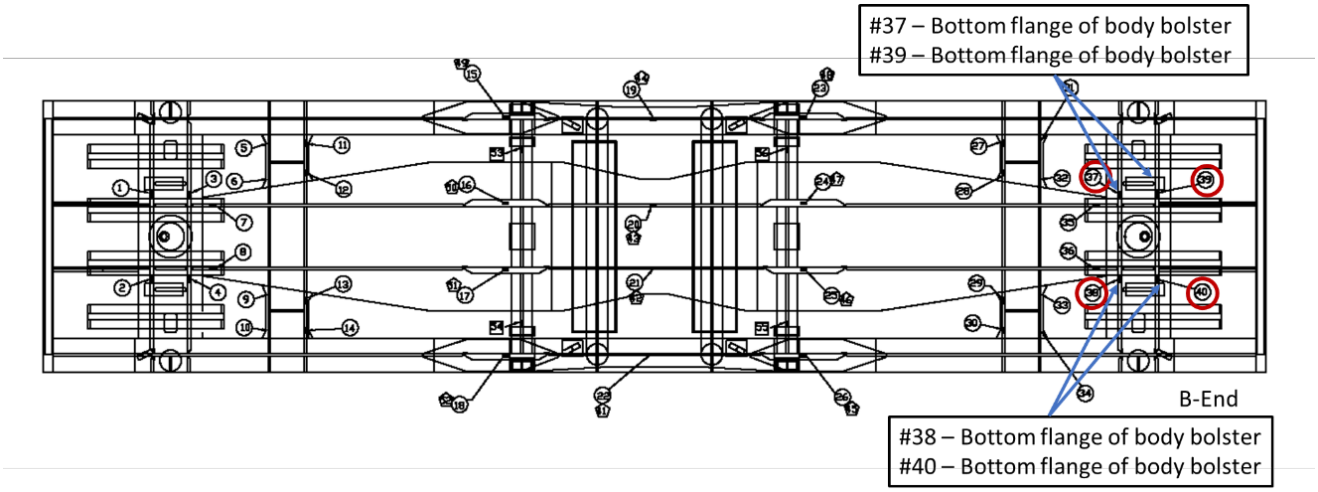

Figure 8. Measurement locations with highest stresses during jacking test

Table 9. Comparison of selected measured stresses with predicted stresses for jacking test

Channel Name	Approximate Location	Normal Stress in the Active Direction of the Strain Gage						
		Measured Stress from Max Test Load (ksi)	Measured Stress from Applied Force (ksi)	Total Stress (ksi)	Yield Stress (ksi)	Total Stress as percent of Yield	Predicted Stress (ksi)	Percent Difference Test vs Predicted
SGBF40	Bottom flange of B-end body bolster. On edge nearest B-end. 2 1/4 inches outboard of center sill bottom flange toward LH side of car.	-2.9	7.5	4.6	60	8%	4.3	NA*
SGBF38	Bottom flange of B-end body bolster. On edge nearest center of car. 2 1/4 inches outboard of center sill bottom flange toward LH side of car.	-2.5	7.4	4.9	60	8%	4.3	NA*
SGBF39	Bottom flange of B-end body bolster. On edge nearest B-end. 2 1/4 inches outboard of center sill bottom flange toward RH side of car.	-3.1	7.2	4.1	60	7%	4.3	NA*
SGBF37	Bottom flange of B-end body bolster. On edge nearest center of car. 2 1/4 inches outboard of center sill bottom flange toward RH side of car.	-2.6	6.5	3.9	60	7%	4.3	NA*

*Not required because measured stress does not exceed 75% of allowable

4.5 Twist

TTCI performed two twist tests as part of the structural tests. The first test, described in Standard S-2043, Paragraph 5.4.5.1, is reported in Section 4.5.1 of this report, "Suspension Twist." This test followed the requirements of MSRP Section C, Part II, Specification M-1001, Paragraph 11.3.3.5. The test was performed in conjunction with the carbody twist equalization test (Standard S-2043, Paragraph 5.2.2). For this test, six wheels on one side of one span bolster were raised 3 inches. This test process was repeated for all four corners of the car.

The second twist test, described in Standard S-2043, Paragraph 5.4.5.2, is detailed in Section 4.5.2 of this report, "Carbody Twist." For this test, the railcar was supported at all four jacking pads, and then one corner was allowed to drop 3 inches.

4.5.1 Suspension Twist

Table 10 through Table 13 show the summary results from the suspension twist test for the locations with the highest measured stress. These locations are highlighted in Figure 9. Standard S-2043, Paragraph 4.1.1.5 says that the allowable design stress for twist load shall be 56 percent of the yield stress. For the grade 80 material this corresponds to 44.8 ksi and for the grade 60 material it corresponds to 33.6 ksi. The maximum measured stress was 40 percent of the material yield.

The Atlas car trucks are connected to the span bolsters. All the strain gages are applied to the carbody. The displacements introduced at the wheels produce forces that are reacted from the ground into the span bolster on the carbody via the trucks, then from the span bolster into the carbody via the carbody centerplate. The FEA model used by the car builder to predict stresses in the carbody was not capable of modeling the complexity of the truck suspension and the centerplate connections.

Table 10. Comparison of selected measured stresses with predicted stresses for suspension twist test with the A-end LH corner lifted 3 inches

Channel Name	Approximate Location	Normal Stress in the Active Direction of the Strain Gage						
		Measured Stress from Max Test Load (ksi)	Measured Stress from Applied Force (ksi)	Total Stress (ksi)	Yield Stress (ksi)	Total Stress as percent of Allowable	Predicted Stress	Percent Difference Test vs Predicted
SGBF26 (highest total stress)	Center of LH side sill bottom flange, approx. 74 1/8 inches from B end body bolster toward center of car.	27	-1.9	25	44.8	56%	NP**	NA*
SGBF32 (highest stress from applied load)	Rear of bottom flange of cross bearer, 18 1/2 inches from B-end body bolster from center of car. 5 3/4 inches outboard of center sill, toward RH side.	-3.2	-2.1	-5.3	33.6	16%	NP**	NA*

* Not required because measured stress does not exceed 75% of allowable

** FEA prediction could not be completed for this test as the wheels are connected to the span bolster and not the carbody

Table 11. Comparison of selected measured stresses with predicted stresses for suspension twist test with the A-end RH corner lifted 3 inches

Channel Name	Approximate Location	Normal Stress in the Active Direction of the Strain Gage						
		Measured Stress from Max Test Load (ksi)	Measured Stress from Applied Force (ksi)	Total Stress (ksi)	Yield Stress (ksi)	Total Stress as percent of Allowable	Predicted Stress	Percent Difference Test vs Predicted
SGBF26 (highest total stress)	Center of LH side sill bottom flange, approx. 74 1/8 inches from B end body bolster toward center of car.	27	1.8	29	44.8	65%	NP**	NA*
SGBF32 (highest stress from applied load)	Rear of bottom flange of cross bearer, 18 1/2 inches from B-end body bolster from center of car. 5 3/4 inches outboard of center sill, toward RH side.	-3.2	2.1	-1.1	33.6	3%	NP**	NA*

* Not required because measured stress does not exceed 75% of allowable

** FEA prediction could not be completed for this test as the wheels are connected to the span bolster and not the carbody.

Table 12. Comparison of selected measured stresses with predicted stresses for suspension twist test with the B-end LH corner lifted 3 inches

Channel Name	Approximate Location	Normal Stress in the Active Direction of the Strain Gage						
		Measured Stress from Max Test Load (ksi)	Measured Stress from Applied Force (ksi)	Total Stress (ksi)	Yield Stress (ksi)	Total Stress as percent of Allowable	Predicted Stress	Percent Difference Test vs Predicted
SGBF26 (highest total stress)	Center of LH side sill bottom flange, approx. 74 1/8 inches from B end body bolster toward center of car.	27	-0.5	26	44.8	58%	NP**	NA*
SGBF9 (highest stress from applied load)	Rear of bottom flange of cross bearer, 18 1/2 inches from A-end body bolster from center of car. 5 3/4 inches outboard of center sill, toward LH side.	-2.4	1.6	-0.8	33.6	2%	NP**	NA*

* Not required because measured stress does not exceed 75% of allowable

** FEA prediction could not be completed for this test as the wheels are connected to the span bolster and not the carbody.

Table 13. Comparison of selected measured stresses with predicted stresses for suspension twist test with the B-end RH corner lifted 3 inches

Channel Name	Approximate Location	Normal Stress in the Active Direction of the Strain Gage						
		Measured Stress from Max Test Load (ksi)	Measured Stress from Applied Force (ksi)	Total Stress (ksi)	Yield Stress (ksi)	Total Stress as percent of Allowable	Predicted Stress	Percent Difference Test vs Predicted
SGBF26 (highest total stress)	Center of LH side sill bottom flange, approx. 74 1/8 inches from B end body bolster toward center of car.	27	-0.5	26	44.8	58%	NP**	NA*
SGBF6 (highest stress from applied load	Rear of bottom flange of cross bearer, 18 1/2 inches from A-end body bolster from center of car. 5 3/4 inches outboard of center sill, toward RH side.	-2.6	1.9	-0.6	33.6	2%	NP**	NA*

* Not required because measured stress does not exceed 75% of allowable

** FEA prediction could not be completed for this test as the wheels are connected to the span bolster and not the carbody.

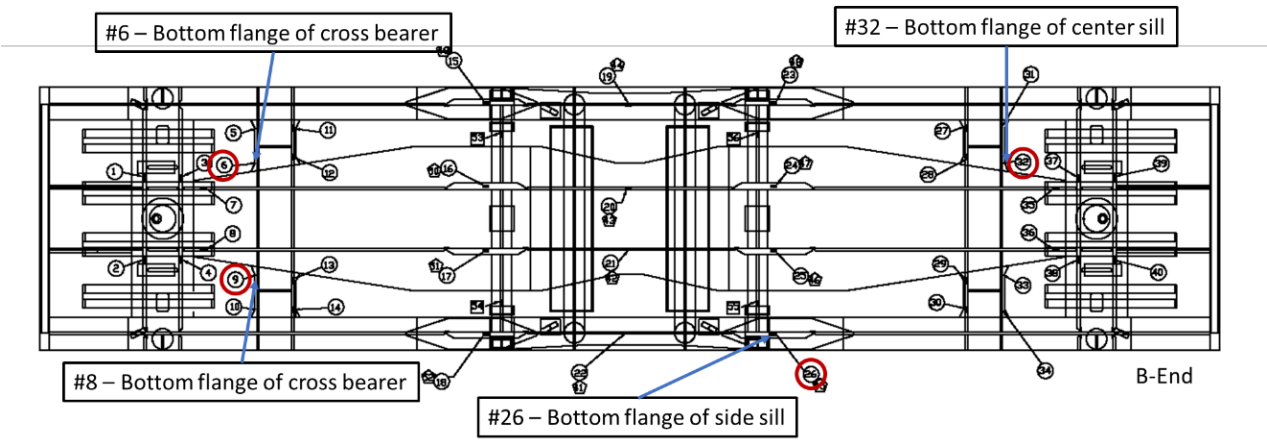

Figure 9. Suspension twist locations

4.5.2 Carbody Twist

Table 14 shows the summary results from the carbody twist test for the locations with the highest measured stress. These locations are highlighted in Figure 10. The maximum measured stress was 43 percent of the material yield.

Table 14. Comparison of selected measured stresses with predicted stresses for carbody twist test

Channel Name	Approximate Location	Normal Stress in the Active Direction of the Strain Gage						
		Measured Stress from Max Test Load (ksi)	Measured Stress with car on Jacks (ksi)	Measured Stress from 3-inch drop (ksi)	Total Stress (ksi)	Yield Stress (ksi)	Total Stress as percent of Yield	Percent Difference Test vs Predicted
SGDP45 (highest total compression stress)	Top of deck plate, above LH side sill web, 66 3/8 inches from line across centermost edges of pin blocks toward center of car (directly above SBGF 26)	-21	-19	-6.7	-26	60	43%	NA*
SGDP45 FEA predictions		NA*	NA*	NA*	NA*			
SGBF26 (Highest total tension stress)	Center of LH side sill bottom flange, approx. 74 1/8 inches from B end body bolster toward center of car.	27	25	5.7	31	72	43%	NA*
SGBF26 FEA predictions		NA*	NA*	NA*	NA*			
SGBF12 (highest stress from applied load)	Rear of bottom flange of #4 cross bearer, RH side between center sill and side sill, near center sill	0.46	-3.8	13	9.2	60	15%	NA*
SGBF12 FEA predictions		NA*	NA*	NA*	NA*			
SGBF29 (#2 ranked stress from applied load)	Front of bottom flange of #1 cross bearer, LH side between center sill and side sill, near center sill	0.46	-4.8	12	7.4	60	12%	NA*
SGBF29 FEA predictions		NA*	NA*	NA*	NA*			

* Not required because measured stress does not exceed 75% of allowable

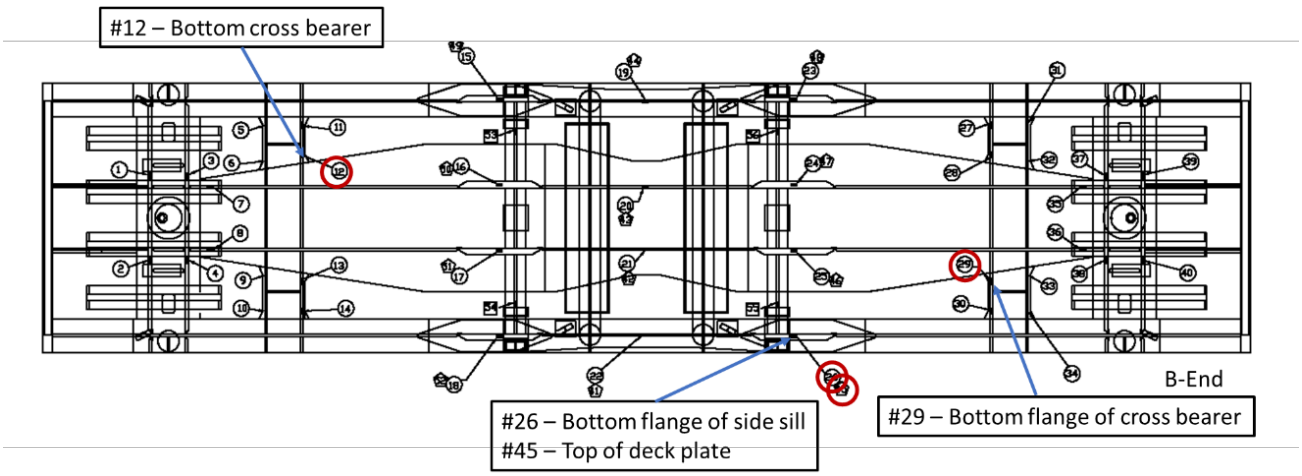

Figure 10. Measurement locations with highest stresses during carbody twist test

4.6 Impact

Table 15 shows the summary results from the impact test for the locations with the highest measured stress. These locations are highlighted in Figure 11.

Standard S-2043, paragraph 4.1.5.9 Allowable Stresses states "All conditions resulting from live and dead loads in combination with impact loads shall follow the guidelines in MSRP Section C Part II, Specification M-1001, paragraph 4.2.2.6." Paragraph 4.2.2.6 states that "such loading may develop the ultimate load carrying capacity of the member being investigated." TTCI used the ultimate stress as the allowable stress for impact tests to comply with the Allowable Stresses statement found in paragraph 4.1.5.9.

The highest stresses were measured at the highest impact speed of 9.6 mph. The coupler load measured on this run was 612 kips. The maximum measured stress was 28 percent of the material yield.

Table 15. Comparison of selected measured stresses with predicted stresses for impact test

Channel Name	Approximate Location	Normal Stress in the Active Direction of the Strain Gage					
		Measured Stress from Max Test Load (ksi)	Measured Stress from Impact Force (ksi)	Total Stress (ksi)	Ultimate Stress (ksi)	Total Stress as percent of Ultimate	Percent Difference Test vs Predicted
SGBF26 (highest total stress)	Center of LH side sill bottom flange, approx. 74 1/8 inches from B end body bolster toward center of car.	27	-6.8	20	90	22%	NA*
SGBF26 FEA predictions		26	-4.1	21.9			
SGBF36 (highest stress from applied load	LH side of bottom flange of center sill – 5 3/16 inches from B-end body bolster toward center of car - aligns with center sill web	3.4	-17	-13	75	17%	NA*
SGBF36 FEA predictions		3	-4	-1			
SGBF35 (#2 rank stress from applied load	RH side of bottom flange of center sill – 5 3/16 inches from B-end body bolster toward center of car - aligns with center sill web	3.4	-17	-13	75	17%	NA*
SGBF35 FEA predictions		3	-4	-1			
SGDP52 (#3 rank stress from applied load	Top of deck plate, above RH center sill web, approx. 2 inches forward of #3 cross bearer	-17	7	-10	75	13%	NA*
SGDP52 FEA predictions		-18	2	-16			

* Not required because measured stress does not exceed 75% of allowable

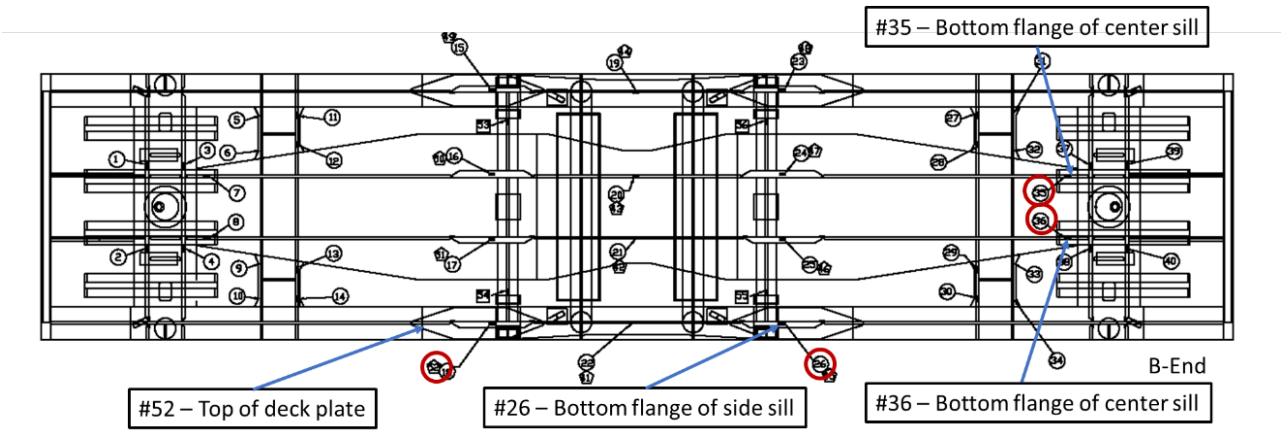

Figure 11. Measurement locations with highest stresses during impact test

5.0 NEW FEA PREDICTIONS

Because none of the measured stresses corresponded with stresses greater than 75 percent of the allowable stress, the tolerance on FEA prediction accuracy does not apply. No new FEA predictions are required.

6.0 REFINING THE DYNAMIC MODEL

Standard S-2043 requires:

"The dynamic model must be refined based on vehicle characterization results if suspension values are measurably different than those used in the original model."

Some of the measured characterization results differ from those used in the original dynamic analysis model. Table 16 provides 1) the suspension stiffness and damping values used for the original model, 2) the values measured during the characterization, 3) the percent difference, 4) information on the origin of the characterization value, and 5) an indication of if and how the characterization value was used to update the model.

Table 16. Comparison of values used in preliminary modeling and values measured during characterization

Parameter		Pre-Test Model Value	Characterization Value	Percent Difference	Notes	Change to model
End Truck Spring vertical stiffness (pound/inch/nest)		31,474	32,472	-3%	Built up from spring component stiffness tests	No change made
End Truck Vertical secondary stiffness (pound/inch/nest)		31,474	35,000	-10%	Characterization value from 0.1 Hz case, minimum and maximum load condition	No change made
End Truck Lateral secondary stiffness (pound/inch/nest)	Min Load	16,976	7,500	118%	Maximum test load, transom restrained	Used 38% of calculated value[6]
	Max Load	18,790	11,500	64%	Maximum test load, transom restrained	Used 58% of calculated value[6]
End Truck Vertical secondary hysteresis width (pound/nest)		5,800	6,000	-3%	Maximum test load	No change made
End Truck Lateral secondary hysteresis width (pound/nest)		5,800	7,900	-27%	Maximum test load, transom restrained	No change made
Middle Truck Spring vertical stiffness (pound/inch/nest)		30,252	31,516	-4%	Built up from spring component stiffness tests	No change made
Middle Truck Vertical secondary stiffness (pound/inch/nest)		30,252	34,500	-12%	Characterization value from 0.1 Hz case, minimum and maximum load condition	No change made
Middle Truck Lateral secondary stiffness (pound/inch/nest)	Min Load	15,595	4,500	233%	Maximum test load, transom restrained, wedges removed	Used 38% of calculated value*
	Max Load	17,363	9,500	84%	Maximum test load, transom restrained, wedges removed	Used 58% of calculated value*
Middle Truck Vertical secondary hysteresis width (pound/nest)		6,000	6,500	-8%	Characterization value from 0.1 Hz case, minimum and maximum load condition	No change made
Middle Truck Lateral secondary hysteresis width (pound/nest)		6,000	7,700	-22%	Maximum test load, transom restrained, wedges installed	No change made
Side bearing preload (pounds)		5000	5240	-5%		No change made

Parameter	Pre-Test Model Value	Characterization Value	Percent Difference	Notes	Change to model
Span Bolster Center plate friction (nondimensional)	0.15	0.17	-12%	Average on the surface. Median of min and max test load values	The friction coefficient was changed to match the characterization value.
Truck Center plate friction (nondimensional)	0.30	0.21	43%	Average on the surface. Median of min and max test load values for the tree trucks tested	The friction coefficient was changed to match the characterization value.
Vertical primary stiffness (pound/inch/pad)	500,000	236,000 288,000	112% 74%	Characterization values range from 194,000 to 288,000 for minimum test load and 213,000 to 510,000 for maximum test load. The average is shown for each load case.	A stiffness of 236,000 is used for minimum test load model and 291,000 is used for maximum test load model.
Lateral primary stiffness (pound/inch/pad)	48,000	35,000 82,000	37% -41%	Characterization values range from 27,000 to 55,000 for minimum test load and 58,000 to 107,000 for maximum test load. The average shown for each load case.	A stiffness of 35,000 is used for minimum test load model and 82,000 is used for maximum test load model.
Longitudinal primary stiffness at axle centerline (pound/inch/pad)	22,500	12.3 13	83% 73%	Data taken from second interaxle test rather than that reported in test report. Characterization values range from 9,900 to 16,100 for minimum test load and 10,100 to 18,400 for maximum test load. The average shown for each load case.	A stiffness of 12,300 is used for minimum test load model and 13,000 is used for maximum test load model.

The lateral secondary suspension stiffness measured during the characterization test was about 58 percent of the value used in the dynamic analysis model for the maximum test load and about 38 percent of the value used for the minimum test load. The measured stiffness is lower because the formula[6] used to estimate the shear stiffness often predicts a higher stiffness than what is found in practice. To match the values from characterization tests, the shear stiffness in the revised dynamic model calculated using the formula were reduced. When compared to the use of Koffman's formula, these modified stiffnesses were 58 percent lower for maximum test load simulations and 38 percent lower for minimum test load simulations. The results of the characterization tests are believed to be more accurate than Koffman's formula.

The original dynamic analysis model used a coefficient of friction value of 0.3 to model the surface between the carbody center plate and the truck center bowl. The coefficient of friction measured during the characterization test was 0.21. The refined dynamic model used a coefficient of friction of 0.21 for this surface. This model used the following:

- A vertical primary pad stiffness of 500,000 pounds per inch per pad for all load conditions.
- A lateral primary pad stiffness of 48,000 pounds per inch per pad for all load conditions.
- A longitudinal primary pad stiffness of 22,500 pounds per inch per pad for all load conditions.

The vertical stiffnesses were measured using CSM 58 primary pads during the characterization tests were about 236,000 pounds per inch and 288,000 pounds per inch per pad for the minimum and maximum test load, respectively. The revised model used these stiffness values for the two test load conditions. Based on the manufacturer's recommendation, a factor of 4X was applied to these values for simulations using CSM 70 primary pads.

The lateral stiffnesses measured with CSM 58 primary pads during the characterization tests were about 35,000 pounds per inch per pad and 82,000 pounds per inch per pad for the minimum and maximum test load, respectively. The revised model used these stiffness values for the two test load conditions. Based on the manufacturer's recommendation, a factor of 1.35X was applied to these values for simulations using CSM 70 primary pads.

While troubleshooting the curving performance in November 2020, TTCI performed a second interaxle longitudinal stiffness test to measure the stiffness of the CSM 70 pads and remeasure the stiffness of the CSM 58 pads. These tests were separate from those presented in the Atlas car single car test report. Figure 12 shows the results of these tests. The longitudinal pad stiffnesses measured during the second interaxle stiffness tests using CSM 58 primary pads were about 12,300 pounds per inch per pad and 13,000 pounds per inch per pad for the minimum and maximum test load, respectively. When this test was performed using the CSM 70 pads the stiffnesses measured were about 28,700 and 31,200 pounds per inch per pad for the minimum and maximum test load, respectively. The revised model used these stiffness values for the two test load conditions with the two pad types.

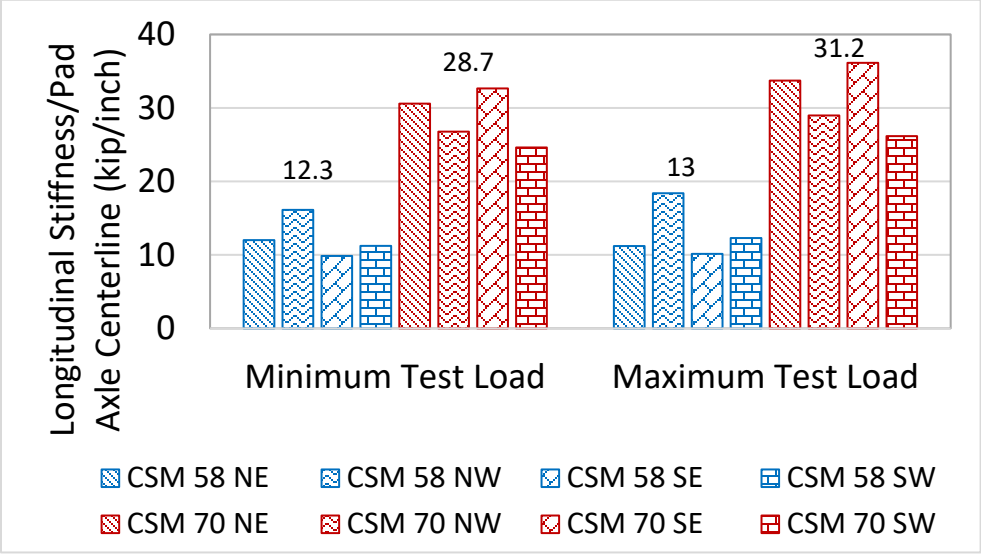

Figure 12. Results of the second interaxle stiffness test with CSM 58 and CSM 70 primary pads

While troubleshooting the hunting performance of Atlas car, TTCI found that the method used to model the connection between the side frame and the primary pad could be altered to better replicate the roll characteristics between the side frame and axle. The original modeling method for this this connection used only a single vertical connection centered at the primary pad located between the side frame and axle. When comparing the predicted lateral suspension displacement with test results, TTCI found that the results matched better when the two connections, separated laterally by the width of the primary pad, were used to model this connection. This new method was implemented in the refined dynamic analysis model.

7.0 NEW DYNAMIC PREDICTIONS

Standard S-2043 states the following:

> *"Test results must be compared to design predictions to verify that the model accurately represents the vehicle. If substantial modifications have been made to the dynamic model, a revised analysis must be performed. The designer may choose to repeat the entire analysis or reanalyze limited cases based on how critically they would be affected by the changes to the model and how large existing margins of safety are. The designer's decisions must be justified through adequate explanation."*

TTCI compared the original and refined dynamic analysis model predictions with the test data to show that the model accurately represented the vehicle. The characterization test results prompted several changes to the dynamic analysis model. As a result, TTCI repeated several portions of the dynamic analysis. The simulation predictions are shown for the original and revised models in Sections 7.1 to 7.10.

Several regimes were simulated using CSM 70 primary pads for comparison with test data to demonstrate model validation and CSM 58 primary pads to demonstrate the expected performance with the primary pad to be used in service. The simulation predictions made using CSM 58 primary

pads were compared to the test data for the hunting and minimum test load dynamic curving where the test data was available. TTCI repeated the following portions of the dynamic analysis because they served to demonstrate the model performance as compared to the test data:

- Twist and roll
- Pitch and bounce
- Yaw and sway
- Dynamic curving
- Single bump test
- Curving with single rail perturbation
- Hunting
- Standard Chapter 11 constant curving
- Limiting spiral negotiation

TTCI repeated the following portions of the dynamic analysis because the original dynamic analysis predictions showed that some metrics were close to or did not meet the criteria.

- Curving with various lubrication conditions
- Turnouts and crossovers
- Buff and draft curving
- Worn component simulation

Because the original dynamic analysis showed a relatively large margin of safety with respect to the criteria for these regimes, the regimes below were not simulated with the revised model:

- Ride quality
- Braking effects on steering

The lightest load modeled during the original dynamic analysis for the Atlas car in 2017 is different than what was tested and modeled during the post-test analysis simulations described in this report. Because of this difference, the original simulation predictions for the lightest car condition will not be compared to the revised predictions for the minimum test load. In 2017, the DOE expected to sometimes move an Atlas car in a Standard S-2043 train without a cask loaded on the car. To meet all dynamic requirements, a ballast load was needed, and Orano designed a ballast load for this purpose. Ballast load properties were used for the “empty” car simulations performed in 2017. Since that time, the DOE determined that any empty Atlas car could be moved using non-Standard S-2043 trains. Because of this determination, the minimum simulated load was changed from the ballast load to a load representing the lightest empty cask that would be carried by a Standard S-2043 train, referred to as the minimum test load. The revised predictions for the maximum test load are consistent with the original predictions for the HI-STAR 190 XL cask. The EEC approved the empty Atlas car for use in non-HLRM trains based on its similarities with the empty Navy M-290 HLRM car. This car has been approved under M-1001 (see Section 4 and Appendix A of [2]).

Most simulation predictions were made using inputs created with measured track geometry. TTCI's experience has shown that simulations with measured track geometry produce better predictions of car performance than those that are obtained with analytic track inputs created with mathematical functions. Because the measured track geometry inputs contain short wavelengths that cause spurious peaks in the data, the 50-millisecond and 3-foot analysis windows described in AAR Chapter 11 and S-2043 are used when analyzing data to produce the most realistic results. The exceptions included some curving with single rail perturbation simulations and special track work simulations of number 7 turnouts and number 7 crossovers that used inputs from mathematically generated inputs.

7.1 Twist and Roll

The simulations of the twist-and-roll regime were conducted according to Standard S-2043, Paragraph 4.3.9.6. The twist-and-roll track tests were conducted according to Standard S-2043, Paragraph 5.5.8. The twist-and-roll regime consists of a series of ten 0.75-inch vertical track deviations offset on each rail to input roll motions to the car.

7.1.1 Minimum Test Load

Table 17 shows the worst-case test results and the simulation predictions for the car loaded with the minimum test load. Figure 13 shows the peak-to-peak roll angle for the results from testing done using CSM 70 pads and modeling predictions using both CSM 70 and CSM 58 primary pads plotted against speed to show the trend in performance. As Figure 13 shows, the simulation predictions and the test results for CSM 70 pads have a lower center roll resonance at the same speed and a similar overall trend. The simulation predictions done using CSM 58 pads show slightly higher lateral acceleration values than the values from the simulation predictions done using CSM 70 pads, but results for other metrics are similar. Only post-test simulation predictions are shown because the pre-test predictions were performed for a load case no longer intended for use (as described in Section 7.0). The twist-and-roll test results and revised simulation predictions **meet** Standard S-2043 criteria for the minimum test load.

Table 17. Twist-and-roll test results and simulation predictions using minimum test load

Criterion	Limiting Value	CSM 70 Pads		CSM 58 Pads
		Test Result	Simulation Prediction Revised Model	Simulation Prediction Revised Model
Roll angle (degree)	4.0	1.4	1.9	1.9
Maximum wheel lateral/vertical (L/V)	0.8	0.27	0.29	0.27
Maximum truck side L/V	0.5	0.19	0.15	0.17
Minimum vertical wheel load (%)	25%	54%	57%	58%
Lateral peak-to-peak acceleration (g)	1.3	0.50	0.29	0.47
Maximum lateral acceleration (g)	0.75	0.26	0.15	0.24
Maximum vertical acceleration (g)	0.90	0.36	0.19	0.20
Maximum vertical suspension deflection (%)	95%	16%	22%	21%

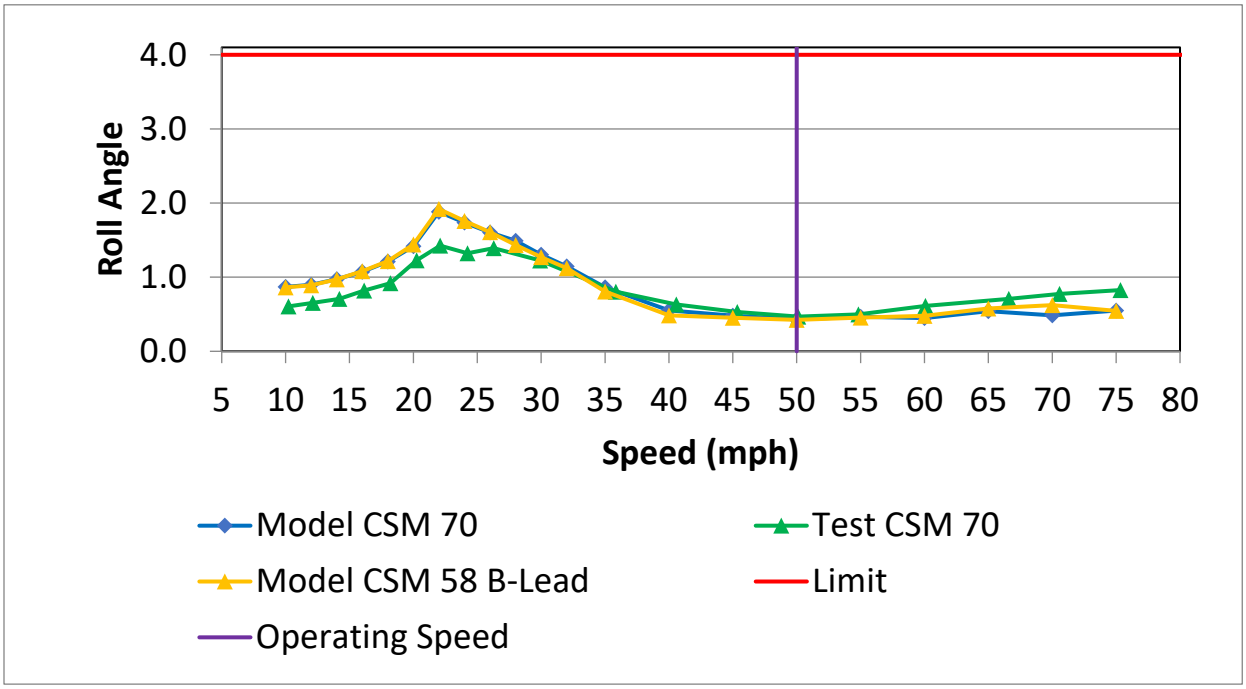

Figure 13. Twist-and-roll test results and simulation predictions of maximum peak-to-peak carbody roll angle with minimum test load

7.1.2 Maximum Test Load

Table 18 shows the worst-case test results and simulation predictions for the car loaded with the maximum test load. Figure 14 shows the peak-to-peak roll angle for test results and modeling predictions done using CSM 70 primary pads plotted against speed to show the trend in performance. Figure 15 shows the peak-to-peak roll angle for the pre-test and refined-models simulation predictions. The test results and simulation predictions (Figure 14) show the lower-center roll resonance at the same speed and similar overall performance trends. The simulation predictions done using CSM 58 pads showed a similar performance to simulation predictions done using CSM 70 pads. The simulation predictions changed very little after changes in model inputs using the characterization results. The revised simulation predictions **meet** Standard S-2043 criteria for the twist and roll tests with maximum test load.

Table 18. Twist-and-roll test results and simulation predictions with maximum test load

Criterion	Limiting Value	CSM 70 Pads		CSM 58 Pads	
		Test Result	Simulation Prediction Revised Model	Simulation Prediction Original Model	Simulation Prediction Revised Model
Roll angle (degree)	4.0	1.3	1.7	2.1	1.8
Maximum wheel lateral/vertical (L/V)	0.8	0.23	0.14	0.14	0.14
Maximum truck side L/V	0.5	0.15	0.08	0.11	0.10
Minimum vertical wheel load (%)	25%	64%	62%	66%	63%
Lateral peak-to-peak acceleration (g)	1.3	0.31	0.34	0.24	0.38
Maximum lateral acceleration (g)	0.75	0.17	0.19	0.13	0.21
Maximum vertical acceleration (g)	0.90	0.20	0.24	0.11	0.25
Maximum vertical suspension deflection (%)	95%	56%	63%	74%	63%

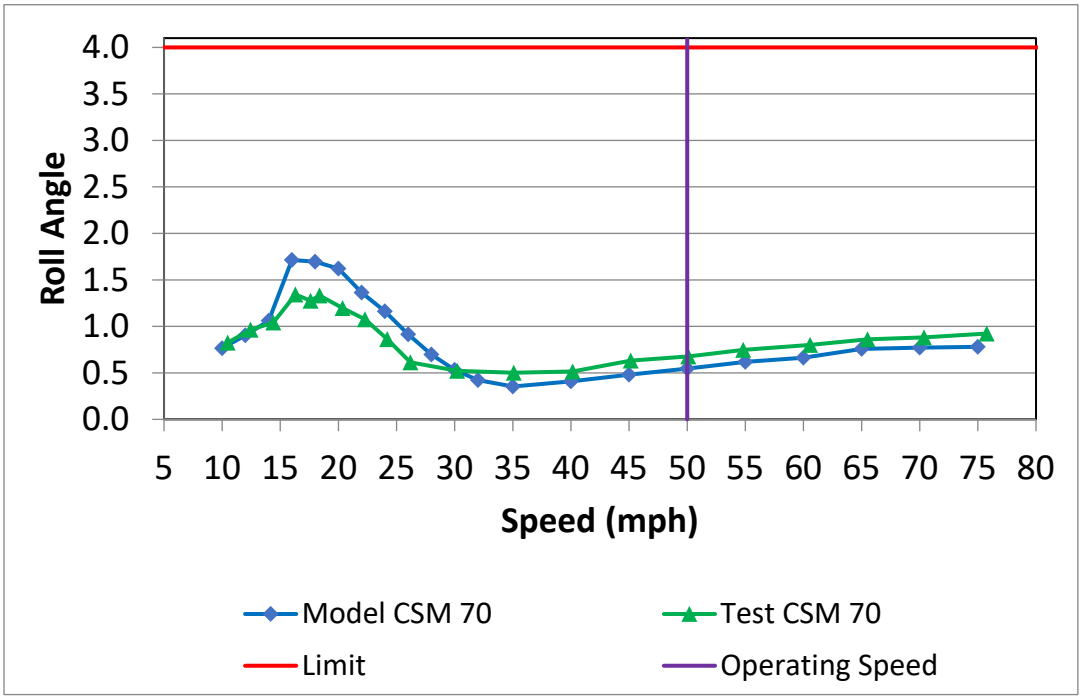

Figure 14. Twist-and-roll test results and simulation predictions of maximum peak-to-peak carbody roll angle with maximum test load using CSM 70 pads

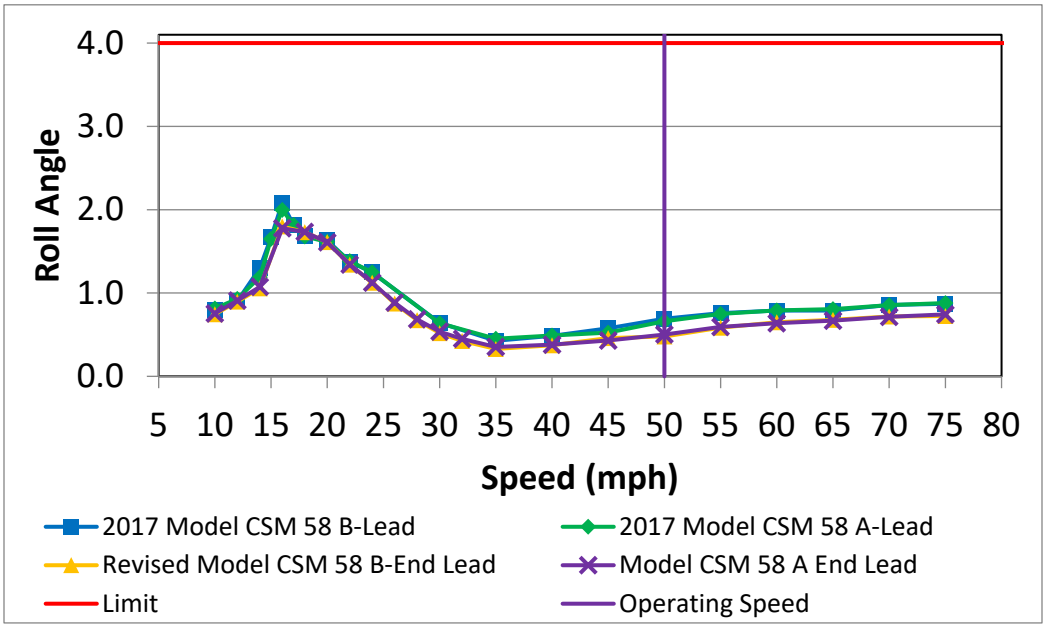

Figure 15. Twist-and-roll pre-test and refined model simulation predictions of maximum peak-to-peak carbody roll angle with maximum test load using CSM 70 pads

7.2 Pitch and Bounce (Chapter 11)

The simulations of the pitch-and-bounce regime were conducted according to Standard S-2043, Paragraph 4.3.9.7. The pitch-and-bounce tests were conducted according to Standard S-2043, Paragraph 5.5.11. The pitch-and-bounce regime consists of a series of ten 0.75-inch vertical track deviations in parallel on each rail to input vertical motions on the car.

Because the truck center spacing of the car (38 feet, 9 inches) is so similar to the wavelength of the perturbations of the standard pitch-and-bounce zone (39 feet), special tests or simulations with inputs at a wavelength equal to the truck center spacing of the car were not performed.

7.2.1 Minimum Test Load

Simulations are required for the minimum test load condition, but testing is not required. Table 19 shows the worst-case simulation predictions for the car loaded with the minimum test load. Figure 16 shows the maximum vertical acceleration for the modeling predictions using CSM 58 primary pads plotted against speed to show the trend in performance. The revised simulation predictions **meet** Standard S-2043 criteria for pitch and bounce done using CSM 58 pads at minimum test load.

Table 19. Pitch and bounce test results and simulation predictions

Criterion	Limiting Value	Simulation Prediction Revised Model
Roll angle (degree)	4.0	0.2
Maximum wheel L/V	0.8	0.18
Maximum truck side L/V	0.5	0.11
Minimum vertical wheel load (%)	25%	61%
Lateral peak-to-peak acceleration (g)	1.3	0.48
Maximum lateral acceleration (g)	0.75	0.26
Maximum vertical acceleration (g)	0.90	0.00
Maximum vertical suspension deflection (%)	95%	0.53

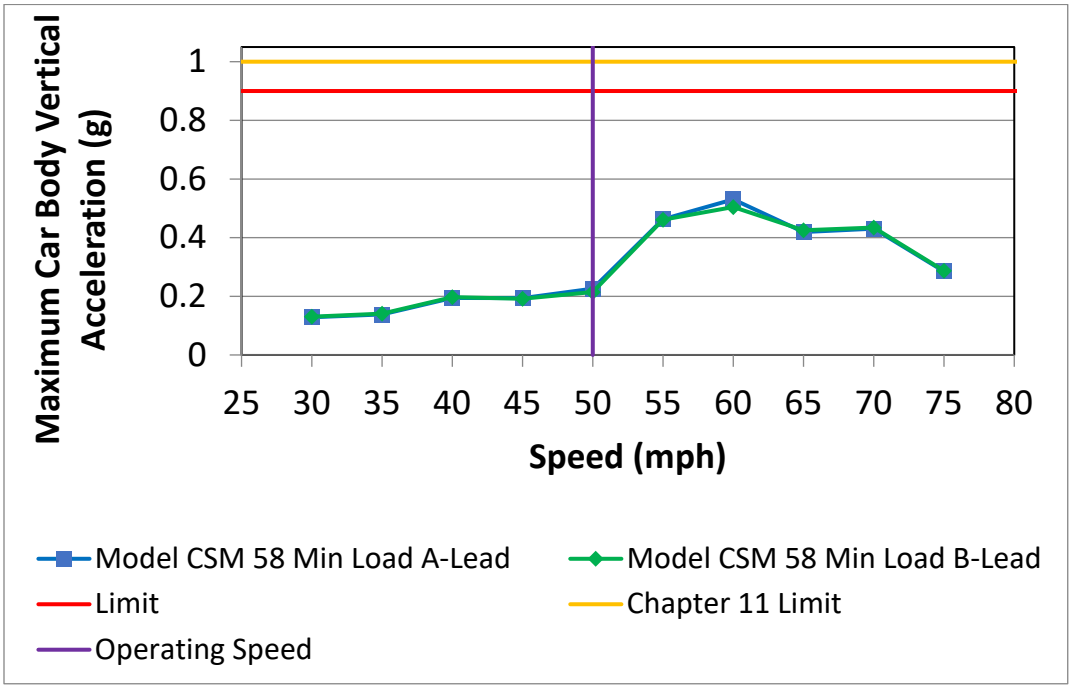

Figure 16. Simulation predictions of maximum vertical carbody acceleration in the pitch and bounce regime with minimum test load

7.2.2 Maximum Test Load

Table 20 shows the worst-case test results and simulation predictions for the car loaded with the maximum test load. Figure 17 shows the test results and modeling predictions of the maximum vertical acceleration using CSM 70 primary pads plotted against speed to show the trend in performance. Figure 18 shows the simulation predictions of maximum vertical acceleration done using CSM 58 primary pads. The maximum vertical acceleration simulation predictions and test results done using CSM 70 primary pads match closely. The simulation predictions done using CSM 58 pads show similar minimum vertical wheel load results, but slightly higher carbody accelerations than the simulation predictions done using CSM 70 pads. The revised simulation predictions showed not only higher lateral/vertical (L/V) ratio and acceleration values but also higher minimum vertical

load values than the original 2017 simulation predictions. The test results and revised simulation predictions **meet** Standard S-2043 criteria for pitch and bounce with maximum test load.

Table 20. Test results and simulations predictions for Pitch and Bounce with maximum test load

Criterion	Limiting Value	CSM 70 Pads		CSM 58 Pads	
		Test Result	Simulation Prediction Revised Model	Simulation Prediction Original Model	Simulation Prediction Revised Model
Roll angle (degree)	4.0	0.2	0.3	0.1	0.3
Maximum wheel lateral/vertical (L/V)	0.8	0.10	0.14	0.06	0.12
Maximum truck side L/V	0.5	0.07	0.09	0.04	0.09
Minimum vertical wheel load (%)	25%	63%	73%	68%	74%
Lateral peak-to-peak acceleration (g)	1.3	0.12	0.25	0.16	0.34
Maximum lateral acceleration (g)	0.75	0.07	0.14	0.08	0.20
Maximum vertical acceleration (g)	0.90	0.25	0.26	0.22	0.38
Maximum vertical suspension deflection (%)	95%	52%	56%	76%	56%

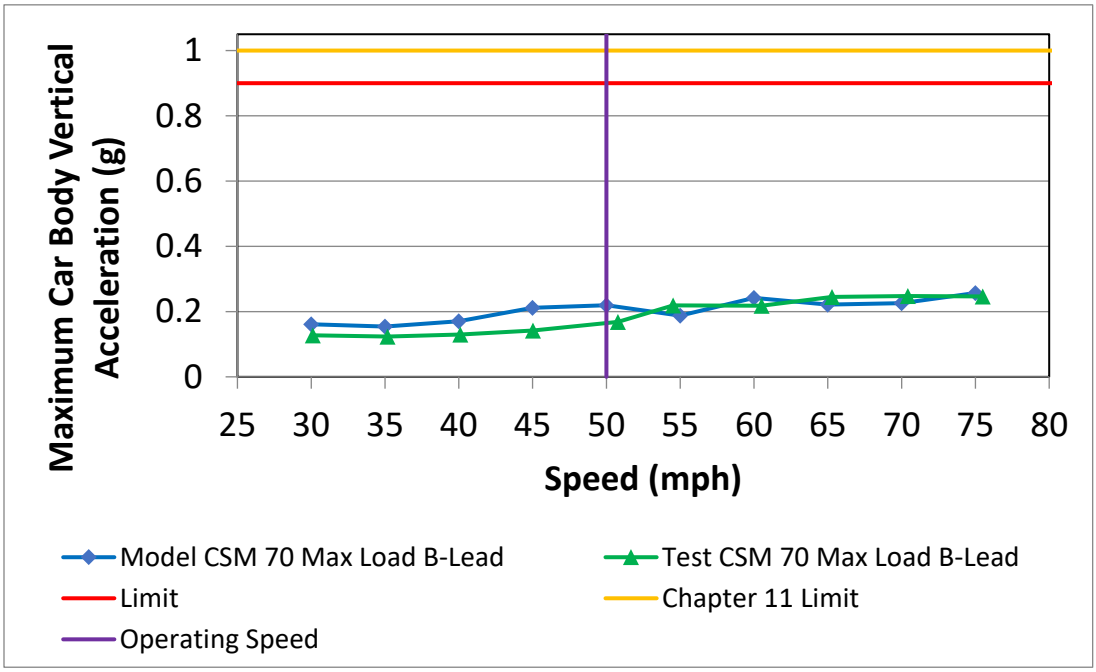

Figure 17. Pitch and bounce test results and simulation predictions of maximum vertical acceleration with CSM 70 Pads at maximum test load

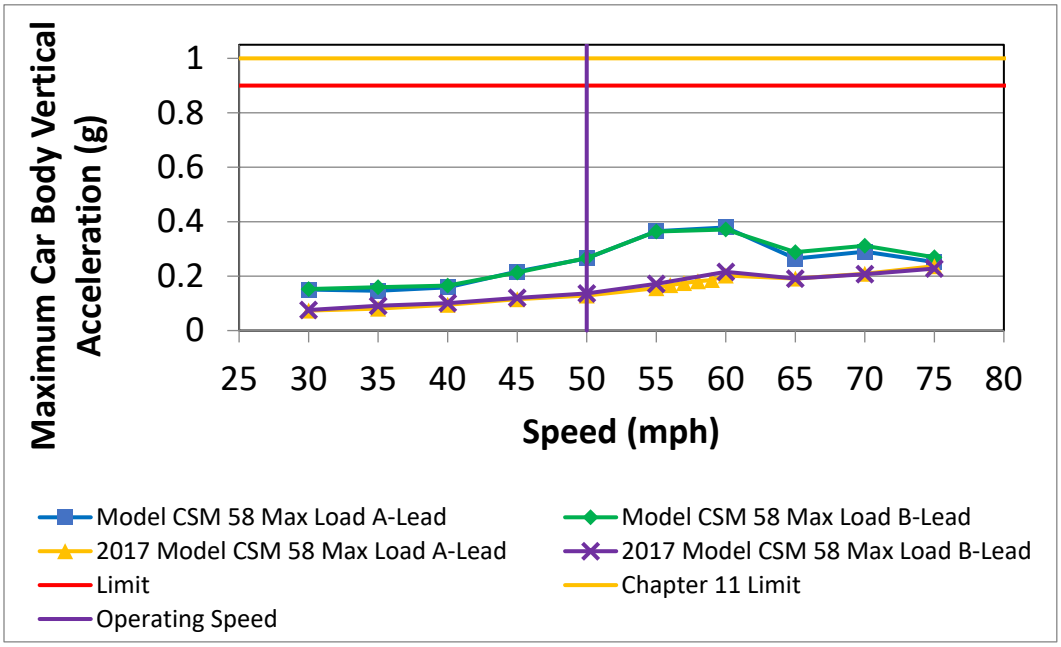

Figure 18. Pitch and bounce simulation predictions of maximum vertical acceleration with CSM 58 Pads at maximum test load

7.3 Yaw and Sway

Simulations of the yaw-and-sway regime were conducted according to Standard S-2043, Paragraph 4.3.9.8. The yaw-and-sway tests were conducted according to Standard S-2043, Paragraph 5.5.9. The yaw-and-sway regime consists of a series of five consecutive 1.25-inch lateral deviations, on a track section with a 1-inch-wide gage, that input lateral and yaw motions on the car.

Table 21 shows the worst-case test results and the simulation predictions for the car loaded with the maximum test load in the yaw-and-sway test regime. Figure 19 shows the test results and modeling predictions of the maximum truck side L/V ratio with CSM 70 primary pads plotted against speed to show the trend in performance. Figure 20 shows the simulation predictions of the maximum truck side L/V ratio with CSM 58 primary pads. The test results and revised simulation predictions **meet** Standard S-2043 criteria for yaw-and-sway with the maximum test load. Using CSM 70 primary pads, the model predicts higher accelerations, higher L/V ratios, and lower vertical wheel loads than those measured in the test. The simulations done using CSM 58 pads showed lower accelerations, lower L/V ratios, and higher vertical wheel loads than simulations done using CSM 70 primary pads. The differences between the original 2017 simulation predictions and the revised simulation predictions were inconsequential relative to Standard S-2043 criteria levels.

Table 21. Yaw-and-sway test results and simulation predictions

Criterion	Limiting Value	CSM 70 Pads		CSM 58 Pads	
		Test Result	Simulation Prediction Revised Model	Simulation Prediction 2017 Model	Simulation Prediction Revised Model
Roll angle (degree)	4.0	0.7	1.2	0.8	1.0
Maximum wheel L/V	0.8	0.53	0.72	0.59	0.55
Maximum truck side L/V	0.5	0.31	0.43	0.30	0.35
Minimum vertical wheel load (%)	25%	68%	55%	56%	66%
Lateral peak-to-peak acceleration (g)	1.3	0.82	1.21	0.67	0.87
Maximum lateral acceleration (g)	0.75	0.44	0.63	0.36	0.47
Maximum vertical acceleration (g)	0.90	0.17	0.28	0.11	0.41
Maximum vertical suspension deflection (%)	95%	58%	61%	70%	59%

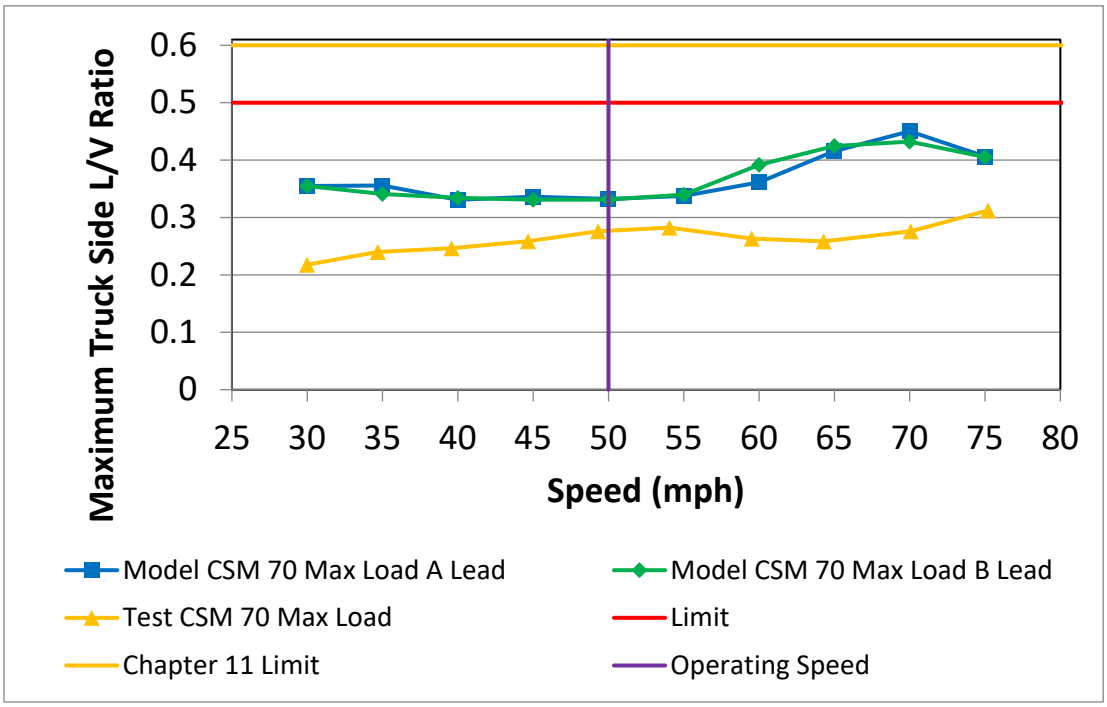

Figure 19. Simulation predictions and test results of maximum truck side L/V ratio in the yaw-and-sway regime with CSM 70 pads and the maximum test load

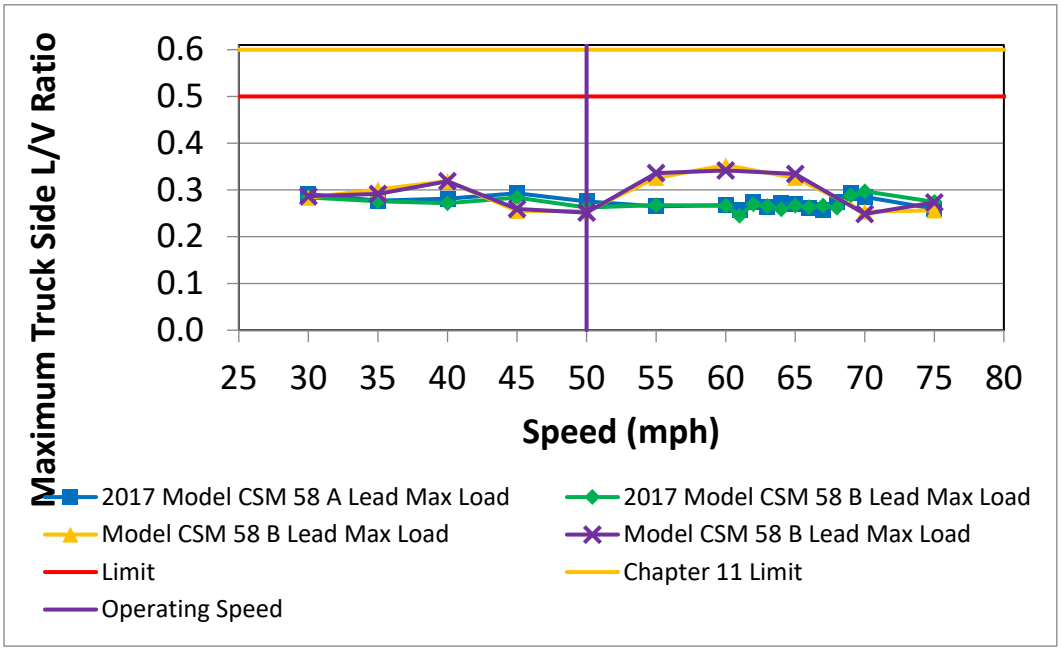

Figure 20. Simulation predictions of maximum truck side L/V ratio in the yaw-and-sway regime with CSM 58 pads and the maximum test load

7.4 Dynamic Curving

Simulations of the dynamic curving regime were conducted according to Standard S-2043, Paragraph 4.3.9.9. The dynamic curving tests were conducted according to Paragraph 5.5.10 of Standard S-2043. The dynamic curve section is on a 10-degree curve with a 4-inch superelevation. The dynamic curving regime consists of a series of 0.5-inch vertical track deviations at a 39-foot wavelength offset on each rail to input roll motions to the car. There are five deviations on the high rail and six deviations on the low rail. At the same time, the track gage changes from 56.5 inches to 57.5 inches to input lateral motions to the car. The simulations and tests were performed at speeds ranging from 10 mph (approximately 3 inches of cant excess) to 32 mph (3 inches of cant deficiency) in increments of 2 mph or less.

7.4.1 Minimum Test Load

Table 22 shows the worst-case test results and the simulation predictions for the car loaded with the minimum test load in the dynamic curving test regime. Figure 21 shows the test results and simulation predictions of the maximum wheel L/V ratio with CSM 70 primary pads plotted against speed to show the trend in performance. Figure 22 shows the test results and simulation predictions of the maximum wheel L/V ratio with CSM 58 primary pads.

The test results did not meet Standard S-2043 criteria for the wheel L/V ratio with CSM 70 pads for dynamic curving with the minimum test load, but all other criteria were met. Figure 23 shows a distance plot of the worst-case test condition. The simulation predictions done using CSM 70 pads did meet Standard S-2043 criteria. Both the test results and revised simulation predictions done using CSM 58 pads **met** Standard S-2043 criteria.

Using CSM 70 primary pads, the model predicts lower wheel L/V ratios and higher minimum vertical wheel loads than those that were measured in the test. The simulations done using CSM 58 pads showed lower L/V ratios than the simulations done using CSM 70 primary pads, but the difference was not as large as what was measured in the test. Only post-test simulation predictions are shown because the pre-test predictions were for a load case no longer intended for use.

Table 22. Dynamic curving test results and simulation predictions

Criterion	Limiting Value	CSM 70 Primary Pad		CSM 58 Primary Pad	
		Test Result	Simulation Prediction Revised Model	Test Result	Simulation Prediction Revised Model
Roll angle (degree)	4.0	0.9	1.0	0.8	1.0
Maximum wheel L/V	0.8	0.90	0.73	0.75	0.71
Maximum truck side L/V	0.5	0.45	0.39	0.39	0.35
Minimum vertical wheel load (%)	25%	31%	54%	40%	53%
Lateral peak-to-peak acceleration (g)	1.3	0.20	0.19	0.19	0.19
Maximum lateral acceleration (g)	0.75	0.16	0.15	0.19	0.16
Maximum vertical acceleration (g)	0.90	0.14	0.12	0.17	0.12
Maximum vertical suspension deflection (%)	95%	26%	23%	22%	23%

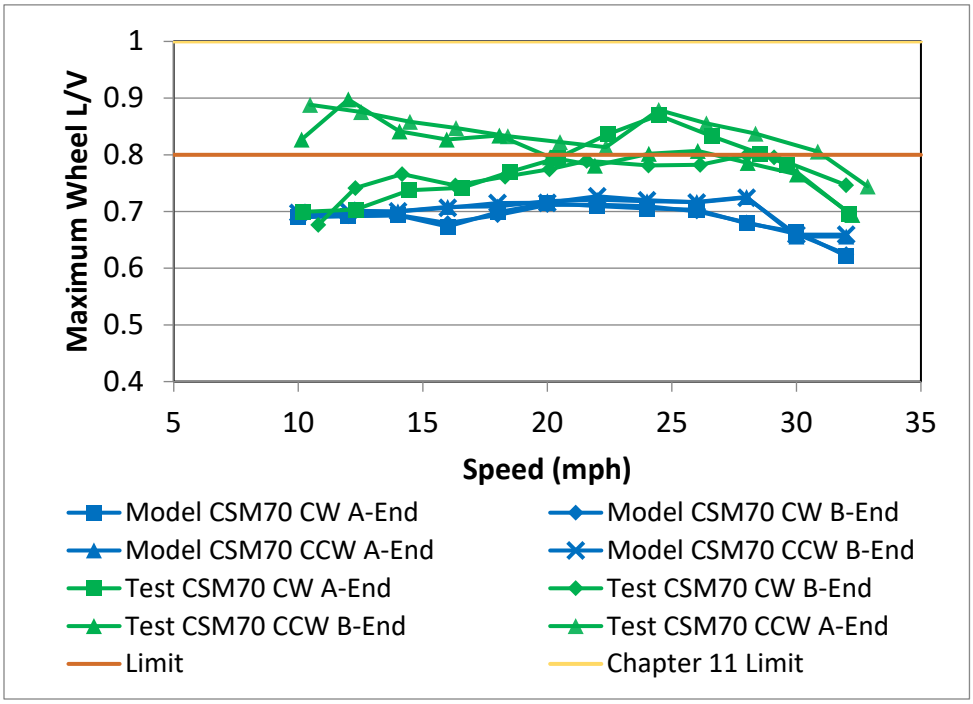

Figure 21. Simulation prediction and test results of maximum wheel L/V ratio in the dynamic curving regime with minimum test load and CSM 70 pads

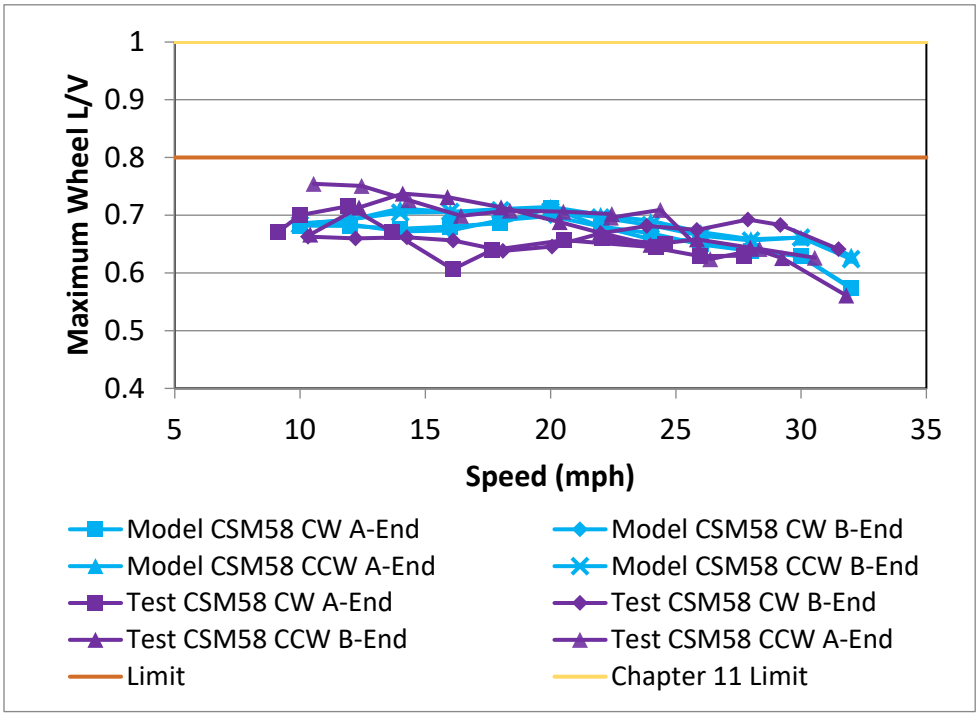

Figure 22. Simulation prediction and test results of maximum wheel L/V ratio in the dynamic curving regime with minimum test load and CSM 58 pads

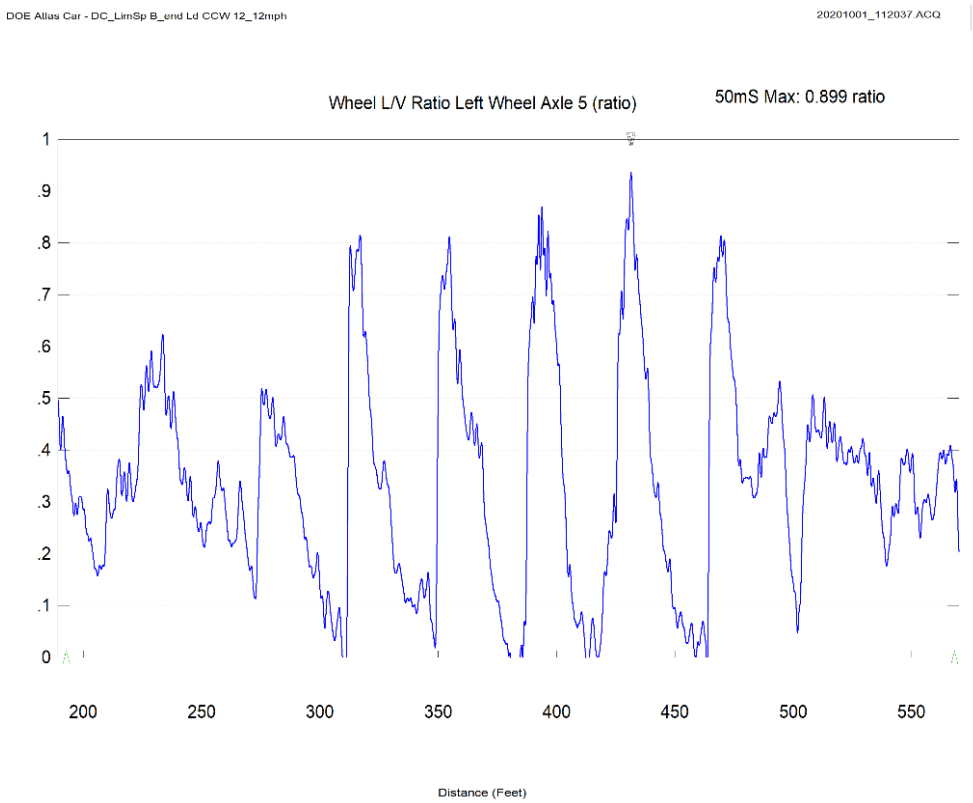

Figure 23. Distance plot of axle 5 lead left wheel L/V ratio during 12 mph run counterclockwise (CCW) through dynamic curve with B-End leading using CSM 70 primary pads

7.4.2 Maximum Test Load

Table 23 shows the worst-case test results and simulation predictions for the car loaded with the maximum test load in the dynamic curving test regime. Figure 24 shows the test results and simulation predictions of the maximum wheel L/V ratio with CSM 70 primary pads plotted against speed to show the trend in performance. Figure 25 shows the original and revised simulation predictions of the maximum wheel L/V ratio with CSM 58 primary pads.

The test results did not meet Standard S-2043 criteria for the wheel L/V ratio with CSM 70 pads for dynamic curving with the maximum test load, but all other criteria were met. The simulation predictions with the revised model using either CSM 70 or CSM 58 pads **met** Standard S-2043 criteria.

Using CSM 70 primary pads, the model predicts lower wheel L/V ratios and higher minimum vertical wheel loads than those that were measured in the test, but the overall trend matches closely, as Figure 24 shows. The simulations done using CSM 58 pads showed lower L/V ratios than the simulations done using CSM 70 primary pads, but the difference was small. The wheel L/V ratios predicted with the original model in 2017 were significantly higher than those predicted with the revised model. This difference is likely explained by the fact that the primary longitudinal stiffness measured in characterization tests and used in the refined model is significantly lower than the original model value.

Table 23. Dynamic curving test results and simulation predictions with maximum test load

Criterion	Limiting Value	CSM 70 Pads		CSM 58 Pads	
		Test Result	Simulation Prediction Revised Model	Simulation Prediction Original Model	Simulation Prediction Revised Model
Roll angle (degree)	4.0	0.8	1.0	1.2	1.0
Maximum wheel lateral/vertical (L/V)	0.8	0.81	0.72	0.88	0.68
Maximum truck side L/V	0.5	0.40	0.37	0.37	0.30
Minimum vertical wheel load (%)	25%	45%	55%	49%	55%
Lateral peak-to-peak acceleration (g)	1.3	0.25	0.12	0.16	0.14
Maximum lateral acceleration (g)	0.75	0.18	0.13	0.13	0.12
Maximum vertical acceleration (g)	0.90	0.11	0.17	0.06	0.25
Maximum vertical suspension deflection (%)	95%	66%	67%	78%	67%

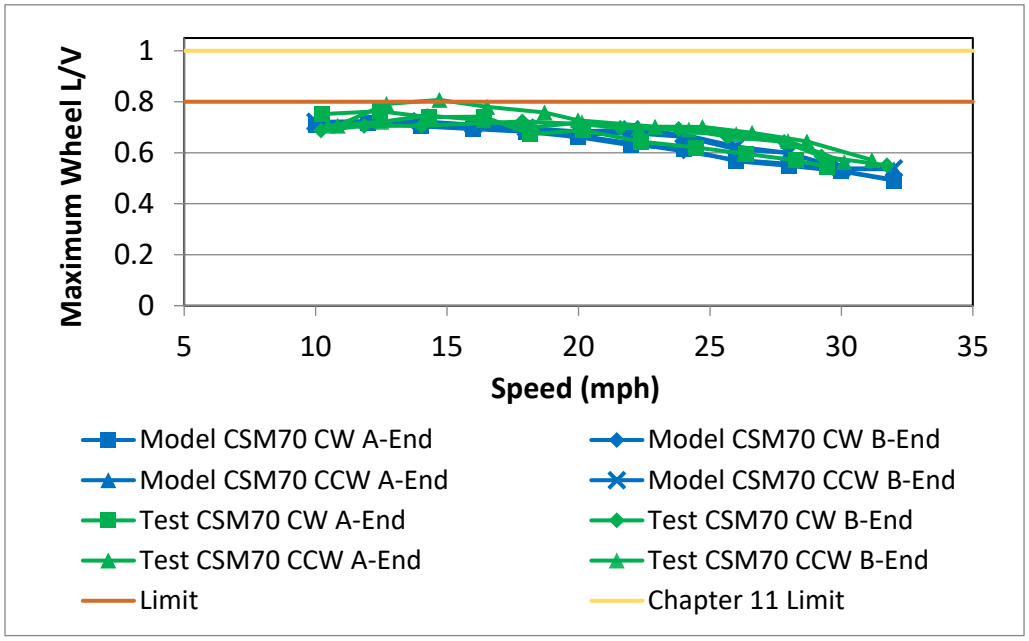

Figure 24. Simulation prediction and test results of maximum wheel L/V ratio in the dynamic curving regime with maximum test load using CSM 70 pads

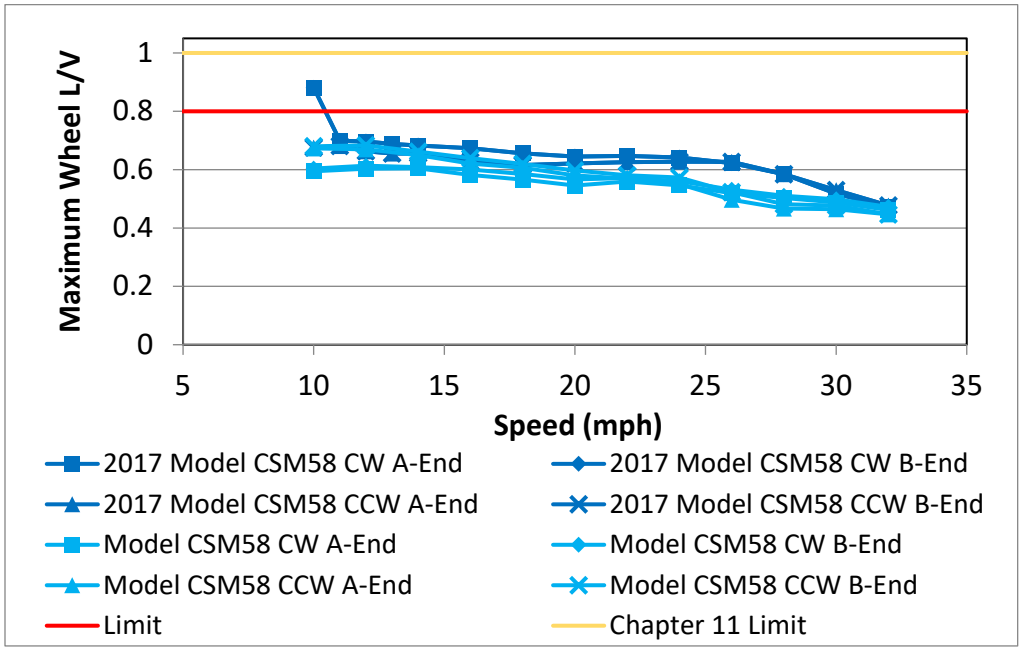

Figure 25. Simulation predictions of maximum wheel L/V ratio in the dynamic curving regime with maximum test load using CSM 70 and CSM 58 pads

7.4.3 Other Various Load Conditions

Table 24 through Table 26 show the worst-case results of simulations of every cask in the dynamic curving regime using the refined model with the different load conditions. The maximum and minimum test load conditions were considered. The simulations for the other casks 16 casks that will be carried on the Atlas car represent those casks in their loaded condition. The maximum wheel L/V

ratio ranged from 0.69 to 0.72, a very narrow window of performance. All simulation predictions for the various load conditions in the dynamic curving regime **met** Standard S-2043 criteria.

Table 24. Dynamic Curving with Various Loads (Part 1 of 3)

Criterion	Limiting Value	Extreme Case		NAC-Intl.			Energy Solutions
		Maximum Test Load	Minimum Test Load	MAGNATRAN	STC	UMS	TS125
Maximum carbody roll angle (degree)	4	0.97	0.97	1.02	1.04	1.04	1.02
Maximum wheel L/V	0.8	0.69	0.71	0.71	0.71	0.71	0.72
Maximum truck side L/V	0.5	0.30	0.35	0.33	0.34	0.34	0.34
Minimum vertical wheel load (%)	25	55.0	52.7	55.5	54.7	54.7	54.6
Peak-to-peak carbody lateral acceleration (g)	1.3	0.12	0.19	0.13	0.15	0.22	0.15
Maximum carbody lateral acceleration (g)	0.75	0.11	0.16	0.13	0.13	0.19	0.15
Maximum carbody vertical acceleration (g)	0.9	0.16	0.12	0.20	0.15	0.16	0.17
Maximum vertical suspension deflection (%)	95	66.8	23.2	46.9	38.0	38.0	40.7

Table 25. Dynamic Curving with Various Loads (Part 2 of 3)

Criterion	Limiting Value	Holtec Intl.		NAC-Intl.		
		HI-STAR-60	HI-STAR-100	HI-STAR-100HB	HI-STAR-180	HI-STAR-190-SL
Maximum carbody roll angle (degree)	4	0.97	1.01	1.02	1.01	0.97
Maximum wheel L/V	0.8	0.71	0.70	0.71	0.70	0.69
Maximum truck side L/V	0.5	0.35	0.32	0.35	0.32	0.31
Minimum vertical wheel load (%)	25	52.2	56.7	53.8	56.7	54.3
Peak-to-peak carbody lateral acceleration (g)	1.3	0.17	0.15	0.16	0.15	0.12
Maximum carbody lateral acceleration (g)	0.75	0.15	0.13	0.13	0.13	0.12
Maximum carbody vertical acceleration (g)	0.9	0.14	0.15	0.12	0.15	0.17
Maximum vertical suspension deflection (%)	95	28.8	44.7	32.6	44.7	61.4

Table 26. Dynamic Curving with Various Loads (Part 3 of 3)

Criterion	Limiting Value	TN Americas LLC						
		AREVA-MP-187	AREVA-MP-197	AREVA-MP197HB	TN-32B	TN-40	TN-40HT	TN-68
Maximum carbody roll angle (degree)	4	1.03	1.04	1.03	1.00	0.99	1.01	1.04
Maximum wheel L/V	0.8	0.70	0.71	0.70	0.70	0.71	0.71	0.72
Maximum truck side L/V	0.5	0.34	0.34	0.33	0.33	0.33	0.34	0.34
Minimum vertical wheel load (%)	25	55.25	54.90	55.63	56.18	55.94	55.80	54.07
Peak-to-peak carbody lateral acceleration (g)	1.3	0.15	0.24	0.20	0.15	0.13	0.14	0.15
Maximum carbody lateral acceleration (g)	0.75	0.14	0.19	0.16	0.14	0.14	0.13	0.14
Maximum carbody vertical acceleration (g)	0.9	0.15	0.15	0.18	0.15	0.15	0.14	0.17
Maximum vertical suspension deflection (%)	95	38.48	36.90	42.38	43.26	44.43	40.41	38.53

7.5 Single Bump Test

Simulations of the single bump regime were conducted according to Standard S-2043, Paragraph 4.3.10.1. The single bump tests were conducted according to Standard S-2043, Paragraph 5.5.13. The single bump test section represents a typical grade crossing with an elevation increase of 1.0 inch over a 7-foot track section, a steady elevation for 20 feet, and then a ramp back down over 7 feet. The simulations and tests were performed at speeds ranging from 30 mph to 75 mph in increments of 5 mph or less.

7.5.1 Minimum Test Load

Table 27 shows the worst-case test results and simulation predictions for the car loaded with the minimum test load in the single bump test regime. Figure 26 shows the test results, the simulation predictions of the minimum vertical wheel load done using CSM 70 primary pads, and simulation predictions done using CSM 58 primary pads plotted against speed to show the trend in performance.

Using CSM 70 primary pads, the model predicts lower minimum vertical wheel loads and higher vertical accelerations than those that were measured in the test, but the overall trend is about the same, as Figure 26 shows. The simulation predictions done using CSM 58 pads were very close to the simulation predictions done using CSM 70 primary pads. Only post-test simulation predictions are shown because the pre-test predictions were for a load case no longer intended for use.

The test results and revised simulation predictions **meet** Standard S-2043 criteria for the single bump test regime with the minimum test load.

Table 27. Single bump test results and simulation predictions with minimum test load

Criterion	Limiting Value	CSM 70 Pads		CSM 58 Pads
		Test Result	Simulation Prediction Revised Model	Simulation Prediction Revised Model
Roll angle (degree)	4.0	0.4	0.2	0.2
Maximum wheel lateral/vertical (L/V)	0.8	0.20	0.10	0.09
Maximum truck side L/V	0.5	0.12	0.07	0.06
Minimum vertical wheel load (%)	25%	66%	59%	61%
Lateral peak-to-peak acceleration (g)	1.3	0.17	0.20	0.18
Maximum lateral acceleration (g)	0.75	0.09	0.10	0.10
Maximum vertical acceleration (g)	0.90	0.37	0.77	0.69
Maximum vertical suspension deflection (%)	95%	18%	36%	34%

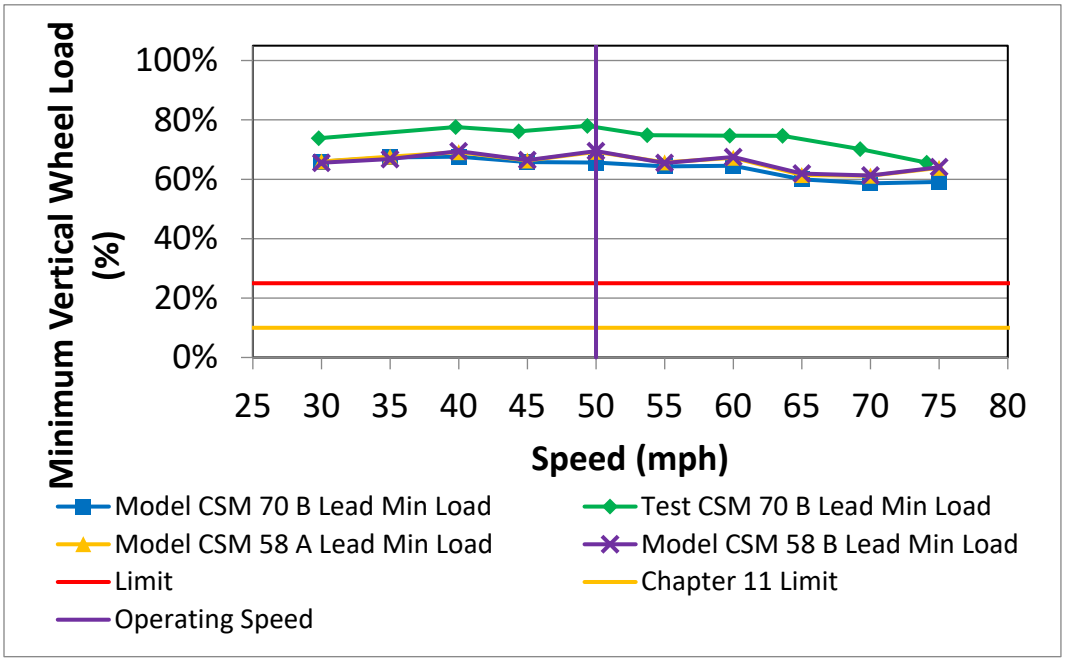

Figure 26. Simulation prediction and test results of minimum vertical wheel load in the single bump regime with minimum test load

7.5.2 Maximum Test Load

Table 28 shows the worst-case test results and simulation predictions for the car loaded with the maximum test load in the single bump test regime. Figure 27 shows test results and simulation predictions of the maximum carbody vertical acceleration done using CSM 70 primary pads plotted against speed to show the trend in performance. Figure 28 shows the original and revised simulation predictions of maximum carbody vertical acceleration done using CSM 58 primary pads.

Using CSM 70 primary pads, the model predicts lower vertical carbody acceleration, 55 mph and below, than what was measured in the test, but, at 60 mph and above, the vertical accelerations match closely, as Figure 27 shows. The simulations done using CSM 58 pads showed a higher carbody vertical acceleration than the simulations done using CSM 70 primary pads. The vertical accelerations predicted by the original model in 2017 were significantly lower than those predicted by the revised model.

The test results and revised simulation predictions **meet** Standard S-2043 criteria for the single bump test regime.

Table 28. Single bump test results and simulation predictions with maximum test load

Criterion	Limiting Value	CSM 70 Pads		CSM 58 Pads	
		Test Result	Simulation Prediction Revised Model	Simulation Prediction Original Model	Simulation Prediction Revised Model
Roll angle (degree)	4.0	0.3	0.3	0.1	0.4
Maximum wheel lateral/vertical (L/V)	0.8	0.13	0.07	0.02	0.06
Maximum truck side L/V	0.5	0.08	0.05	0.02	0.05
Minimum vertical wheel load (%)	25%	71%	67%	71%	69%
Lateral peak-to-peak acceleration (g)	1.3	0.17	0.15	0.05	0.14
Maximum lateral acceleration (g)	0.75	0.09	0.09	0.03	0.09
Maximum vertical acceleration (g)	0.90	0.37	0.39	0.22	0.55
Maximum vertical suspension deflection (%)	95%	52%	62%	72%	62%

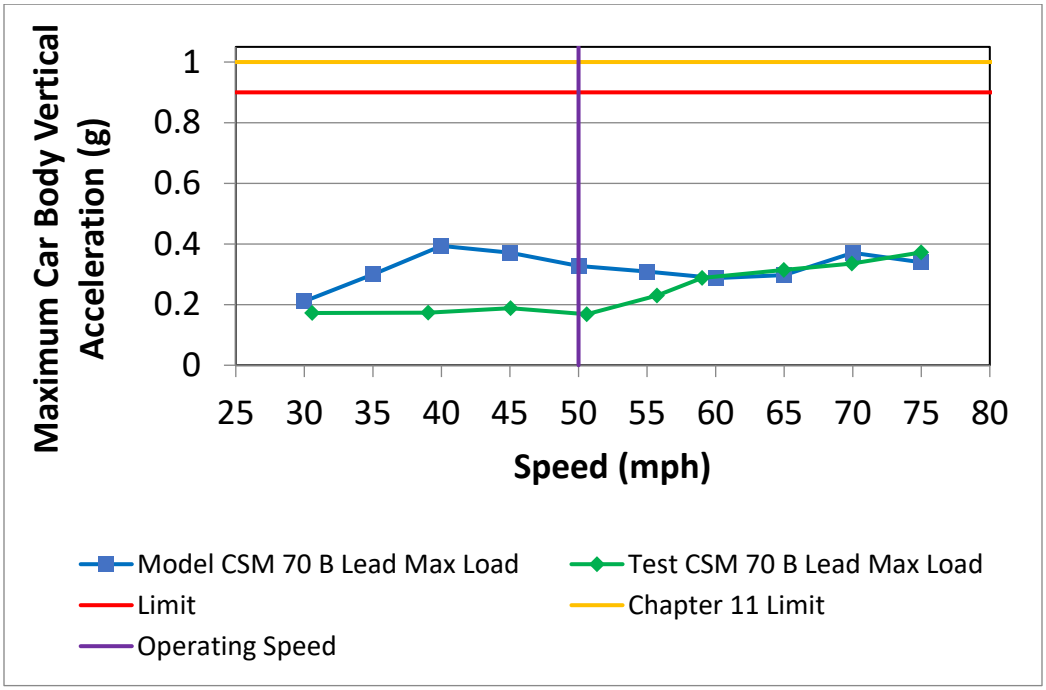

Figure 27. Simulation prediction and test results of maximum vertical carbody acceleration in the single bump test regime with maximum test load using CSM 70 pads

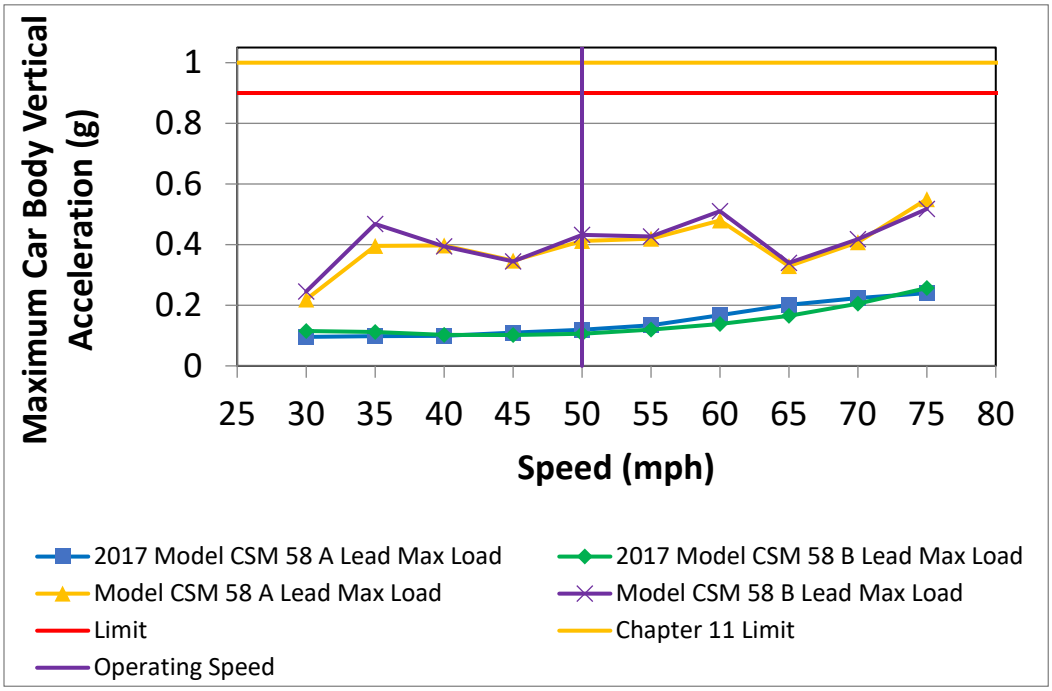

Figure 28. Original (2017) and revised simulation predictions of maximum vertical carbody acceleration in the single bump test regime with maximum test load using CSM 58 pads

7.6 Curving with Single Rail Perturbation

Simulations of the curving with a single-rail perturbation regime were conducted according to Standard S-2043, Paragraph 4.3.10.2. The tests of the curving with single rail perturbation regime were conducted according to Standard S-2043, Paragraph 5.5.15. Simulations were made for 1-, 2-, and 3-inch outside rail dips and 1-, 2-, and 3-inch inside rail bumps in a 12-degree curve with zero superelevation. The inside rail bump was a flat-topped ramp with an elevation change over 6 track feet, a steady elevation over 12 track feet, and then a ramp back down over 6 track feet. The outside rail dip was the reverse.

The tests were performed with 2-inch amplitude perturbations. Simulations were performed using measured track geometry from the test zone for comparison with the test results. Measured inputs were not available for the other bump and dip amplitudes so ideal track inputs were used. The outside rail dip predictions and the test results are presented here because the dip section was the most severe condition for both the simulations and the tests. TTCI used 50-millisecond windows when processing wheel force statistics.

7.6.1 Minimum Test Load

Table 29 shows the worst-case test results and simulation predictions for the car loaded with the minimum test load in the curve with single rail perturbation, 2-inch dip regime. The simulation predictions shown in Table 29 used measured track geometry as input. Figure 29 shows the test results and the simulation predictions of the maximum wheel L/V ratio with CSM 70 primary pads plotted against speed to show the trend in performance. Figure 30 shows the simulations predictions

of the maximum wheel L/V ratio with CSM 70 and CSM 58 primary pads plotted together to show the trend and the difference in performance between the two pads.

Using CSM 70 primary pads, the model predicts higher maximum wheel L/V ratios and higher truck side L/V ratios than those that were measured in the test. The simulation predictions of the wheel L/V ratios were all at a similar level regardless of the simulation direction or speed, whereas the test results were much more variable.

The simulations done using CSM 58 pads predicted lower wheel L/V ratios and lower truck side L/V ratios than the ratios that were predicted using CSM 70 pads. Only post-test simulation predictions are shown because the pre-test predictions were for a load case no longer intended for use.

Table 29. Curving with 2-inch rail dip test results and simulation predictions using measured track inputs with minimum test load

Criterion	Limiting Value	CSM 70		CSM 58
		Test Result	Simulation Prediction Revised Model	Simulation Prediction Revised Model
Roll angle (degree)	4.0	0.8	1.6	1.6
Maximum wheel L/V	0.8	0.88	1.01	0.80
Maximum truck side L/V	0.5	0.50	0.54	0.39
Minimum vertical wheel load (%)	25%	39%	47%	49%
Lateral peak-to-peak acceleration (g)	1.3	0.23	0.14	0.19
Maximum lateral acceleration (g)	0.75	0.17	0.09	0.13
Maximum vertical acceleration (g)	0.90	0.28	0.09	0.09
Maximum vertical suspension deflection (%)	95%	21%	28%	27%

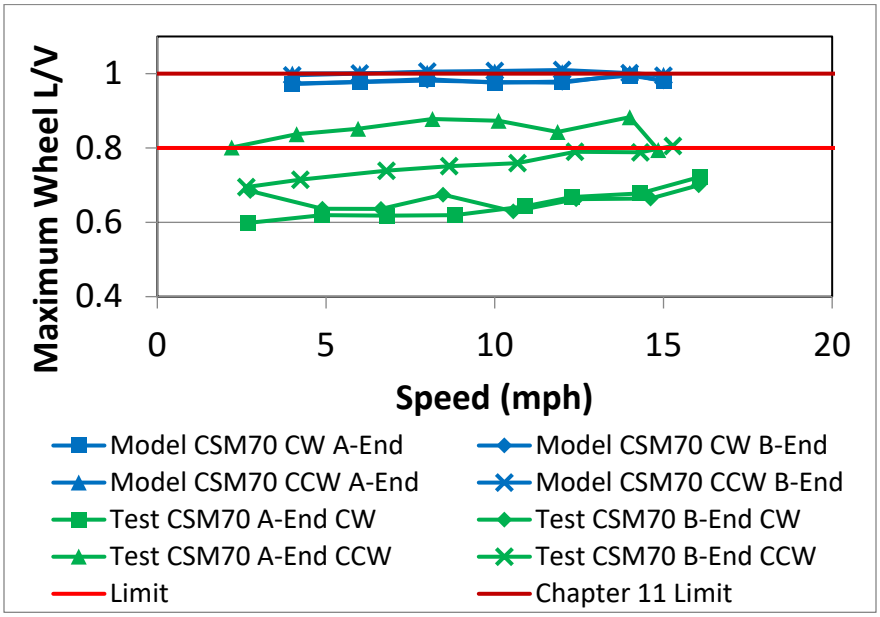

Figure 29. Simulation predictions and test results using CSM 70 primary pads of maximum wheel L/V ratio in the curve with single dip regime with minimum test load

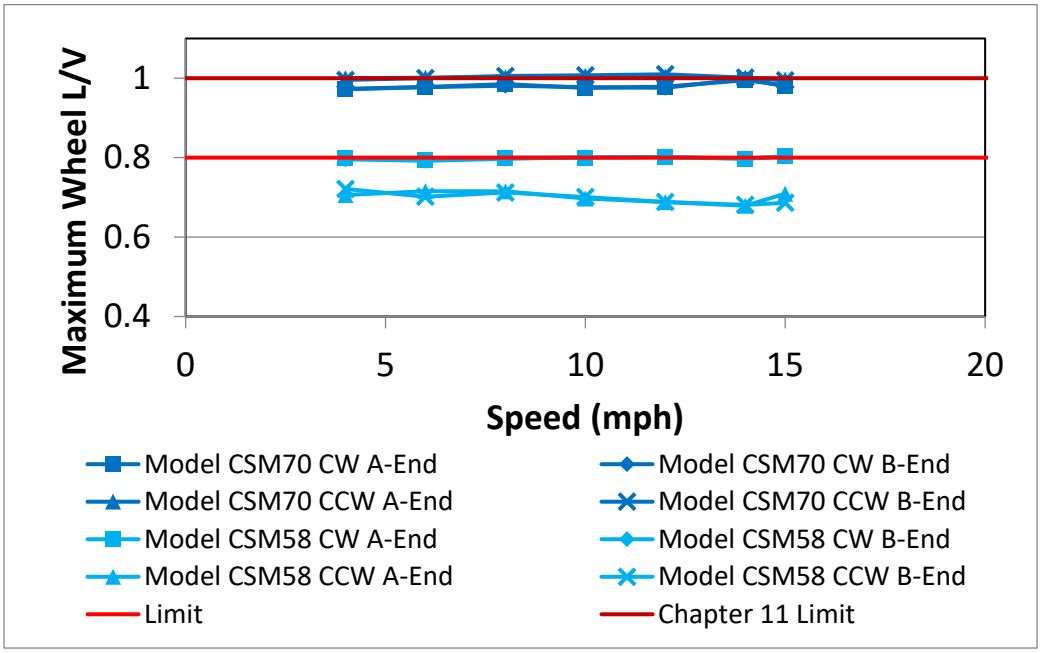

Figure 30. Simulation predictions using CSM 70 and CSM 58 primary pads of maximum wheel L/V ratio in the curve with single dip regime with minimum test load

Table 30 shows the worst-case simulation predictions for the car loaded with the minimum test load in the curve with a single rail perturbation regime with 1-, 2-, and 3-inch bumps using CSM 58 pads. Table 31 shows the worst-case simulation predictions for the car loaded with the minimum test load in the curve with a single rail perturbation regime with 1-, 2-, and 3-inch dips. The simulation predictions shown in Table 30 and Table 31 used ideal track geometry as input.

Table 30. Simulation prediction for curve with single rail perturbation bump section at varying amplitudes with minimum test load

Criterion	Limiting Value	Simulation Predictions Revised Model CSM 58 Pads		
		1-inch	2-inch	3-inch
Roll angle (degree)	4.0	0.4	1.6	4.2
Maximum wheel L/V	0.8	0.49	0.58	0.68
Maximum truck side L/V	0.5	0.27	0.30	0.32
Minimum vertical wheel load (%)	25%	60%	51%	39%
Lateral peak-to-peak acceleration (g)	1.3	0.07	0.16	0.26
Maximum lateral acceleration (g)	0.75	0.04	0.08	0.14
Maximum vertical acceleration (g)	0.90	0.07	0.09	0.14
Maximum vertical suspension deflection (%)	95%	22%	30%	43%

Table 31. Simulation prediction for curve with single rail perturbation dip section at varying amplitudes with minimum test load

Criterion	Limiting Value	Simulation Predictions Revised Model CSM 58 Pads		
		1-inch	2-inch	3-inch
Roll angle (degree)	4.0	0.4	1.1	3.1
Maximum wheel L/V	0.8	0.52	0.63	0.80
Maximum truck side L/V	0.5	0.30	0.33	0.38
Minimum vertical wheel load (%)	25%	53%	44%	36%
Lateral peak-to-peak acceleration (g)	1.3	0.07	0.14	0.23
Maximum lateral acceleration (g)	0.75	0.03	0.06	0.13
Maximum vertical acceleration (g)	0.90	0.06	0.08	0.11
Maximum vertical suspension deflection (%)	95%	21%	28%	34%

The test results and simulation predictions did not meet Standard S-2043 criteria for the maximum wheel L/V ratio or maximum truck side L/V ratio with CSM 70 pads for the curve with a single rail perturbation 2-inch dip regime with minimum test load, but all other criteria were met. The revised simulation predictions done using CSM 58 pads **met** Standard S-2043 criteria for the curve with a single rail perturbation 2-inch dip regime (measured) with minimum test load. The maximum wheel L/V ratio **met (did not exceed)** the limit of 0.8.

Simulation predictions of ideal track input with 1-, 2-, and 3-inch bumps and dips did not meet Standard S-2043 criteria for the maximum peak-to-peak roll angle in the 3-inch bump simulations. By itself, the 3-inch bump and dip regimes roll the track about 3 degrees, so very little suspension deflection is allowed within the 4-degree peak-to-peak Standard S-2043 limit. Therefore, on behalf of the DOE, TTCI is requesting an exception from the AAR EEC. All other criteria were met, although the maximum wheel L/V ratio was at the limit of 0.8 in the 3-inch dip simulations.

7.6.2 Maximum Test Load

Table 32 shows the worst-case test results and simulation predictions for the car loaded with the maximum test load in the curve with a single rail perturbation, 2-inch dip regime. The simulation predictions shown in Table 32 used measured track geometry as input. Figure 31 shows test results and simulation predictions of the maximum wheel L/V ratio using CSM 70 primary pads and simulation results using CSM 58 primary pads plotted against speed to show the trend in performance.

Using CSM 70 primary pads, the model predicts higher maximum wheel L/V ratios and higher truck side L/V ratios than those that were measured in the test. The simulation predictions of wheel L/V ratios were all at a similar level regardless of the simulation direction or speed, whereas the test results were much more variable.

The simulations done using CSM 58 pads predicted lower wheel L/V ratios and lower truck side L/V ratios than those that were predicted with CSM 70 pads. Only the post-test simulation predictions are shown because the pre-test predictions were not made using a measured track input.

The simulation predictions done using CSM 70 pads did not meet Standard S-2043 criteria for the maximum wheel L/V ratio for the curve with a single rail perturbation 2-inch dip regime with a maximum test load, but all other criteria were met. The results from testing done using CSM 70 pads and revised simulation predictions done using CSM 58 pads **met** Standard S-2043 criteria for the curve with a single rail perturbation, 2-inch dip regime with maximum test load.

Table 32. Curving with 2-inch rail dip test results and simulation predictions using measured track inputs with maximum test load

Criterion	Limiting Value	CSM 70 Pads		CSM 58 Pads
		Test Result	Simulation Prediction Revised Model	Simulation Prediction Revised Model
Roll angle (degree)	4.0	1.6	2.2	2.2
Maximum wheel lateral/vertical (L/V)	0.8	0.79	0.90	0.52
Maximum truck side L/V	0.5	0.44	0.45	0.31
Minimum vertical wheel load (%)	25%	45%	49%	51%
Lateral peak-to-peak acceleration (g)	1.3	0.16	0.18	0.19
Maximum lateral acceleration (g)	0.75	0.14	0.12	0.12
Maximum vertical acceleration (g)	0.90	0.15	0.09	0.09
Maximum vertical suspension deflection (%)	95%	81%	74%	73%

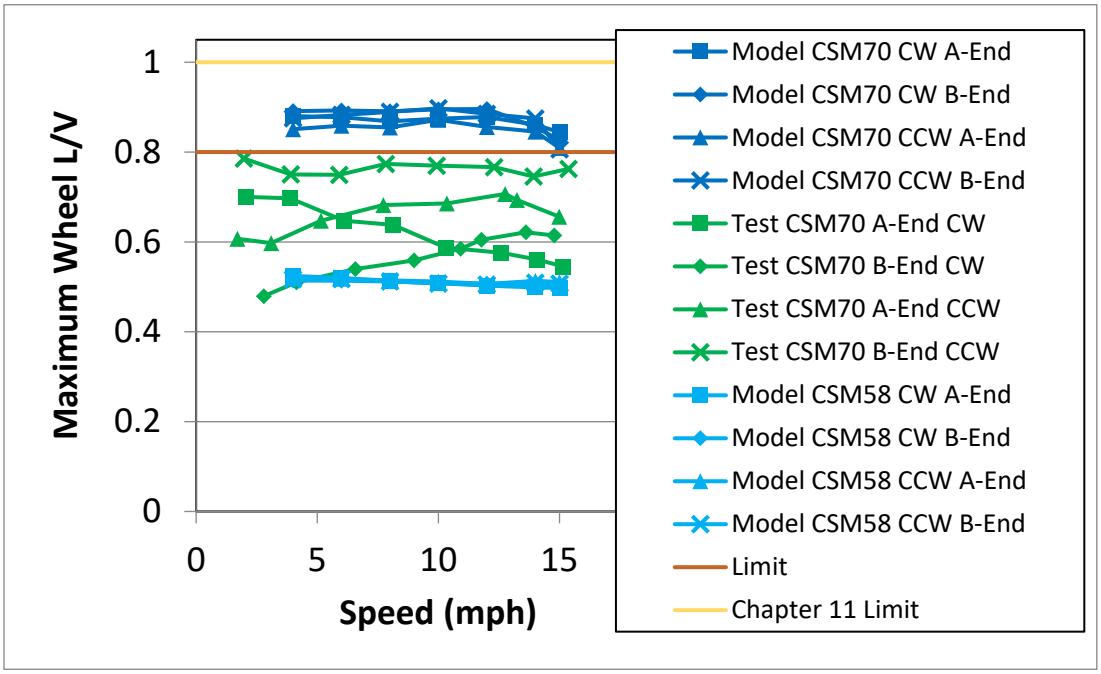

Figure 31. Simulation prediction and test results of maximum wheel L/V ratio in the curving with single rail perturbation dip regime with maximum test load using CSM 70 and CSM 58 pads

Table 33 shows the worst-case simulation predictions for the car loaded with the maximum test load in the curve with single rail perturbation regime with 1-, 2-, and 3-inch bumps. Table 34 shows the worst-case simulation predictions for the car loaded with the maximum test load in the curve with single rail perturbation regime with 1-, 2-, and 3-inch dips. The simulation predictions shown in Table 33 and Table 34 used CSM 58 pads and ideal track geometry as input. The simulation predictions over the 3-inch bump and the 3-inch dip did not meet the maximum peak-to-peak roll angle criteria. All other criteria were met.

The wheel L/V ratios predicted with the revised model were more than 45 percent lower than those predicted with the original model. The difference between wheel L/V ratio predictions is likely because the primary pad stiffness measured in the characterization test was much lower than the value used in the original model. The original and revised predictions for other metrics were closer.

Table 33. Simulation prediction for curve with single rail perturbation bump section at varying amplitudes with maximum test load

Criterion	Limiting Value	Simulation Predictions Revised Model CSM 58 Pads					
		1-inch		2-inch		3-inch	
		Original	Revised	Original	Revised	Original	Revised
Roll angle (degree)	4.0	0.5	0.4	3.0	2.8	5.0	4.7
Maximum wheel L/V	0.8	0.53	0.25	0.59	0.30	0.64	0.33
Maximum truck side L/V	0.5	0.29	0.19	0.33	0.19	0.33	0.23
Minimum vertical wheel load (%)	25%	58	60	53	52	38	40
Lateral peak-to-peak acceleration (g)	1.3	0.05	0.07	0.14	0.12	0.21	0.18
Maximum lateral acceleration (g)	0.75	0.05	0.03	0.08	0.06	0.12	0.11
Maximum vertical acceleration (g)	0.90	0.04	0.07	0.08	0.12	0.07	0.13
Maximum vertical suspension deflection (%)	95%	77	63	86	79	94	92

Table 34. Simulation prediction for curve with single rail perturbation dip section at varying amplitudes with maximum test load

Criterion	Limiting Value	Simulation Predictions Revised Model CSM 58 Pads					
		1-inch		2-inch		3-inch	
		Original	Revised	Original	Revised	Original	Revised
Roll angle (degree)	4.0	0.5	0.5	2.6	2.6	4.5	4.5
Maximum wheel L/V	0.8	0.57	0.28	0.68	0.36	0.79	0.43
Maximum truck side L/V	0.5	0.32	0.20	0.35	0.19	0.38	0.24
Minimum vertical wheel load (%)	25%	64	61	56	49	44	40
Lateral peak-to-peak acceleration (g)	1.3	0.06	0.07	0.11	0.12	0.19	0.19
Maximum lateral acceleration (g)	0.75	0.05	0.03	0.07	0.07	0.10	0.11
Maximum vertical acceleration (g)	0.90	0.04	0.06	0.07	0.10	0.06	0.13
Maximum vertical suspension deflection (%)	95%	73	63	82	75	88	89

7.7 Hunting

Simulations of the hunting regime were conducted according to Standard S-2043, Paragraph 4.3.11.3.1. The hunting tests were conducted according to Standard S-2043, Paragraph 5.5.7. The simulations used inputs from the measured track geometry of the test site, a 5,500-foot section of tangent track on the TTC Railroad Test Track (RTT).

7.7.1 Minimum Test Load

Table 35 shows the worst-case test results and simulation predictions for the car loaded with the minimum test load in the hunting test regime. Figure 32 shows the test results and simulation predictions of the standard deviation of carbody lateral acceleration over 2,000 feet using CSM 70 primary pads plotted against speed to show the trend in performance. Figure 33 shows the test results and simulation predictions of the standard deviation of carbody lateral acceleration over 2,000 feet with CSM 58 primary pads.

Using CSM 70 primary pads, the model predicts higher lateral accelerations than those that were measured in the test, but the overall trend matches closely, as shown in Figure 32. The simulations done using CSM 58 pads predicted higher lateral accelerations at speeds of 65 mph and below, but lower lateral accelerations above 65 mph. Only post-test simulation predictions are shown because the pre-test predictions were for a load case no longer intended for use.

The test results and simulation predictions done using CSM 70 pads met Standard S-2043 criteria. The test results and revised simulation predictions done using CSM 58 pads **did not meet** the Standard S-2043 carbody lateral acceleration standard deviation criteria at speeds above 65 mph, but all other criteria were met.

Table 35. Hunting test results and simulation predictions with minimum test load

Criterion	Limiting Value	CSM 70 Pads		CSM 58 Pads	
		Test Result	Simulation Prediction Revised Model	Test Result	Simulation Prediction Revised Model
Roll angle (degree)	4.0	0.5	0.2	0.7	0.2
Maximum wheel lateral/vertical (L/V)	0.8	Not Measured*	0.14	Not Measured*	0.24
Maximum truck side L/V	0.5	Not Measured*	0.09	Not Measured*	0.15
Minimum vertical wheel load (%)	25%	Not Measured*	71%	Not Measured*	69%
Lateral peak-to-peak acceleration (g)	1.3	0.17	0.35	0.80	0.57
Maximum lateral acceleration (g)	0.75	0.10	0.19	0.43	0.31
Lateral Carbody Acceleration Standard Deviation (g)	0.13	0.03	0.05	0.22	0.14
Maximum vertical acceleration (g)	0.90	0.27	0.18	0.28	0.32
Maximum vertical suspension deflection (%)	95%	7%	17%	10%	16%

* L/V and vertical wheel load data is not available for high-speed stability tests with KR wheels (IWS required to obtain those measurements).

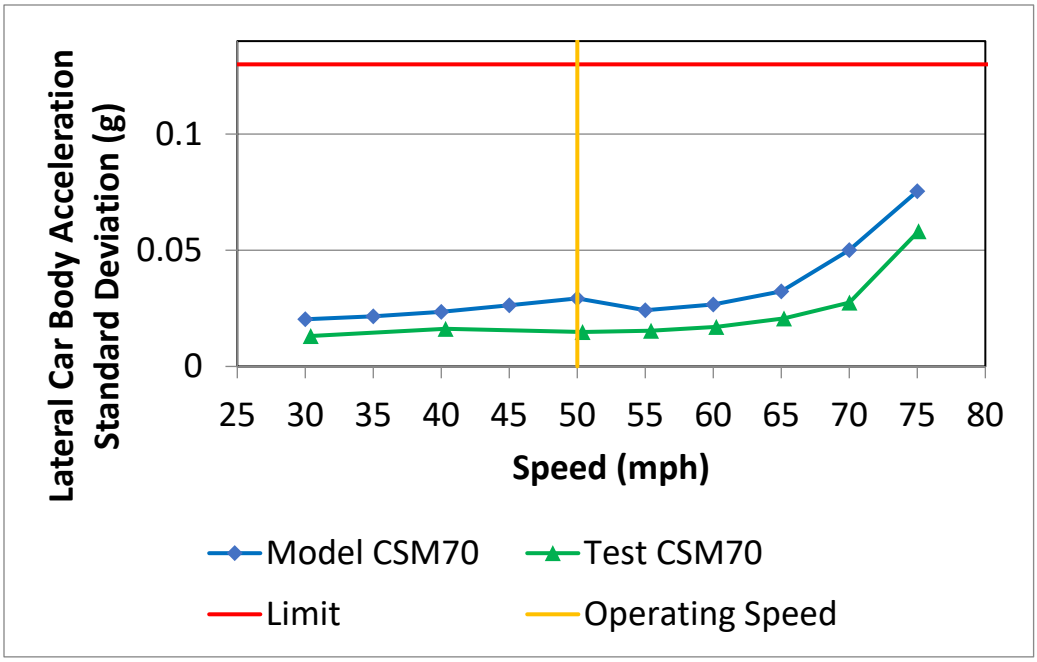

Figure 32. Simulation prediction and test results of the standard deviation of carbody lateral acceleration over 2,000 feet with minimum test load using CSM 70 pads and KR profile wheels

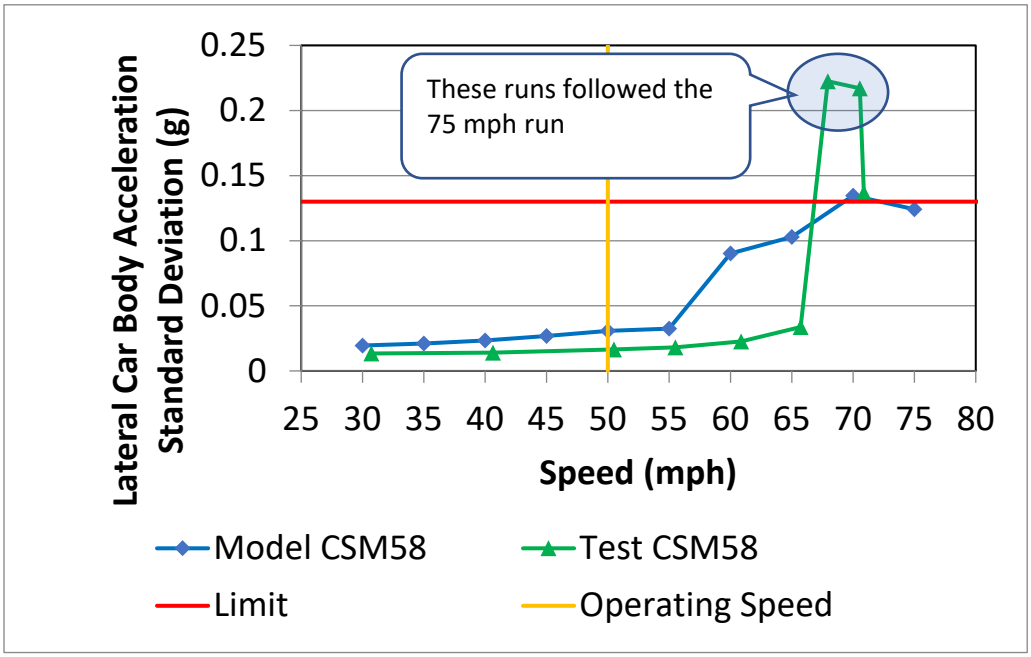

Figure 33. Simulation prediction and test results of the standard deviation of carbody lateral acceleration over 2,000 feet with minimum test load using CSM 58 pads and KR profile wheels

7.7.2 Maximum Test Load

Table 36 shows the worst-case test results and simulation predictions for the car loaded with the maximum test load in the hunting test regime. Figure 34 shows the test results and simulation predictions for the standard deviation of carbody lateral acceleration over 2,000 feet using CSM 70 primary pads plotted against speed to show the trend in performance. Figure 35 shows the test results and simulation predictions of the standard deviation of carbody lateral acceleration over 2,000 feet using CSM 58 primary pads. Using either CSM 70 or CSM 58 primary pads, the model predicts higher lateral accelerations than those that were measured in the test at speeds below 70 mph, and it predicts lower lateral accelerations at speeds above 70 mph, as shown in Figure 34 and Figure 35.

The pre-test (2017) simulations done using CSM 58 primary pads do not match test data as well as the revised model, except at 75 mph. The pre-test simulations show wheel loads much lower than what was predicted in the revised simulations. This difference between the simulations and the predictions is because the data analysis for the pre-test simulation included data from the curve spirals (entry and exit) and a significant portion of the curve at each end of the tangent test zone. By contrast, data from the revised simulations was only processed data in the tangent track portion consistent with the requirements of Standard S-2043. More details on the pre-test simulations are available in Walker and Trevithick [2].

Test results and revised simulation predictions done using both CSM 70 and CSM 58 pads **met** Standard S-2043 criteria for hunting with maximum test load.

Table 36. Hunting test results and simulation predictions with maximum test load

Criterion	Limiting Value	CSM 70 Pads		CSM 58 Pads		
		Test Result	Simulation Prediction Revised Model	Test Result	Simulation Prediction Original Model	Simulation Prediction Revised Model
Roll angle (degree)	4.0	0.6	0.3	0.6	3.7	0.3
Maximum wheel lateral/vertical (L/V)	0.8	Not Measured*	0.09	Not Measured*	0.20	0.09
Maximum truck side L/V	0.5	Not Measured*	0.08	Not Measured*	0.17	0.08
Minimum vertical wheel load (%)	25%	Not Measured*	81%	Not Measured*	25%	81%
Lateral peak-to-peak acceleration (g)	1.3	0.18	0.21	0.34	0.37	0.33
Maximum lateral acceleration (g)	0.75	0.09	0.13	0.24	0.25	0.18
Lateral Carbody Acceleration Standard Deviation (g)	0.13	0.03	0.03	0.04	0.09	0.07
Maximum vertical acceleration (g)	0.90	0.18	0.30	0.25	0.13	0.34
Maximum vertical suspension deflection (%)	95%	47%	53%	63%	86%	87%

* L/V and vertical wheel load data is not available for high-speed stability tests with KR wheels (IWS required).

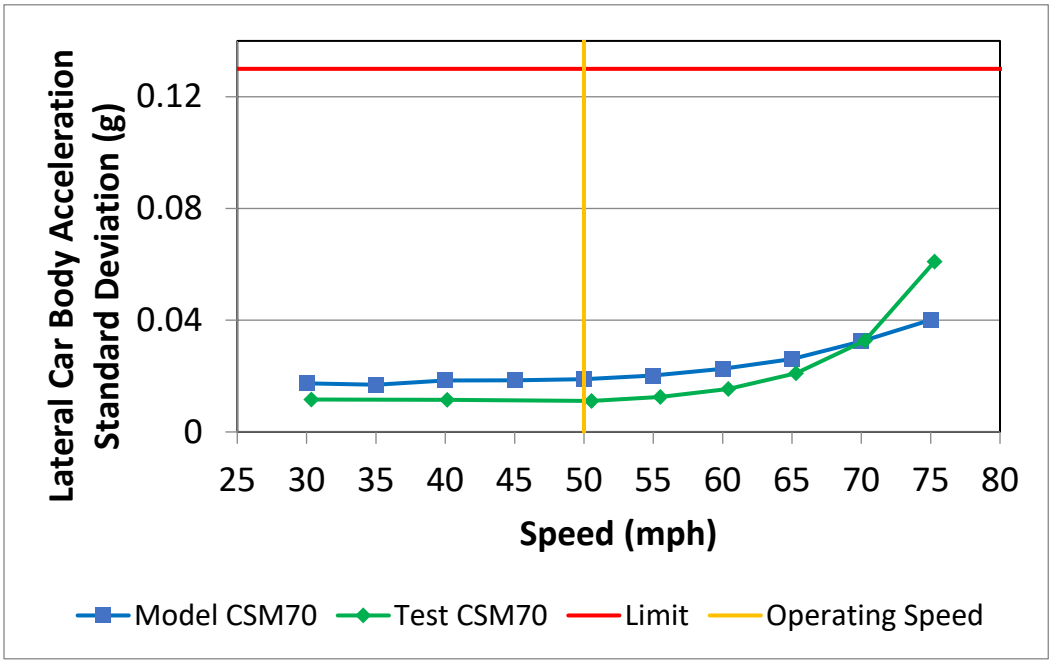

Figure 34. Simulation prediction and test results of maximum wheel L/V ratio in the dynamic curving regime with maximum test load using CSM 70 pads

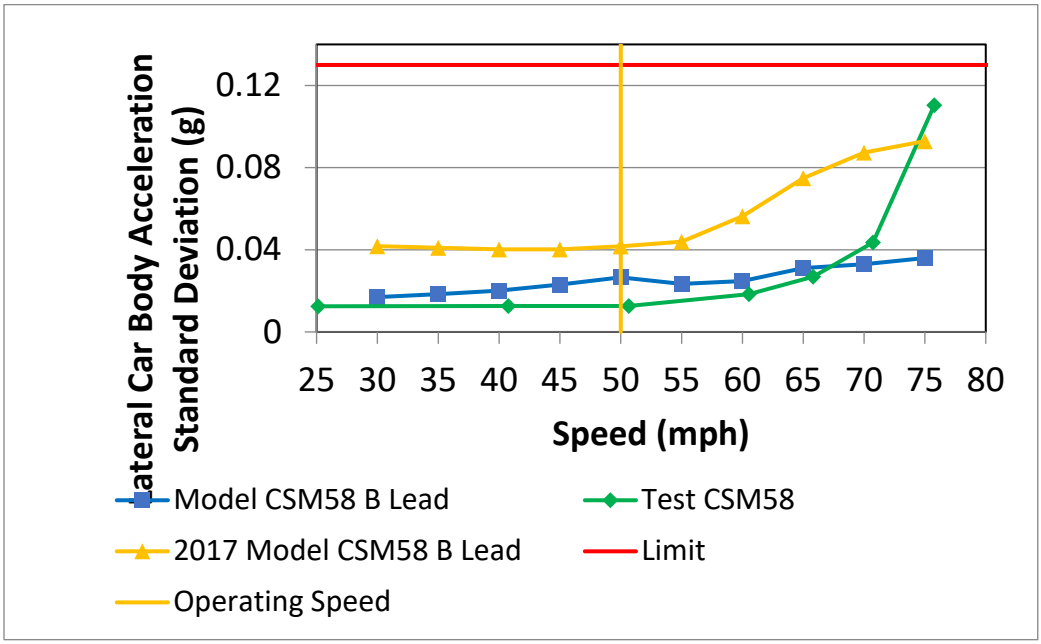

Figure 35. Simulation predictions of maximum wheel L/V ratio in the dynamic curving regime with maximum test load using CSM 70 and CSM 58 pads

7.8 Constant Curving

Simulations of the constant curving regime were conducted according to Standard S-2043, Paragraph 4.3.11.4. The constant curving tests were conducted according to Standard S-2043, Paragraph 5.5.16.

The constant curving regime was modeled using measured track geometry from the 7.5-, 10-, and 12-degree curves of the Wheel-Rail Mechanisms (WRM) loop at the TTC.

Simulation predictions presented for constant curving include the 95th percentile wheel L/V ratio for the steady curve portion of the inputs. This criterion is not listed in Table 4.1 of the Standard S-2043 design paragraph but is listed in Table 5.1 of the Standard S-2043 single car test paragraph. The 95th percentile wheel L/V ratio is relevant to these simulations because the simulations are performed with measured track geometry inputs rather than ideal track geometry.

7.8.1 Minimum Test Load

Table 37 shows the worst-case test results and simulation predictions for the car loaded with the minimum test load in the constant curving test regime. Figure 36 shows the test results and simulation predictions of the maximum wheel L/V ratio plotted against speed to show the trend in performance. The test results are shown for CSM 70 pads and simulation results are shown for both CSM 70 and CSM 58 pads.

Using CSM 70 primary pads, the model predicts lower maximum wheel L/V ratios than those that were measured in the test, but the overall trend matches, and the magnitude was in the same range as the test data, as Figure 36 shows. The simulations done using CSM 58 pads predicted lower wheel L/V ratios than simulations done using CSM 70 pads. Only post-test simulation predictions are shown because the pre-test predictions were for a load case no longer intended for use.

The test results did not meet the criteria for the maximum wheel L/V ratio or the 95th percentile wheel L/V ratio using CSM 70 pads. The final choice of CSM 58 pads over CSM 70 pads was made to improve curving performance. The simulation predictions using both CSM 70 and CSM 58 pads with the revised model **met** Standard S-2043 criteria, although the 95th percentile wheel L/V ratio was at the limit of 0.6 for CSM 70 pads.

Table 37. Constant curving test results and simulation predictions with minimum test load

Criterion	Limiting Value	CSM 70		CSM 58
		Test Result	Simulation Prediction Revised Model	Simulation Prediction Revised Model
Roll angle (degree)	4.0	0.3	0.76	0.77
Maximum wheel L/V	0.8	0.86	0.68	0.52
95% Wheel L/V	0.6	0.66	0.60	0.47
Maximum truck side L/V	0.5	0.47	0.36	0.34
Minimum vertical wheel load (%)	25	54	52.5	52.7
Lateral peak-to-peak acceleration (g)	1.3	0.19	0.23	0.15
Maximum lateral acceleration (g)	0.75	0.17	0.17	0.14
Maximum vertical acceleration (g)	0.90	0.12	0.16	0.15
Maximum vertical suspension deflection (%)	95	18	25.5	25.1

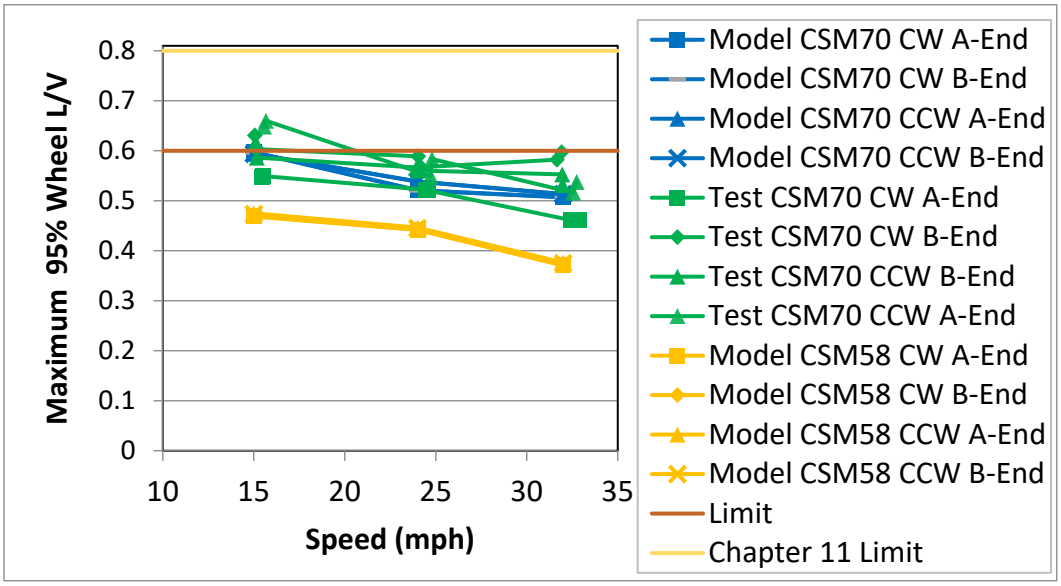

Figure 36. Test Results and Simulation Predictions of the 95 Percentile Wheel L/V Ratio in the 12-degree Constant Curve with CSM 70 and CSM 58 Primary Pads for Minimum Test Load

7.8.2 Maximum Test Load

Table 38 shows the worst-case test results and simulation predictions for the car loaded with the maximum test load in the constant curving test regime. Figure 37 shows the test results and simulation predictions for the maximum wheel L/V ratio plotted against speed to show the trend in performance. The results are shown tests done using CSM 70 pads, and the results are shown for simulations done with both CSM 70 and CSM 58 pads.

Using CSM 70 primary pads, the model predicts lower maximum wheel L/V ratios than were measured in the test, but the overall trend matches, and the magnitude was in the same range as the test data, as Figure 37 shows. The simulations done using CSM 58 pads predicted lower wheel L/V ratios than simulations done with CSM 70 pads. Only post-test simulation predictions are shown because the pre-test predictions were for a load case no longer intended for use.

The test results did not meet the criteria for the maximum wheel L/V ratio or the 95th percentile wheel L/V ratio with CSM 70 pads. The simulation predictions done using both CSM 70 and CSM 58 pads with the revised model **met** Standard S-2043 criteria.

Table 38. Constant curving test results and simulation predictions with maximum test load

Criterion	Limiting Value	CSM 70		CSM 58	
		Test Result	Simulation Prediction Revised Model	Simulation Prediction Original Model	Simulation Prediction Revised Model
Roll angle (degree)	4.0	0.5	0.95	1.7	0.97
Maximum wheel L/V	0.8	0.73	0.65	0.64	0.41
95% Wheel L/V	0.6	0.63	0.57	0.54	0.35
Maximum truck side L/V	0.5	0.38	0.34	0.36	0.28
Minimum vertical wheel load (%)	25	50	56.3	56	55.4
Lateral peak-to-peak acceleration (g)	1.3	0.17	0.15	0.19	0.15
Maximum lateral acceleration (g)	0.75	0.17	0.13	0.16	0.13
Maximum vertical acceleration (g)	0.90	0.09	0.16	0.12	0.15
Maximum vertical suspension deflection (%)	95	50	69.4	76	69.0

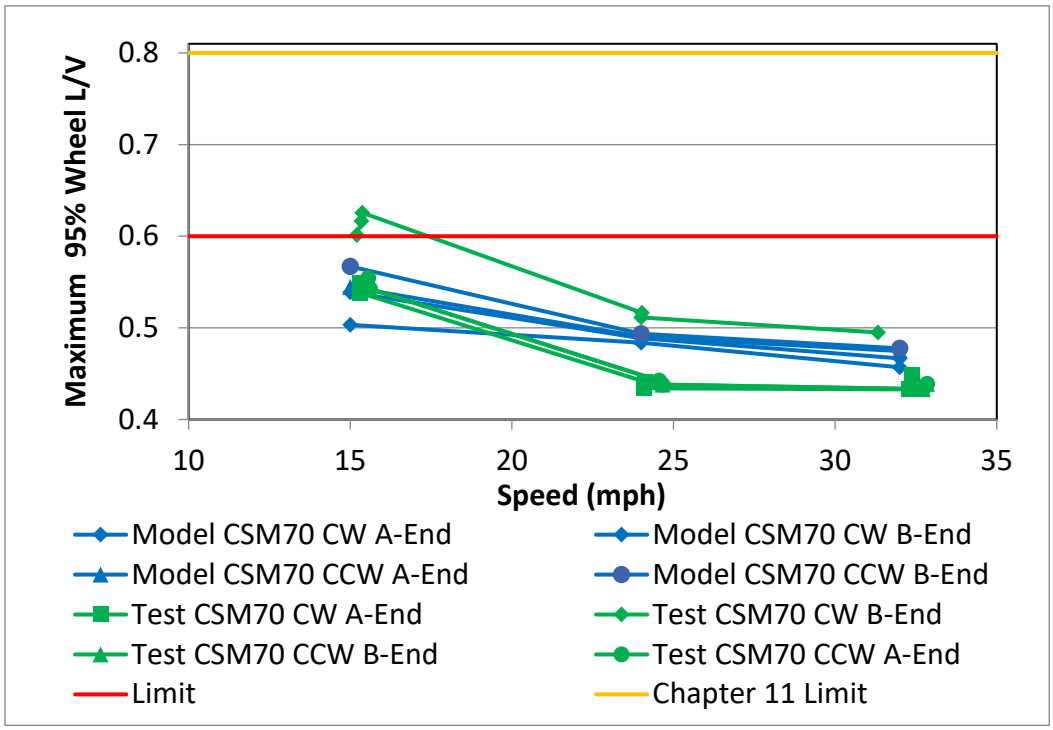

Figure 37. Test Results and Simulation Predictions of the 95 Percentile Wheel L/V Ratio in the 12-degree Constant Curve with CSM 70 Primary Pads for Maximum Test Load

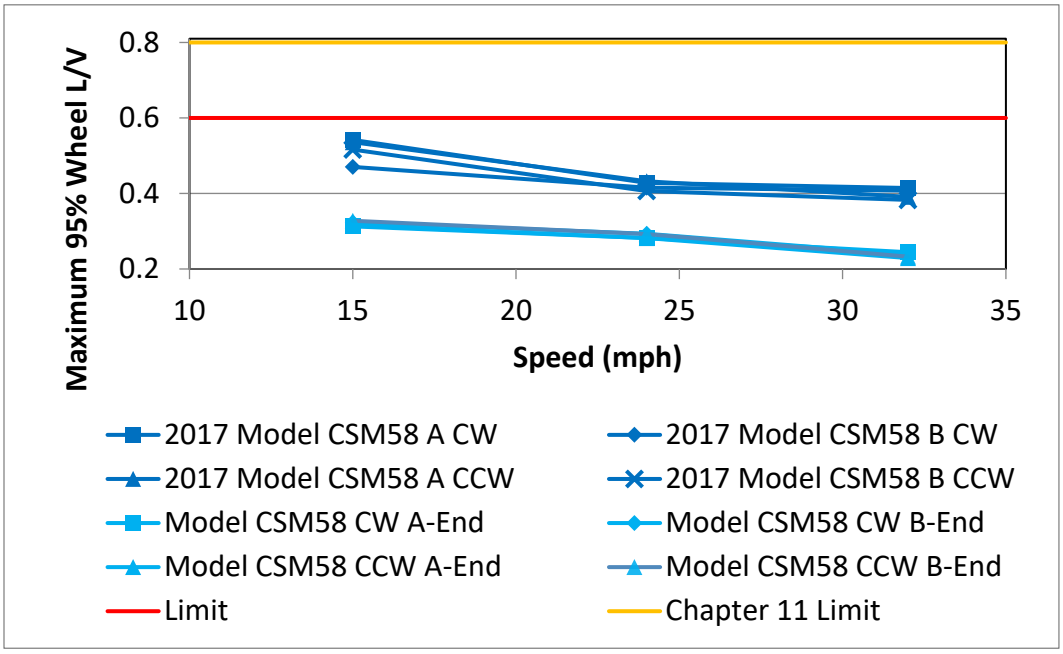

Figure 38. Original (20170 and Revised Simulation Predictions of the 95 Percentile Wheel L/V Ratio in the 12-degree Constant Curve with CSM 58 Primary Pads for Maximum Test Load

7.9 Curving with Various Lubrication Conditions

The simulations of curving with various lubrication conditions were performed according to Standard S-2043, Paragraph 4.3.11.5. The constant curving simulations were repeated in a 10-degree curve with the coefficient of friction conditions shown in Table 39. The simulations were performed using both a new wheel profile on a new rail profile and a hollow-worn wheel profile on a worn rail profile. Figure 39 shows the worn wheel and rail profiles used for the simulations. In this plot, the right side is the high rail (outside rail). The gap between the rail profile (in red) and the wheel profile (in blue) on the gage corner of the rail represents a two-point contact condition. The lubrication and profile conditions are designed to test the performance when the wheelset cannot provide normal steering forces due to the wear.

Table 39. Wheel/rail Coefficients of Friction for the Curving with Various Lubrication Conditions Regime

Friction Coefficient	High Rail Crown	High Rail Gage Face	Low Rail Crown
Case 1	0.5	0.5	0.5
Case 2	0.5	0.2	0.5
Case 3	0.5	0.2	0.2
Case 4	0.2	0.2	0.5

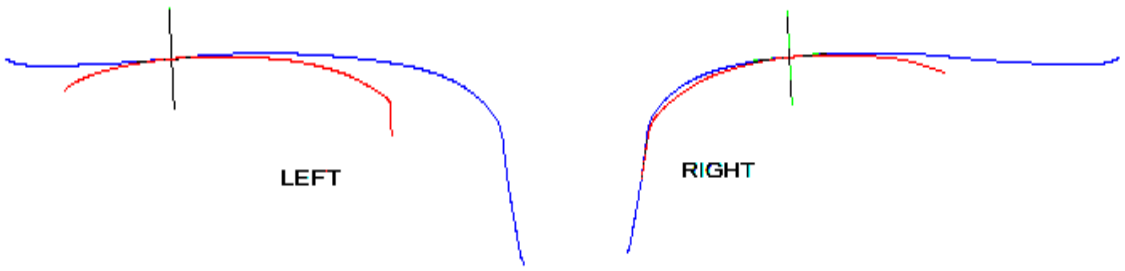

Figure 39. Worn Wheel Profiles on the Ground Rail Profiles
(The Wheelset is Shifted to the High Rail in the Position it Would be in a Left-Hand Curve)

7.9.1 Minimum Test Load

(1) New Profiles

Table 40 shows the simulation predictions for the four friction cases with the new wheel profiles at the minimum test load. The simulations of Cases 1, 2, and 3 meet Standard S-2043 criteria. Although it does meet the corresponding AAR Chapter 11 criterion, the Case 4 simulation does **not meet** the Standard S-2043 Paragraph 5 criterion for 95th percentile wheel L/V ratios. The AAR Chapter 11 criterion is 0.8 for 95th percentile single wheel L/V ratio.

Table 40. Simulation Results for Curving with Rail Lubrication Cases 1-4 and New Wheels and Rails, with Minimum Test Load

Criterion	Limiting Value	Case 1 New	Case 2 New	Case 3 New	Case 4 New
Maximum carbody roll angle (degree)	4.0	0.68	0.67	0.67	0.65
Maximum wheel L/V	0.80	0.63	0.66	0.39	0.72
Maximum truck side L/V	0.50	0.36	0.36	0.25	0.43
Minimum vertical wheel load (%)	25	52	52	52	53
Peak-to-peak carbody lateral acceleration (g)	1.30	0.23	0.23	0.28	0.25
Maximum carbody lateral acceleration (g)	0.75	0.17	0.17	0.20	0.19
Lateral carbody acceleration standard deviation (g)	0.13	0.03	0.03	0.04	0.04
Maximum carbody vertical acceleration (g)	0.90	0.15	0.15	0.14	0.14
Maximum vertical suspension deflection (%)	95	22	22	22	22
95% Wheel L/V Ratio	0.60	0.48	0.50	0.33	0.62

(2) Worn Profiles

Table 41 shows simulation predictions for the four friction cases with hollow-worn wheel profiles and worn rail profiles. The simulations of Case 3 meet all Standard S-2043 criteria. The simulations of Cases 1, 2, and 4 do not meet Standard S-2043 criteria for truck side L/V ratios (0.5 threshold).

Although AAR Chapter 11 limits do not apply to this regime, it may be noted that cases 1 and 4 meet the AAR Chapter 11 criterion for truck side L/V ratios (0.6), but Case 2 does not. The Case 2 simulations also do not meet Standard S-2043 criteria for the 95th percentile wheel L/V ratio (0.6), but they do meet the AAR Chapter 11 criterion of 0.8.

Table 41. Simulation Predictions for Curving with Rail Lubrication Cases 1-4 and Hollow Worn Wheels and Ground Rails, with Minimum Test Load

Criterion	Limiting Value	Case 1 Worn	Case 2 Worn	Case 3 Worn	Case 4 Worn
Maximum carbody roll angle (degree)	4.0	0.63	0.65	0.64	0.65
Maximum wheel L/V	0.80	0.67	0.74	0.43	0.68
Maximum truck side L/V	0.50	**0.53**	**0.61**	0.30	**0.58**
Minimum vertical wheel load (%)	25	52	51	53	52
Peak-to-peak carbody lateral acceleration (g)	1.30	0.30	0.30	0.28	0.30
Maximum carbody lateral acceleration (g)	0.75	0.20	0.20	0.20	0.20
Lateral carbody acceleration standard deviation (g)	0.13	0.04	0.04	0.04	0.04
Maximum carbody vertical acceleration (g)	0.90	0.16	0.17	0.17	0.17
Maximum vertical suspension deflection (%)	95	22	22	22	22
95% Wheel L/V Ratio	0.60	0.56	**0.64**	0.37	0.59

Figure 40 shows a plot of the wheel L/V ratio versus distance for the worst worn-case simulation and the underbalance speed for the Case 2 lubrication condition with worn wheel profiles. Figure 41 shows a plot of the truck side L/V ratio versus distance for the worst-case simulation and the underbalance speed for the Case 4 lubrication with worn wheel profiles. Figure 42 shows a plot of the 95th percentile wheel L/V ratio versus speed for the Case 2 lubrication condition with the worn wheel profile for both directions of travel, with the worst-case result of car orientation shown (either A- or B-end leading). Figure 43 shows a plot of the truck side L/V ratio versus the speed for the Case 2 lubrication condition with the worn wheel profile.

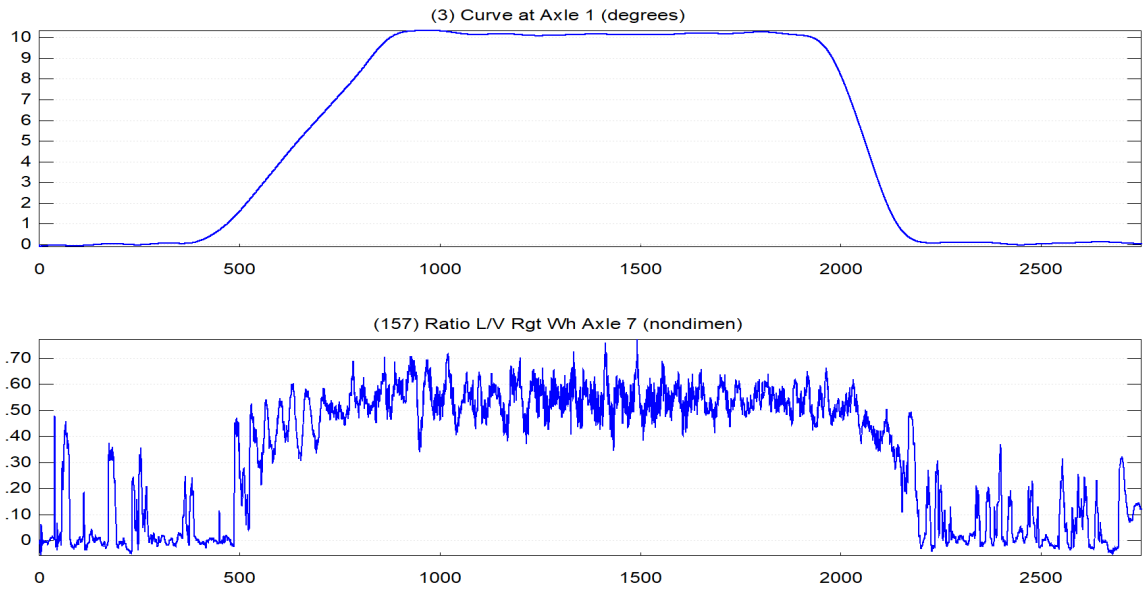

Figure 40. Plot of Wheel L/V Ratio versus distance for Case 2 friction with worn profiles, CCW, A-leading. Plot shows data for the lead axle of the trailing span bolster.

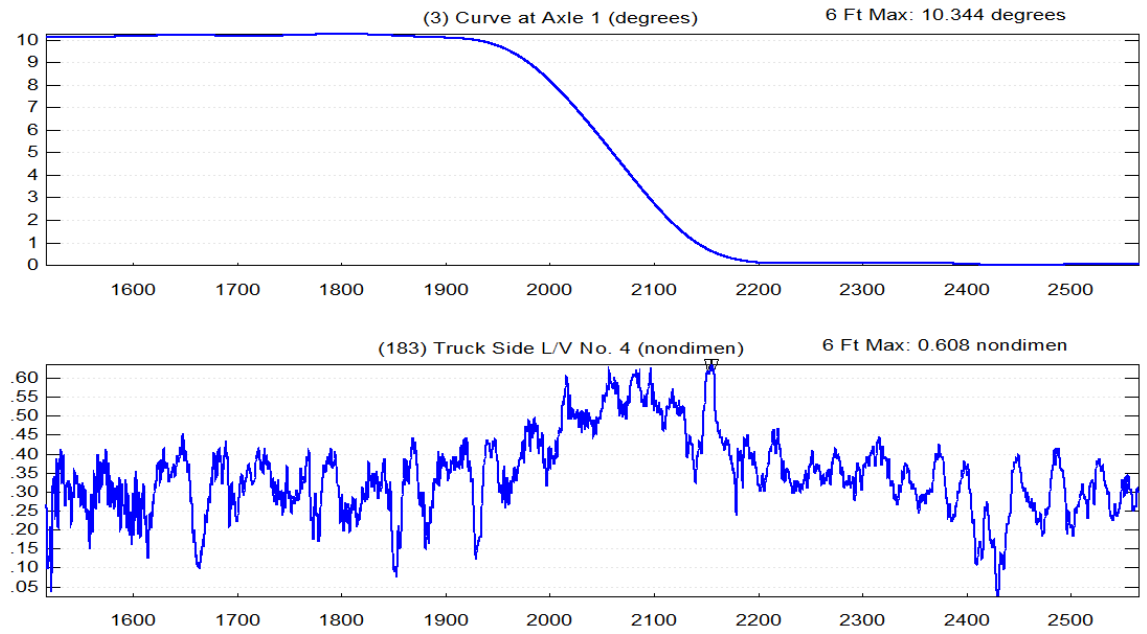

Figure 41. Plot of Truck Side L/V Ratio versus distance for Case 2 friction with worn profiles, CCW, B-leading. Plot shows data for the high rail of the middle truck on the lead span bolster.

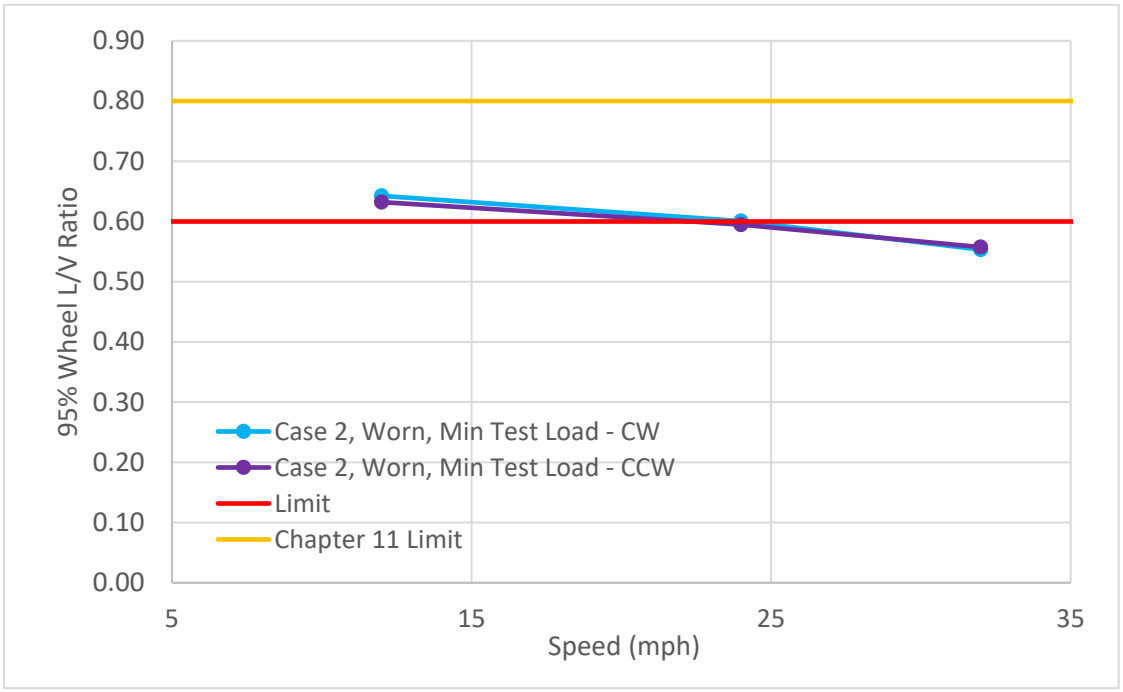

Figure 42. Atlas car with minimum test load 95-Percent Wheel L/V Ratio for curving with Case 2 lubrication and worn wheel and rail profiles

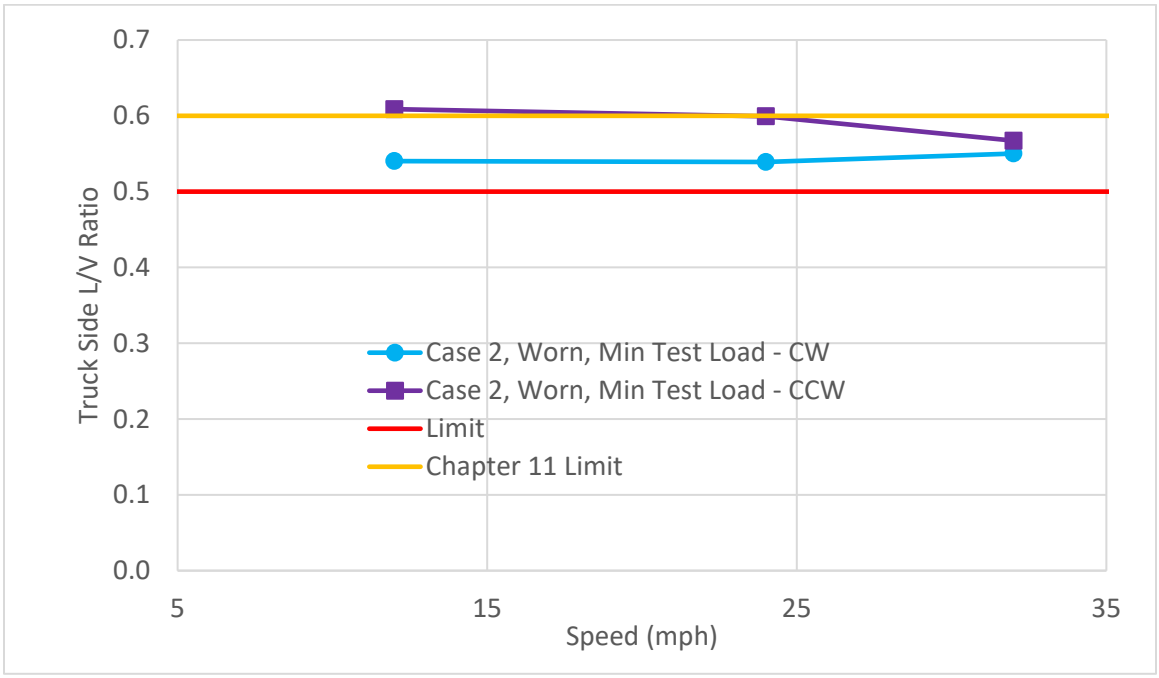

Figure 43. Minimum Test Load Truck Side L/V Ratio for curving with Case 2 lubrication and worn wheel and rail profiles

7.9.2 Maximum Test Load

(1) New Profiles

Table 42 shows the simulation predictions at the maximum test load for the four friction cases with new wheel and rail profiles. The table shows the worst-case results for any simulation, clockwise (CW) or CCW with A-end and B-end leading. The revised simulated performance of the car loaded with the HI-STAR 190 XL cask (maximum test load) **meets** Standard S-2043 criteria for curving under all the lubrication condition cases when considering new wheel and rail profiles. Figure 44 shows the plot of the maximum wheel L/V ratio against speed for Case 4 lubrication conditions with new wheel profiles to demonstrate the trend in performance.

Table 42. Simulation predictions for Curving with Rail Lubrication Cases 1–4 and New Wheels and Rails, Car Loaded with the Maximum Test Load

Criterion	Limiting Value	Case 1 New	Case 2 New	Case 3 New	Case 4 New
Maximum carbody roll angle (degree)	4.0	0.69	0.69	0.68	0.66
Maximum wheel L/V	0.80	0.64	0.67	0.38	0.71
Maximum truck side L/V	0.50	0.30	0.33	0.22	0.43
Minimum vertical wheel load (%)	25	55	55	56	56
Peak-to-peak carbody lateral acceleration (g)	1.30	0.27	0.28	0.22	0.23
Maximum carbody lateral acceleration (g)	0.75	0.20	0.22	0.15	0.17
Lateral carbody acceleration standard deviation (g)	0.13	0.03	0.03	0.03	0.03
Maximum carbody vertical acceleration (g)	0.90	0.21	0.21	0.20	0.20
Maximum vertical suspension deflection (%)	95	67	67	67	67
95% Wheel L/V Ratio	0.60	0.37	0.41	0.27	0.56

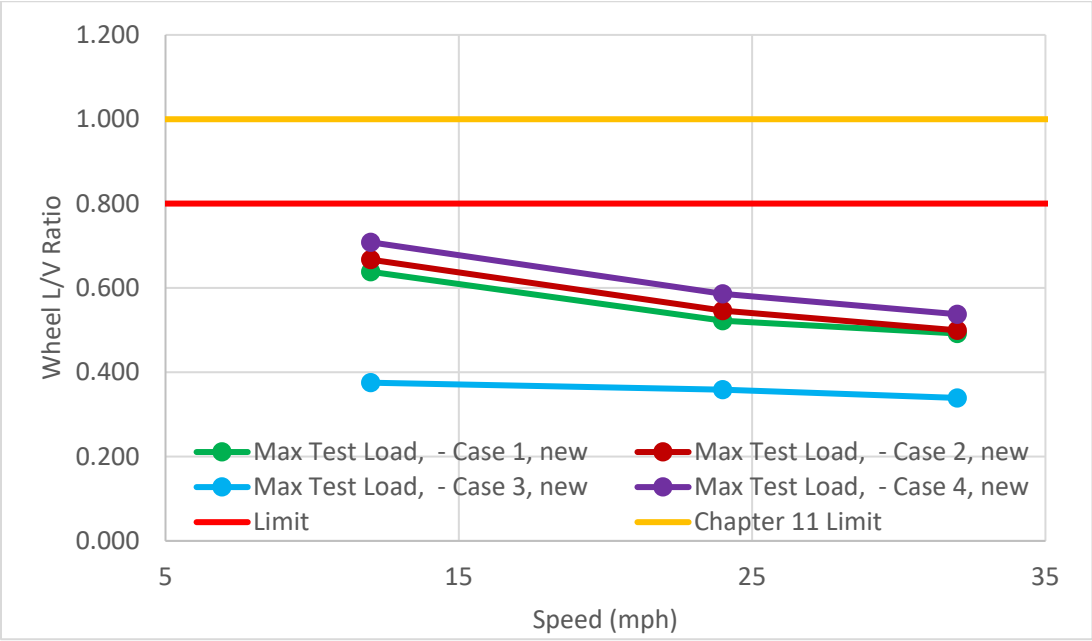

Figure 44. Predictions of Wheel L/V Ratio for multiple lubrication cases with new wheel and rail profiles (most severe results shown)

(2) Worn Profiles

Table 43 shows the simulation predictions of the car loaded with the maximum test load for the four friction cases with hollow worn wheel profiles and ground rail profiles. The table shows the worst-case results for runs in the CW and CCW directions with the A-end and B-end leading. The simulations of Case 3 meet all Standard S-2043 criteria. The simulations of Cases 1, 2, and 4 **do not meet** Standard S-2043 criteria for truck side L/V ratios, although they do meet the corresponding AAR Chapter 11 criteria. The AAR Chapter 11 criterion for truck side L/V ratio is 0.6. The Case 2 and Case 4 simulations predictions **do not meet** the Standard S-2043 limit for the 95 percent wheel L/V ratio although these predictions do meet the corresponding AAR Chapter 11 criteria. Therefore, on behalf of the Department of Energy, TTCI is requesting an exception from the AAR EEC.

Table 43. Simulation predictions for Curving with Rail Lubrication Cases 1–4 and Hollow Worn Wheels and Ground Rails, Car Loaded with the Maximum Test Load

Criterion	Limiting Value	Case 1 Worn	Case 2 Worn	Case 3 Worn	Case 4 Worn
Maximum carbody roll angle (degree)	4.0	0.72	0.74	0.73	0.71
Maximum wheel L/V	0.80	0.66	0.73	0.40	0.68
Maximum truck side L/V	0.50	0.52	0.60	0.25	0.58
Minimum vertical wheel load (%)	25	56	55	56	56
Peak-to-peak carbody lateral acceleration (g)	1.30	0.28	0.28	0.26	0.28
Maximum carbody lateral acceleration (g)	0.75	0.17	0.18	0.17	0.17
Lateral carbody acceleration standard deviation (g)	0.13	0.04	0.04	0.04	0.04
Maximum carbody vertical acceleration (g)	0.90	0.20	0.20	0.20	0.20
Maximum vertical suspension deflection (%)	95	68	67	67	67
95% Wheel L/V Ratio	0.60	0.57	0.66	0.33	0.61

Figure 45 shows a plot of the maximum truck side L/V versus speed for the CW and CCW with the worst-case A- or B-end leading results (Case 2), and both minimum and maximum test load conditions are shown. Figure 46 shows a plot of the maximum 95 percent wheel L/V ratio versus speed for the CW and CCW with the worst-case A- or B-end leading results (Case 2), and both minimum and maximum test load conditions are shown. Figure 47 shows a plot of the maximum truck side L/V ratio versus speed for Case 4, with both the minimum and maximum test load conditions shown for comparison. Figure 48 shows a plot of the truck side L/V ratio versus distance for the 12 mph CCW run with the B-end leading. The plot shows the data for the middle truck of the lead span bolster. The peak value occurs in the exit spiral of the curve.

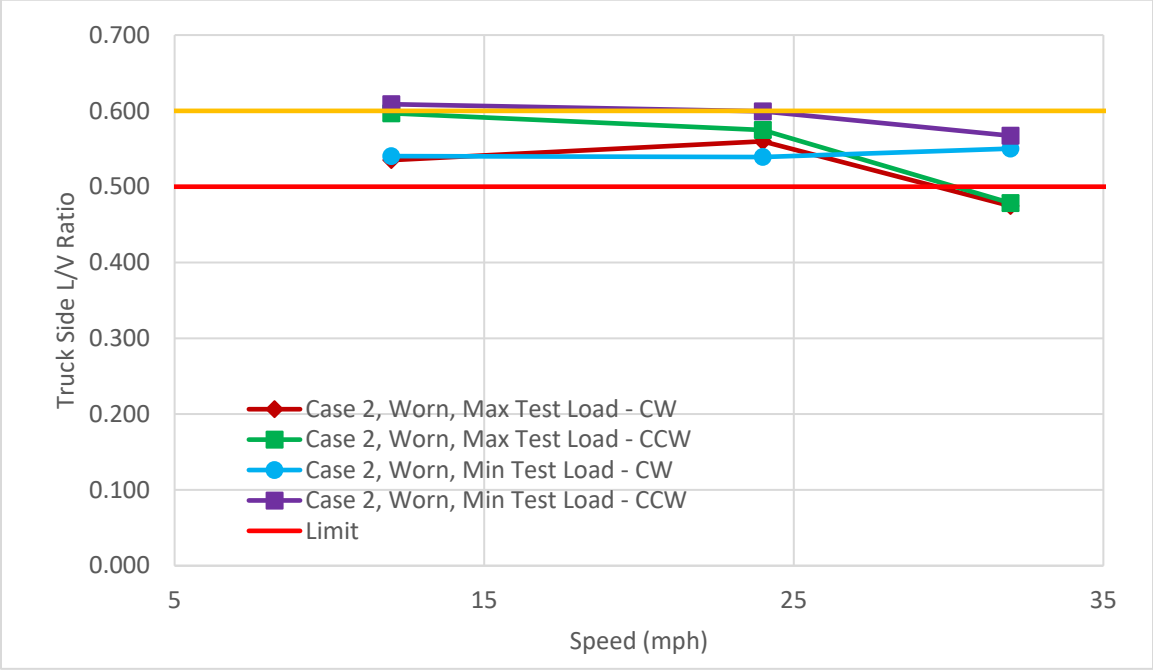

Figure 45. Predictions of Truck Side L/V Ratio for Case 2 lubrication with worn wheel and rail profiles for both directions of travel, with most severe results shown, at maximum and minimum test load.

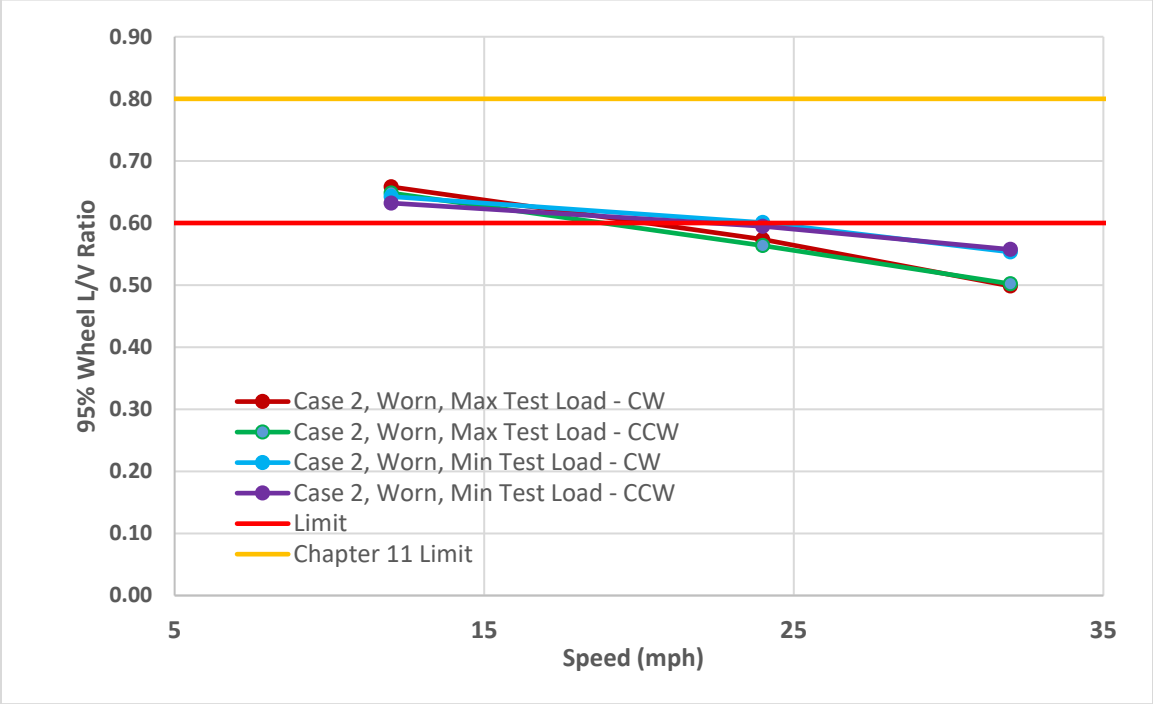

Figure 46. Predictions of 95% Wheel L/V Ratio for Case 2 lubrication with worn wheel and rail profiles for both directions of travel, with most severe results shown, at maximum and minimum test loads

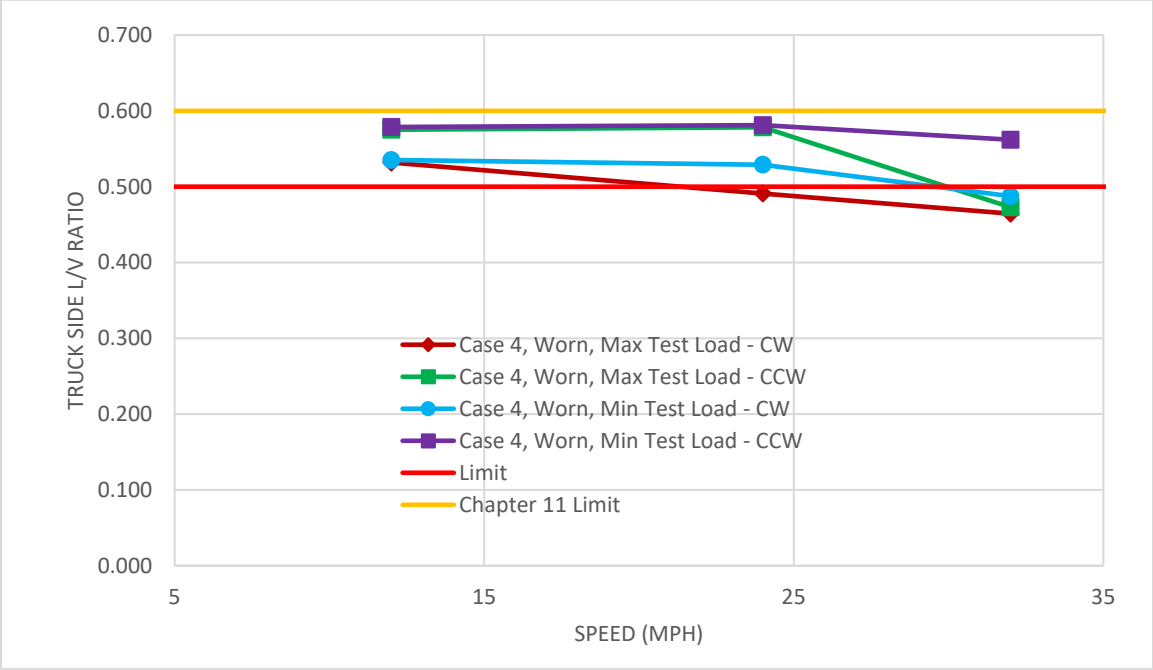

Figure 47. Predictions of Truck Side L/V Ratio for Case 4 lubrication with worn wheel and rail profiles for both directions of travel, with most severe results shown, at maximum and minimum test loads

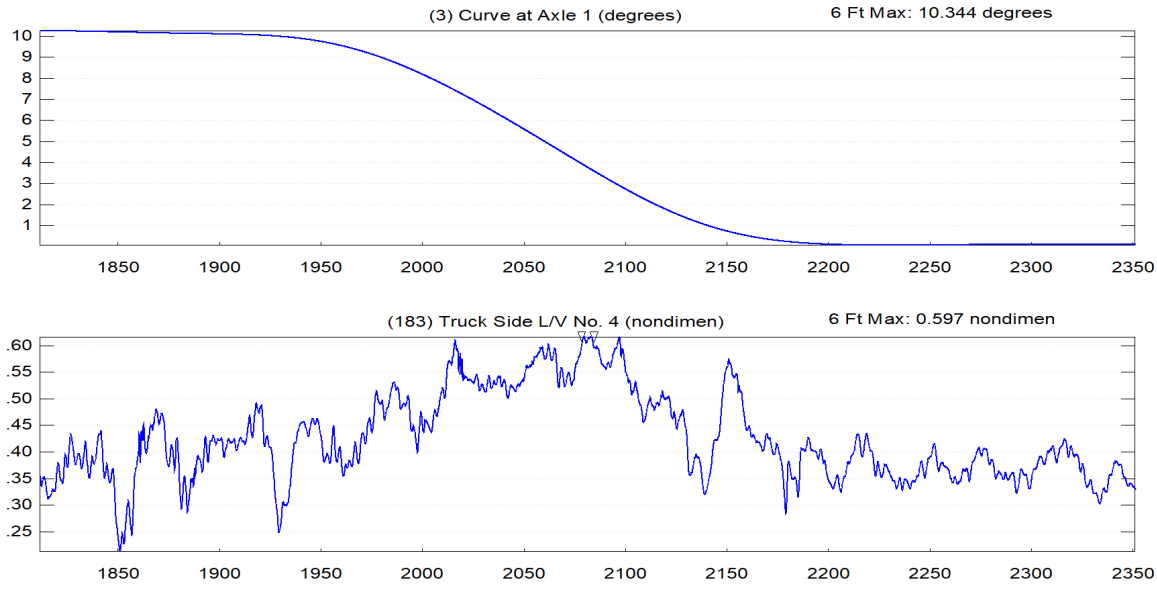

Figure 48. Plot of Truck Side L/V Ratio versus distance for Case 2 friction with worn wheel and rail profiles. The plot shows data for the high rail of the middle truck on the lead span bolster

Figure 49 and Figure 50 show how lubrication impacts the results of the various cases, for both the truck side L/V ratios and the 95th percentile wheel L/V ratios, respectively.

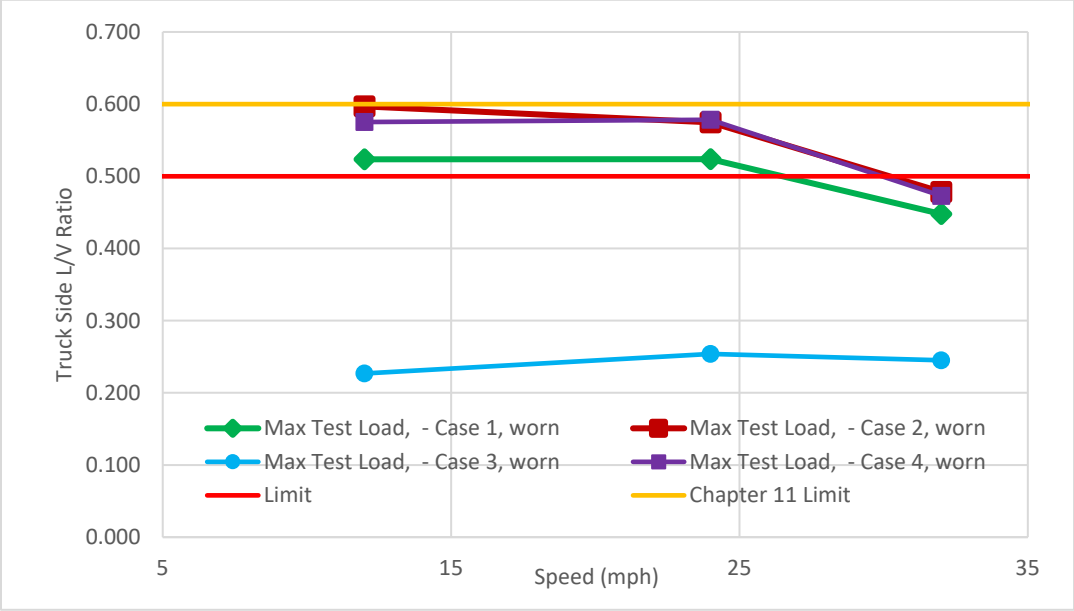

Figure 49. Worst-case predictions for Truck Side L/V Ratio at all lubrication cases of worn wheel and rail profiles, at maximum test load

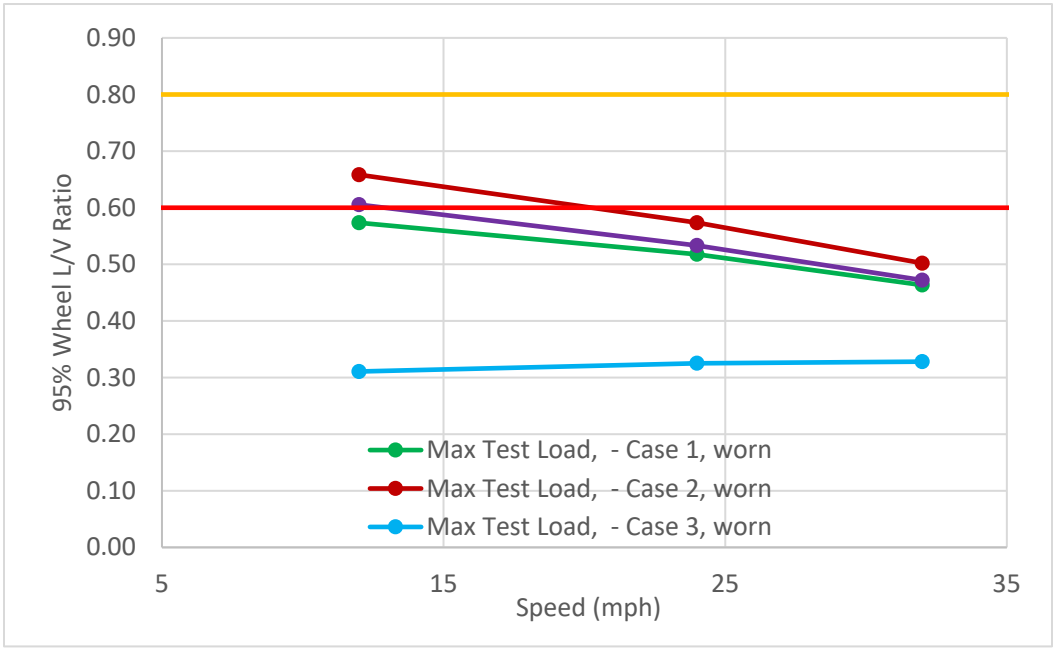

Figure 50. Worst-case predictions for 95 percentile Wheel L/V Ratio at all lubrication cases of worn wheel and rail profiles, at maximum test load

7.10 Limiting Spiral Negotiation

The simulations of the limiting spiral regime were conducted according to Standard S-2043, Paragraph 4.3.11.6. The limiting spiral has a steady curvature change from 0 to 10 degrees and a steady superelevation change from 0 inch to 4 3/8 inches in 89 feet.

7.10.1 Minimum Test Load

Table 44 shows the worst-case test results and the simulation predictions for the car loaded with the minimum test load in the limiting spiral test regime. Figure 51 shows the test results and the simulation predictions of the maximum wheel L/V ratio with CSM 70 primary pads plotted against speed to show the trend in performance. Figure 52 shows test results and simulation predictions of maximum wheel L/V ratio with CSM 58 primary pads.

Using CSM 70 primary pads, the model predicts lower wheel L/V ratios and higher minimum vertical wheel loads than those that were measured in the test, but the overall trend matches closely, as shown in Figure 51. The simulations done using CSM 58 pads showed lower L/V ratios than simulations done using CSM 70 primary pads, but the test results showed higher wheel L/V ratios with CSM 58 primary pads than those with CSM 70 pads. Only post-test simulation predictions are shown because the pre-test predictions were for a load case no longer intended for use.

The test and revised simulation results **meet** Standard S-2043 criteria for the limiting spiral regime at the minimum test load.

Table 44. Limiting spiral test results and simulation predictions with minimum test load

Criterion	Limiting Value	CSM 70 Pads		CSM 58 Pads	
		Test Result	Simulation Prediction Revised Model	Test Result	Simulation Prediction Revised Model
Roll angle (degree)	4.0	1.5	0.7	1.6	0.8
Maximum wheel lateral/vertical (L/V)	0.8	0.67	0.62	0.69	0.50
Maximum truck side L/V	0.5	0.38	0.35	0.42	0.27
Minimum vertical wheel load (%)	25%	42%	55%	56%	54%
Lateral peak-to-peak acceleration (g)	1.3	0.15	0.12	0.18	0.16
Maximum lateral acceleration (g)	0.75	0.13	0.10	0.16	0.11
Maximum vertical acceleration (g)	0.90	0.09	0.13	0.16	0.23
Maximum vertical suspension deflection (%)	95%	29%	24%	16%	24%

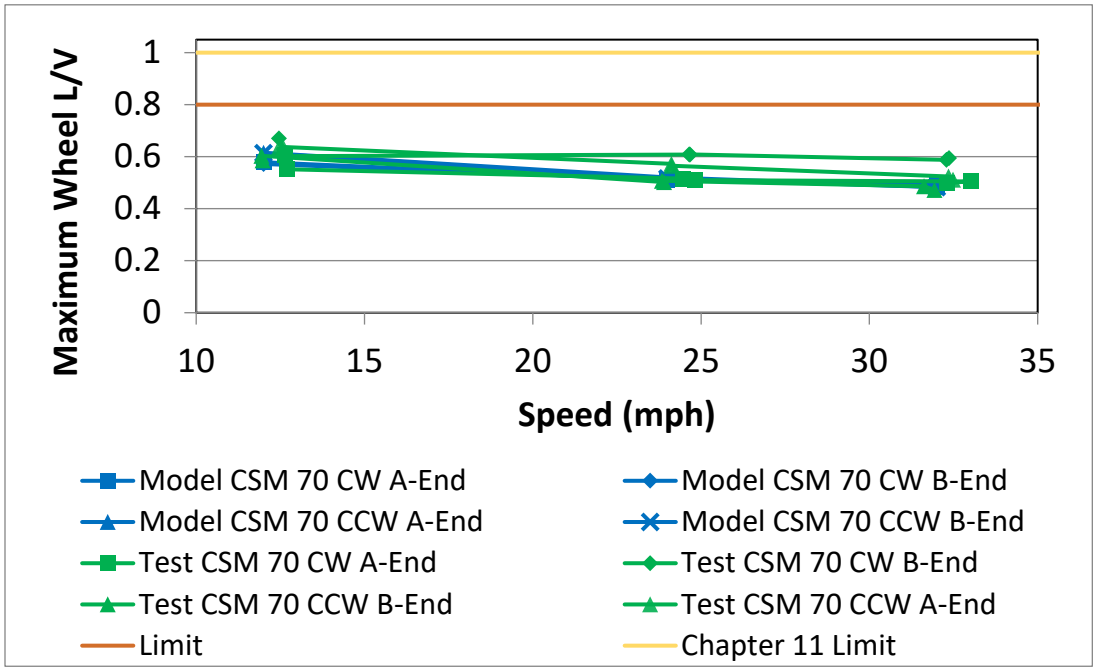

Figure 51. Simulation prediction and test results of maximum wheel L/V ratio in the limiting spiral regime with minimum test load using CSM 70 pads

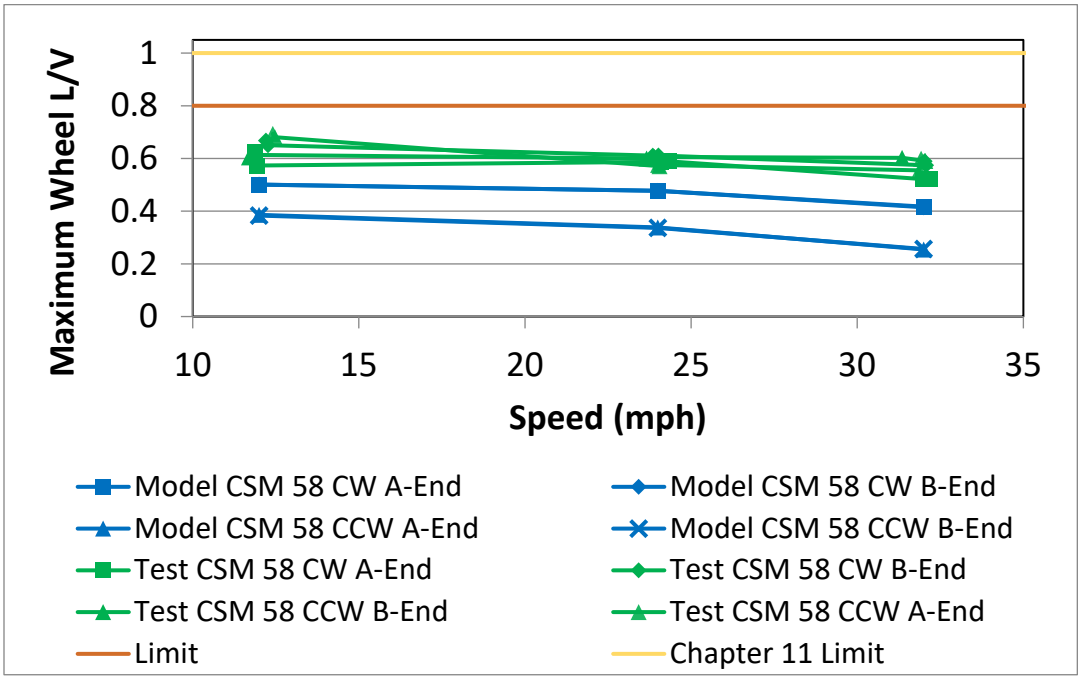

Figure 52. Simulation prediction and test results of maximum wheel L/V ratio in the limiting spiral regime with minimum test load using CSM 58 pads

7.10.2 Maximum Test Load

Table 45 shows the worst-case test results and simulation predictions for the car loaded with the maximum test load in the limiting spiral test regime. Figure 53 shows the test results and simulation predictions of the maximum wheel L/V ratio with CSM 70 primary pads plotted against speed to show the trend in performance. Figure 54 shows the original and revised simulation predictions of maximum wheel L/V ratio with CSM 58 primary pads.

Using CSM 70 primary pads, the model predicts lower wheel L/V ratios and higher minimum vertical wheel loads than those that were measured in the test. The simulations done with CSM 58 pads showed lower L/V ratios than simulations done using CSM 70 primary pads, but the difference was small. The wheel L/V ratios predicted with the original model in 2017 were about 10 percent higher than those predicted with the revised model.

The test and revised simulation results **meet** Standard S-2043 criteria for the limiting spiral regime at maximum test load.

Table 45. Dynamic curving test results and simulation predictions with maximum test load

Criterion	Limiting Value	CSM 70 Pads		CSM 58 Pads	
		Test Result	Simulation Prediction Revised Model	Simulation Prediction Original Model	Simulation Prediction Revised Model
Roll angle (degree)	4.0	1.3	1.0	2.3	1.0
Maximum wheel lateral/vertical (L/V)	0.8	0.74	0.52	0.49	0.44
Maximum truck side L/V	0.5	0.39	0.30	0.31	0.21
Minimum vertical wheel load (%)	25%	52%	60%	54%	59%
Lateral peak-to-peak acceleration (g)	1.3	0.12	0.11	0.13	0.14
Maximum lateral acceleration (g)	0.75	0.13	0.08	0.11	0.11
Maximum vertical acceleration (g)	0.90	0.17	0.17	0.07	0.28
Maximum vertical suspension deflection (%)	95%	68%	69%	78%	69%

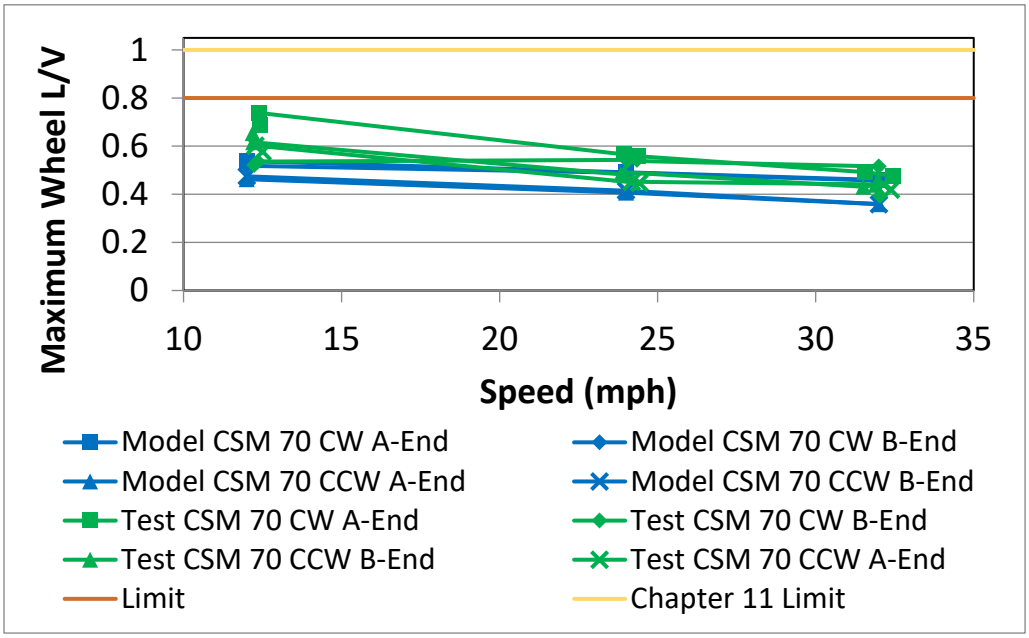

Figure 53. Simulation prediction and test results of maximum wheel L/V ratio in the dynamic curving regime with maximum test load using CSM 70 pads

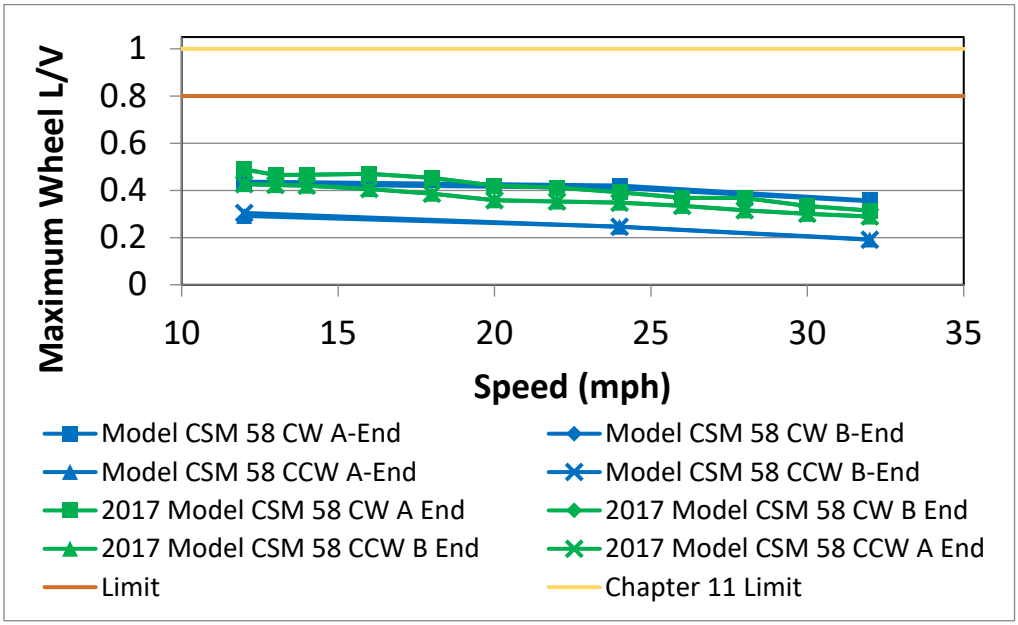

Figure 54. Simulation predictions of maximum wheel L/V ratio in the dynamic curving regime with maximum test load using CSM 70 and CSM 58 pads

7.11 Special Trackwork: Turnouts and Crossovers (Standard S-2043, Paragraph 4.3.11.7)

The simulations of the turnout and crossover regime were conducted according to Standard S-2043, Paragraph 4.3.11.7. The original simulations were performed using a No. 7 AREMA straight point turnout and a No. 7 crossover on 13-foot track centers at speeds up to 15 mph. Additional revised

simulations were performed only for the No. 7 crossover, because, while the preliminary simulation predictions met Standard S-2043 criteria in the turnout, the predictions did not meet all Standard S-2043 criteria in the crossover (the crossover was the most severe case).

Because TTCI does not have measured track geometry available for a No. 7 crossover it used ideal track inputs. These inputs included track geometry deviations due to the switch riser, the turnout entry angles, and the closure curves. The changing rail geometry was modeled based on the unworn shapes of the components. The nominal clearance of the guardrails at the frogs were modeled as well. TTCI used 50-millisecond windows when processing wheel force statistics because the changes in rail profiles along the track introduced extremely short duration, unrealistic spikes in the simulation predictions.

7.11.1 Minimum Test Load – Turnouts and Crossovers

Table 46 shows the worst-case simulation predictions for the crossover regime. The revised simulation predictions **met** Standard S-2043 criteria for the No. 7 crossover at the minimum test load, with the maximum truck side L/V ratio equal to the criterion of 0.5. Figure 55 shows a plot of the truck side L/V ratio in the crossover. Only the post-test simulation predictions are shown because the pre-test predictions were for a load case no longer intended for use.

Table 46. Crossover Simulation Predictions with Minimum Test Load

Criterion	Limiting Value	No. 7 Crossover A-Lead	No. 7 Crossover B-Lead
Maximum carbody roll angle (degree)	4.0	0.1	0.1
Maximum wheel L/V	0.80	0.78	0.78
Maximum truck side L/V	0.50	0.50	0.50
Minimum vertical wheel load (%)	25	57%	56%
Peak-to-peak carbody lateral acceleration (g)	1.30	0.35	0.41
Maximum carbody lateral acceleration (g)	0.75	0.15	0.25
Maximum carbody vertical acceleration (g)	0.90	0.53	0.52
Maximum vertical suspension deflection (%)	95	24%	23%

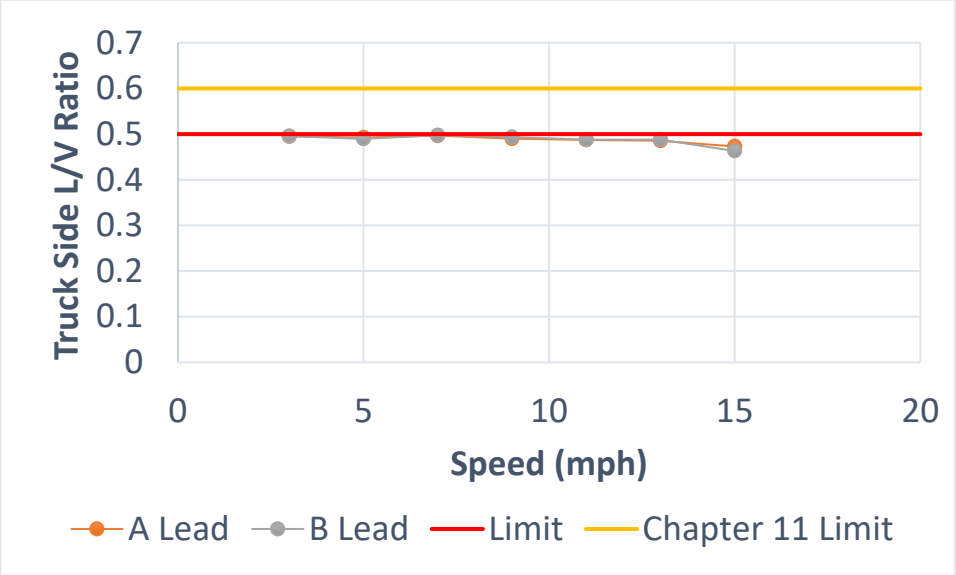

Figure 55. Simulation Predictions of Truck side L/V Ratio on No. 7 Crossovers for Original Simulations of Atlas Car with Minimum Test Load

7.11.2 Maximum Test Load – Turnouts and Crossovers

Table 47 shows the worst-case simulation predictions for the crossover regime. Figure 56 shows a plot of the maximum truck side L/V versus speed to show the trend in performance. The original simulation predictions did not meet the Standard S-2043 criterion for the truck side L/V ratio in the No. 7 crossover, but all other criteria were met. The revised simulation predictions **met** all Standard S-2043 criteria because the measured primary longitudinal stiffness used in the revised model was lower and more representative of the actual vehicle than what was used in the original model.

Table 47. Crossover Simulation Predictions, Car Loaded at Maximum Load

		Original		Revised	
Criterion	**Limiting Value**	**No. 7 Crossover A-Lead**	**No. 7 Crossover B-Lead**	**No. 7 Crossover A-Lead**	**No. 7 Crossover B-Lead**
Maximum carbody roll angle (degree)	4.0	0.3	0.3	0.3	0.3
Maximum wheel L/V	0.80	0.65	0.67	0.61	0.60
Maximum truck side L/V	0.50	0.51	0.52	0.48	0.48
Minimum vertical wheel load (%)	25	64	65	62	69
Peak-to-peak carbody lateral acceleration (g)	1.30	0.22	0.24	0.30	0.54
Maximum carbody lateral acceleration (g)	0.75	0.13	0.13	0.25	0.23
Maximum carbody vertical acceleration (g)	0.90	0.10	0.09	0.09	0.36
Maximum vertical suspension deflection (%)	95	73	75	64	61

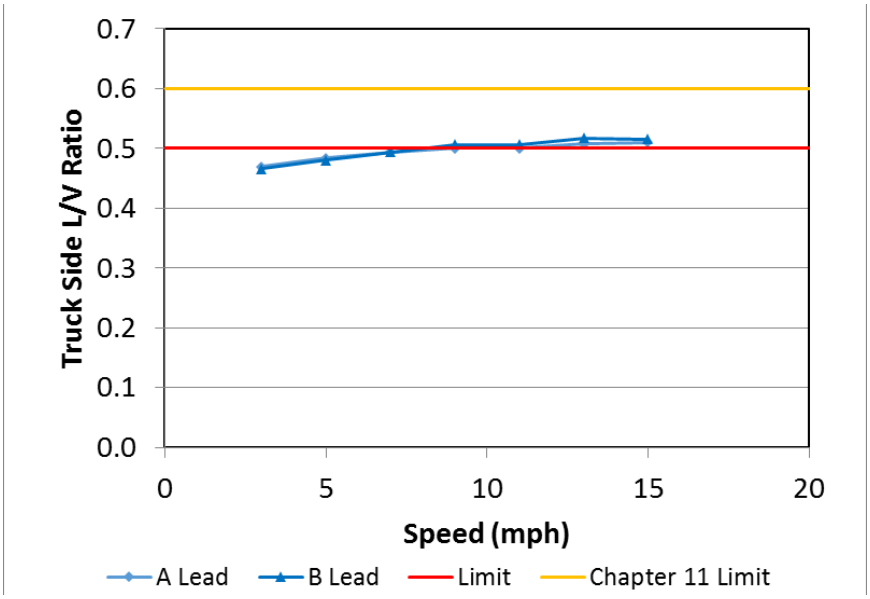

(a)

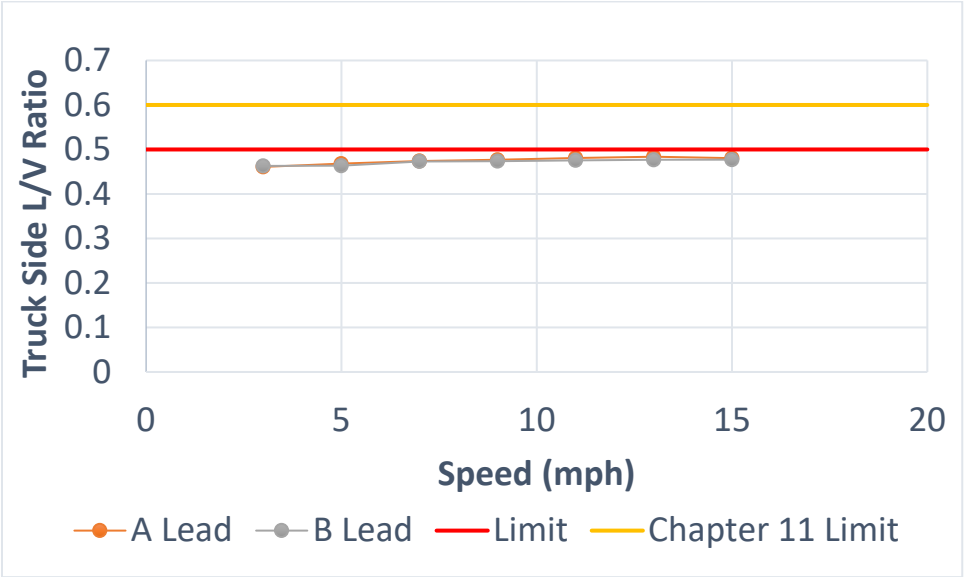

(b)

Figure 56. Simulation Predictions of Truck Side L/V Ratio on No. 7 Crossover. Original Simulations (a) and revised simulations (b) at maximum load

7.12 Buff and Draft Curving

The simulations of the buff and draft curving regime were conducted according to Standard S-2043, Paragraph 4.3.13. The simulations were performed using measured track geometry of the 12-degree curve of the WRM loop at the TTC. The simulations were designed to simulate the cask car coupled to the following:

- A base car as described in the AAR MSRP Section C-II, Standard M-1001 Chapter 2, Paragraph 2.1.4.2.3.

- A long car with 90-foot-long over strikers, 66-foot-long truck centers, 60-inch-long couplers, and conventional draft gear.
- A like car.
- A buffer car–the car the cask car will be coupled to in HLRM service.

The in-train forces were calculated for a 12-degree curve for each of the coupled car geometries, and the load was applied to the coupler as an external force, made up of two components: one lateral and one longitudinal.

Table 48 shows the worst-case simulation predictions for draft force cases, and Table 49 shows the worst-case simulation predictions for the buff force cases. Figure 57 shows a plot of the maximum truck side L/V ratio for the four draft force cases modeled in both the original and revised simulations. Similarly, Figure 58 shows the plot of the buff maximum truck side L/V ratios. All revised simulation predictions **meet** all Standard S-2043 criteria for all buff and draft curving cases.

Table 48. Revised Simulation Predictions for 250,000 Draft Force, Minimum Test Load

Criterion	Limiting Value	Base	Long	Like	Buffer Car
Maximum carbody roll angle (degree)	4.0	0.8	0.6	0.8	0.7
Maximum wheel L/V	0.80	0.55	0.50	0.55	0.50
Maximum truck side L/V	0.50	0.47	0.34	0.47	0.35
Minimum vertical wheel load (%)	25	46	57	46	56
Peak-to-peak carbody lateral acceleration (g)	1.30	0.18	0.17	0.16	0.16
Maximum carbody lateral acceleration (g)	0.75	0.12	0.12	0.12	0.12
Lateral carbody acceleration standard deviation (g)	0.13	0.00	0.00	0.00	0.00
Maximum carbody vertical acceleration (g)	0.90	0.11	0.12	0.12	0.12
Maximum vertical suspension deflection (%)	95	19	19	20	18

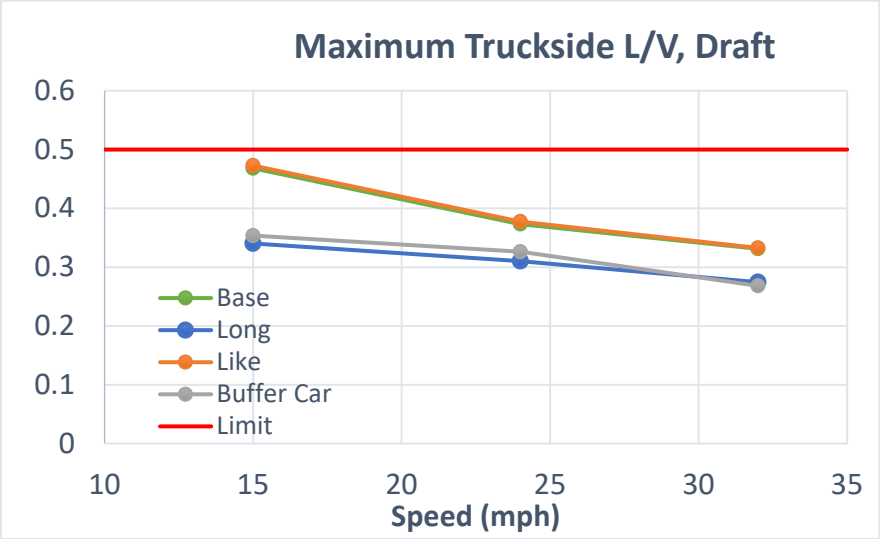

Figure 57. Truck Side L/V Ratio for Curving Simulations Under 250,000 Pounds Draft Force for Revised Simulations with the Minimum Test Load

Table 49. Revised Simulation Predictions for 250,000 Buff Force, Minimum Test Load

Criterion	Limiting Value	Base	Long	Like	Buffer Car
Maximum carbody roll angle (degree)	4.0	0.7	0.8	0.7	0.7
Maximum wheel L/V	0.80	0.52	0.55	0.52	0.52
Maximum truck side L/V	0.50	0.39	0.39	0.40	0.37
Minimum vertical wheel load (%)	25	55	53	55	56
Peak-to-peak carbody lateral acceleration (g)	1.30	0.15	0.15	0.15	0.17
Maximum carbody lateral acceleration (g)	0.75	0.11	0.11	0.11	0.12
Maximum carbody vertical acceleration (g)	0.90	0.12	0.12	0.10	0.13
Maximum vertical suspension deflection (%)	95	35	31	36	32

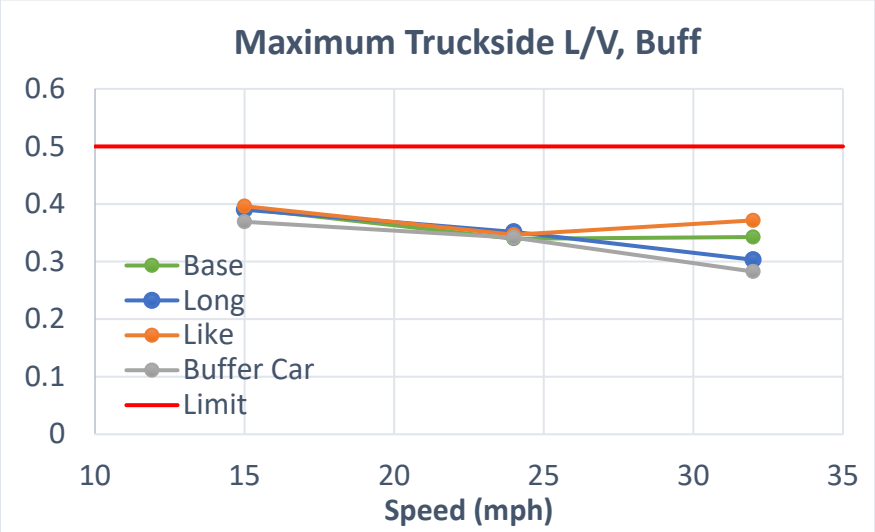

Figure 58. Truck Side L/V Ratio for Curving Simulations Under 250,000 Pounds Buff Force for Revised Simulations with the Minimum Test Load

7.13 Worn Component Simulations

The worn component simulations were conducted according to Standard S-2043, Paragraph 4.3.15. The wear of the following components was simulated:

- Constant Contact Side Bearings (CCSB)
- Center plate
- Primary pad
- Friction wedges
- Broken springs

The hunting, dynamic curving, constant curving, and twist-and-roll worn component simulations were performed with the minimum test load because this configuration generally produced the worst performance. The pitch-and-bounce simulations for the worn wedge and broken spring conditions were performed with the maximum test load condition.

In Sections 7.13.1 to 7.13.5, the worst-case simulation predictions for the worn components are summarized in tables together with the criteria and base line predictions for the new condition car. In cases where the component wear causes the performance to degrade such that the car does not meet criteria, plots are shown to demonstrate the trend in performance. Only simulation predictions with the revised model are shown in Sections 7.13.1 to 7.13.5 because, except for the simulation in the pitch and bounce regime, the load conditions are not comparable.

7.13.1 Worn Constant Contact Side Bearings

The wear in a CCSB may result in a loss of side bearing preload. The wear of the carbody centerplate or the truck center bowl may result in a reduction of the CCSB setup height. To examine the effect of these types of CCSB wear, simulations were performed with the following:

- The CCSB having half the stiffness and half the preload of new CCSB (3,000-pound nominal preload). This condition will reduce the both the turning moment and the the roll stiffness between the truck bolster and the span bolster.
- The setup height of the new CCSB reduced to 4 7/8 inch. This reduction will increase the turning moment between the truck bolster and span bolster. It will also increase the roll stiffness and reduce the roll clearance between the truck bolster and span bolster.

The performance of the car with worn CCSB was checked during dynamic curving, hunting, and twist and roll simulation with the minimum test load.

Table 50 shows the worst-case simulation predictions for the baseline, low preload, and tight clearance conditions. All performance criteria were **met** for the dynamic curving simulations with worn CCSB. Figure 59 shows a plot of the maximum wheel L/V ratio versus speed for the baseline case and the two worn CCSB cases to show the trend in performance.

Table 50. Simulation Predictions of the Atlas Cask Car with Worn CCSB in Dynamic Curving

Criterion	Limiting Value	Revised Models		
		Baseline	CCSB, Low Preload	CCSB, Tight Clearance
Maximum carbody roll angle (degree)	4.0	0.97	0.95	0.99
Maximum wheel L/V	0.80	0.71	0.71	0.71
Maximum truck side L/V	0.50	0.35	0.35	0.35
Minimum vertical wheel load (%)	25	52.69	52.51	53.22
Peak-to-peak carbody lateral acceleration (g)	1.30	0.19	0.18	0.23
Maximum carbody lateral acceleration (g)	0.75	0.16	0.16	0.18
Maximum carbody vertical acceleration (g)	0.90	0.12	0.11	0.12
Maximum vertical suspension deflection (%)	95	23.22	23.19	24.01

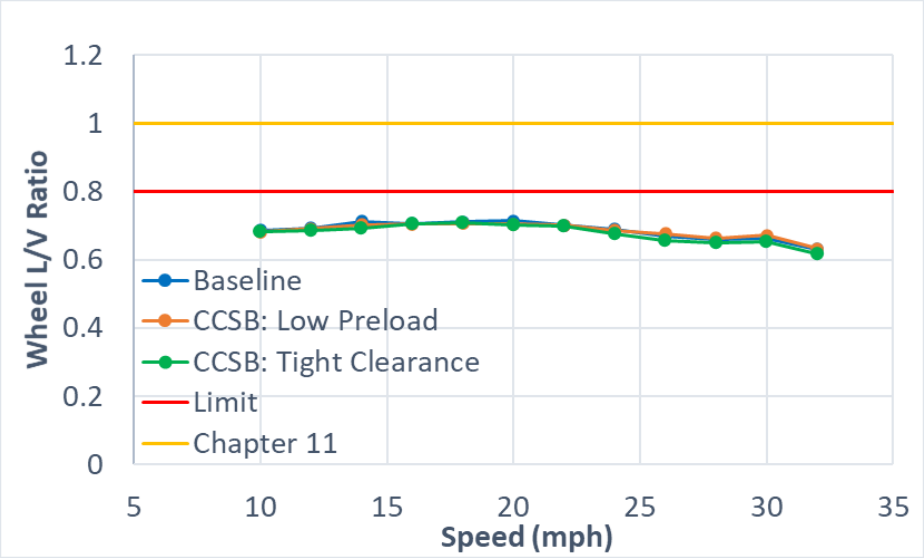

Figure 59. Single Wheel L/V Ratio for Worn CCSB Cases

Table 51 shows a comparison of the hunting simulation predictions for unworn baseline and the worn CCSB simulations. Similar to the test results, the baseline simulations and the "Low Preload" worn CCSB condition did not meet the Standard S-2043 criterion for the maximum standard deviation of carbody lateral acceleration. All other Standard S-2043 criteria were met.

As the CCSB preload is reduced, the hunting performance deteriorates. Figure 60 shows the standard deviation of the carbody lateral acceleration over 2,000 feet, and all configurations show a severely deteriorated performance at speeds above 50 mph, although the tight bearing clearance does not exceed the limit. All worn side bearing performance **meets** Standard S-2043 criteria up to 60 mph. This speed is above the limiting operating speed of the cask car in HLRM service.

Table 51. Simulation Predictions of the Atlas Cask Car with Worn CCSB in Hunting

Criterion	Limiting Value	Revised Models		
		Baseline	CCSB, Low Preload	CCSB, Tight Clearance
Maximum carbody roll angle (degree)	4.0	0.30	0.41	0.27
Maximum wheel L/V	0.80	0.28	0.39	0.21
Maximum truck side L/V	0.50	0.14	0.21	0.15
Minimum vertical wheel load (%)	25	71.1	61.4	70.6
Peak-to-peak carbody lateral acceleration (g)	1.30	0.59	0.64	0.55
Maximum carbody lateral acceleration (g)	0.75	0.31	0.36	0.31
Lateral carbody acceleration standard deviation (g)	0.13	0.14	0.17	0.11
Maximum carbody vertical acceleration (g)	0.90	0.32	0.17	0.17
Maximum vertical suspension deflection (%)	95	16.5	16.1	16.8

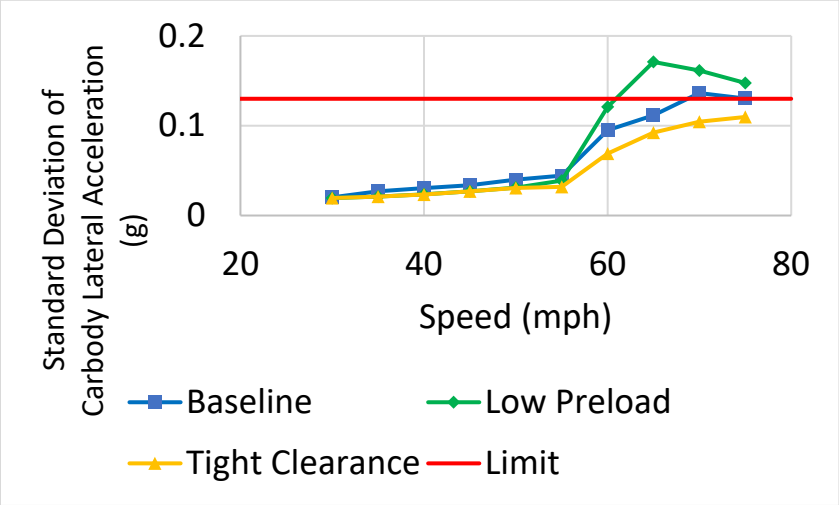

Figure 60. Maximum Carbody Lateral Acceleration for CCSB Wear Cases Plotted Against Speed

Table 52 shows a comparison of twist-and-roll simulation predictions for the baseline and worn CCSB simulations. The simulation predictions for the worn CCSB **meet** Standard S-2043 criteria for twist and roll simulations.

Table 52. Simulation Predictions of the Atlas Cask Car with Worn CCSB in Twist and Roll

Criterion	Limiting Value	Baseline	CCSB, Low Preload	CCSB, Tight Clearance
Maximum carbody roll angle (degree)	4.0	1.9	2.0	1.9
Maximum wheel L/V	0.80	0.27	0.30	0.17
Maximum truck side L/V	0.50	0.17	0.17	0.12
Minimum vertical wheel load (%)	25	58	58	59
Peak-to-peak carbody lateral acceleration (g)	1.30	0.53	0.54	0.46
Maximum carbody lateral acceleration (g)	0.75	0.29	0.27	0.25
Maximum carbody vertical acceleration (g)	0.90	0.24	0.24	0.23
Maximum vertical suspension deflection (%)	95	21	22	21

7.13.2 Centerplate

To examine the effect of centerplate wear, simulations were performed with centerplate friction increased from 0.3 for the baseline case to 0.5 for the worn case. Table 53 shows a comparison of the constant curving simulation predictions for the baseline and worn centerplate simulations. The simulation predictions for worn centerplates **meet** Standard S-2043 criteria for constant curving.

Table 53. Simulation Predictions of the Atlas Cask Car with Worn Centerplate in Constant Curving

Criterion	Limiting Value	Baseline	Worn Centerplate
Maximum carbody roll angle (degree)	4.0	0.77	0.77
Maximum wheel L/V	0.80	0.52	0.52
Maximum truck side L/V	0.50	0.34	0.34
Minimum vertical wheel load (%)	25	52.7	53.4
Peak-to-peak carbody lateral acceleration (g)	1.30	0.15	0.15
Maximum carbody lateral acceleration (g)	0.75	0.14	0.14
Maximum carbody vertical acceleration (g)	0.90	0.15	0.14
Maximum vertical suspension deflection (%)	95	24.8	24.9

Table 54 shows a comparison of the dynamic curving simulation predictions for the baseline and worn centerplate simulations. The simulation predictions for the baseline and worn simulation **meet** the criteria for dynamic curving (the tested car also met this performance specification).

Table 54. Simulation Predictions of the Atlas Cask Car with Worn Centerplate in Dynamic Curving

Criterion	Limiting Value	Baseline	Centerplate Wear
Maximum carbody roll angle (degree)	4.0	0.97	1.01
Maximum wheel L/V	0.80	0.71	0.71
Maximum truck side L/V	0.50	0.35	0.35
Minimum vertical wheel load (%)	25	52.69	53.56
Peak-to-peak carbody lateral acceleration (g)	1.30	0.19	0.19
Maximum carbody lateral acceleration (g)	0.75	0.16	0.17
Maximum carbody vertical acceleration (g)	0.90	0.12	0.11
Maximum vertical suspension deflection (%)	95	23.22	24.05

Table 55 shows a comparison of the hunting simulation predictions for baseline and worn centerplate simulations. The baseline simulation predictions **did not meet** the criteria for a standard deviation of the lateral carbody acceleration over 2,000 feet. All worn centerplate performances meet Standard S-2043 criteria up to 65 mph. This speed is above the limiting operating speed of the cask car in HLRM service. Figure 61 plots the lateral carbody acceleration standard deviation against vehicle speed, and the worn centerplate condition is marginally more favorable than the baseline condition. All other criteria were met for hunting with worn centerplates.

Table 55. Simulation Predictions of the Atlas Cask Car with Worn Centerplate in Hunting

Criterion	Limiting Value	Baseline	Centerplate Wear
Maximum carbody roll angle (degree)	4.0	0.3	0.3
Maximum wheel L/V	0.80	0.28	0.19
Maximum truck side L/V	0.50	0.14	0.13
Minimum vertical wheel load (%)	25	71	70
Peak-to-peak carbody lateral acceleration (g)	1.30	0.59	0.57
Maximum carbody lateral acceleration (g)	0.75	0.31	0.31
Lateral carbody acceleration standard deviation (g)	0.13	0.14	0.13
Maximum carbody vertical acceleration (g)	0.90	0.32	0.17
Maximum vertical suspension deflection (%)	95	16	16

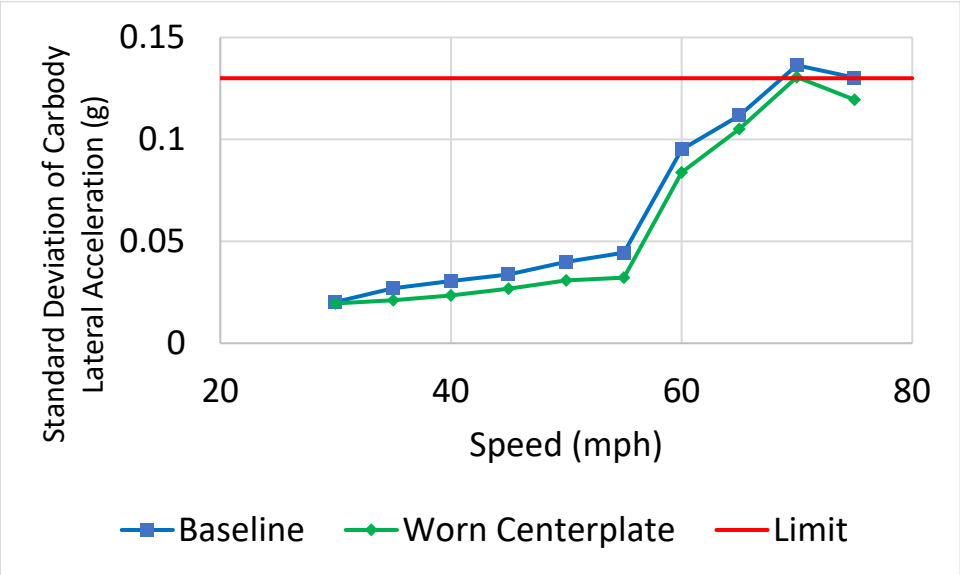

Figure 61. Hunting stability, considering centerplate wear

7.13.3 Primary Pad

It is not clear how the primary pads of the Swing Motion® trucks will wear over time. To examine the possible impact of various changes, the worn primary pads were simulated with both lower and higher longitudinal and lateral stiffness. For the lower stiffness runs, the stiffness was reduced by a factor of 2. For the higher stiffness runs, the stiffness was increased by a factor of 20.

Table 56 shows a comparison of the constant curving simulation predictions for the baseline and worn primary pad simulations. The simulation predictions for the worn primary pads **meet** Standard S-2043 criteria for constant curving.

Table 56. Simulation Predictions of the Atlas Cask Car with Worn Primary Pads in Constant Curving

Criterion	Limiting Value	Baseline	Soft Primary Pad	Stiff Primary Pad
Maximum carbody roll angle (degree)	4.0	0.77	0.77	0.77
Maximum wheel L/V	0.80	0.52	0.43	0.71
Maximum truck side L/V	0.50	0.34	0.29	0.37
Minimum vertical wheel load (%)	25	52.70	52.50	53.60
Peak-to-peak carbody lateral acceleration (g)	1.30	0.15	0.15	0.22
Maximum carbody lateral acceleration (g)	0.75	0.14	0.12	0.19
Maximum carbody vertical acceleration (g)	0.90	0.15	0.15	0.16
Maximum vertical suspension deflection (%)	95	24.80	24.54	25.06

Table 57 shows a comparison of the dynamic curving simulation predictions for the baseline and worn primary pad simulations. The simulation predictions showed that both baseline and worn pad conditions **met** the Standard S-2043 criteria for the wheel L/V ratio for dynamic curving.

Table 57. Simulation Predictions of the Atlas Cask Car with Worn Primary Pads in Dynamic Curving

Criterion	Limiting Value	Baseline	Soft Primary Pad	Stiff Primary Pad
Maximum carbody roll angle (degree)	4.0	0.97	0.91	1.04
Maximum wheel L/V	0.80	0.71	0.66	0.75
Maximum truck side L/V	0.50	0.35	0.33	0.39
Minimum vertical wheel load (%)	25	52.69	52.67	53.61
Peak-to-peak carbody lateral acceleration (g)	1.30	0.19	0.18	0.22
Maximum carbody lateral acceleration (g)	0.75	0.16	0.18	0.19
Maximum carbody vertical acceleration (g)	0.90	0.12	0.12	0.13
Maximum vertical suspension deflection (%)	95	23.22	23.93	24.36

Table 58 shows a comparison of hunting simulation predictions for baseline and worn primary pad simulations. The simulation predictions do not meet the Standard S-2043 criterion for the maximum standard deviation of lateral carbody acceleration over 2,000 feet. The trends of lateral carbody acceleration standard deviation versus speed are shown in Figure 62, where, if the pads deteriorate in a significantly softer condition, then the stable vehicle speed is significantly reduced.

All other criteria, including peak-to-peak carbody lateral acceleration and maximum carbody lateral acceleration, were **met** for hunting with worn primary pads.

Table 58. Simulation Predictions of the Atlas Cask Car with Worn Primary Pads in Hunting

Criterion	Limiting Value	Baseline	Soft Primary Pad	Stiff Primary Pad
Maximum carbody roll angle (degree)	4.0	0.3	0.4	0.5
Maximum wheel L/V	0.80	0.28	0.35	0.43
Maximum truck side L/V	0.50	0.14	0.20	0.26
Minimum vertical wheel load (%)	25	71	62	55
Peak-to-peak carbody lateral acceleration (g)	1.30	0.59	0.74	0.73
Maximum carbody lateral acceleration (g)	0.75	0.31	0.40	0.40
Lateral carbody acceleration standard deviation (g)	0.13	0.14	0.19	0.20
Maximum carbody vertical acceleration (g)	0.90	0.32	0.18	0.23
Maximum vertical suspension deflection (%)	95	17	19	20

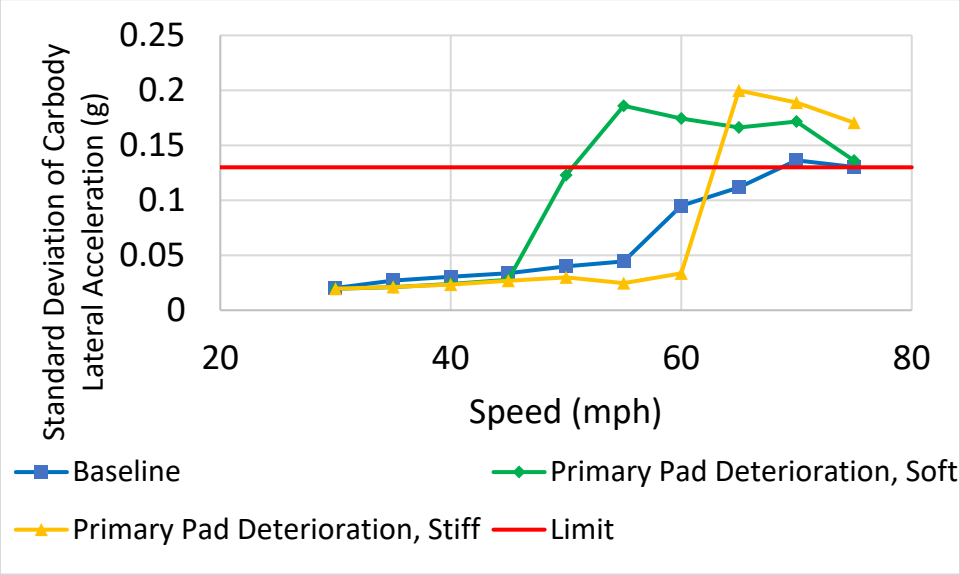

Figure 62. Hunting stability, considering primary pad deterioration

7.13.4 Friction Wedges

The wedge rise limit for the Swing Motion® trucks used in the cask car is 11/16 inch. The worn wedge simulations were performed with the wedges at this state of wear in all locations.

Table 59 shows a comparison of the dynamic curving simulation predictions for baseline and the worn friction wedge simulations. The simulation predictions for dynamic curving with worn wedges **met** Standard S-2043 criteria.

Table 59. Simulation Predictions of the Atlas Cask Car with Worn Friction Wedges in Dynamic Curving

Criterion	Limiting Value	Baseline	Friction Wedge Wear
Maximum carbody roll angle (degree)	4.0	1.0	1.0
Maximum wheel L/V	0.80	0.71	0.70
Maximum truck side L/V	0.50	0.35	0.35
Minimum vertical wheel load (%)	25	53	54
Peak-to-peak carbody lateral acceleration (g)	1.30	0.19	0.17
Maximum carbody lateral acceleration (g)	0.75	0.16	0.14
Maximum carbody vertical acceleration (g)	0.90	0.12	0.17
Maximum vertical suspension deflection (%)	95	23	24

Table 60 shows a comparison of the pitch-and-bounce simulation predictions for the baseline and worn friction wedge simulations. The pitch-and-bounce simulations were performed for the maximum test load condition. The simulation predictions for the **worn** friction wedges met Standard S-2043 pitch-and-bounce criteria.

Table 60. Simulation Predictions of the Atlas Cask Car with Worn Friction Wedges in Pitch and Bounce

Criterion	Limiting Value	Baseline	Friction Wedge Wear
Maximum carbody roll angle (degree)	4.0	0.3	0.3
Maximum wheel L/V	0.80	0.12	0.14
Maximum truck side L/V	0.50	0.09	0.09
Minimum vertical wheel load (%)	25	74	72
Peak-to-peak carbody lateral acceleration (g)	1.30	0.34	0.29
Maximum carbody lateral acceleration (g)	0.75	0.17	0.14
Maximum carbody vertical acceleration (g)	0.90	0.38	0.29
Maximum vertical suspension deflection (%)	95	56	56

Table 61 shows a comparison of the twist-and-roll simulation predictions for the baseline and worn friction wedges. The simulation predictions for the worn friction wedges **meet** Standard S-2043 twist-and-roll criteria.

Table 61. Simulation Predictions of the Atlas Cask Car with Worn Friction Wedges in Twist and Roll

Criterion	Limiting Value	Baseline	Worn Friction Wedges
Maximum carbody roll angle (degree)	4.0	1.9	1.8
Maximum wheel L/V	0.80	0.27	0.18
Maximum truck side L/V	0.50	0.17	0.12
Minimum vertical wheel load (%)	25	58	59
Peak-to-peak carbody lateral acceleration (g)	1.30	0.53	0.42
Maximum carbody lateral acceleration (g)	0.75	0.29	0.21
Maximum carbody vertical acceleration (g)	0.90	0.24	0.36
Maximum vertical suspension deflection (%)	95	21	22

7.13.5 Broken Spring

The cask car uses different springs in the end trucks than those used in the center trucks of a span bolster. Broken spring simulations were done with one 1-96 spring removed from the spring nest of the leading truck of the trailing span bolster to represent a broken or missing spring. This location was chosen because the modeling and testing of the Atlas railcar showed that this location is critical for the dynamic curving regime. The dynamic curving and twist-and-roll simulations were performed for the minimum test load condition, and pitch-and-bounce simulations were performed for the maximum test load condition.

Table 62 shows a comparison of the dynamic curving simulation predictions for the baseline and broken spring simulations. The simulation predictions **met** the Standard S-2043 criteria for dynamic curving with a broken spring.

Table 62. Simulation Predictions of the Atlas Cask Car with a Broken Spring in Dynamic Curving

Criterion	Limiting Value	Baseline	Broken spring
Maximum carbody roll angle (degree)	4.0	1.0	1.0
Maximum wheel L/V	0.80	0.71	0.71
Maximum truck side L/V	0.50	0.35	0.37
Minimum vertical wheel load (%)	25	53	53
Peak-to-peak carbody lateral acceleration (g)	1.30	0.19	0.17
Maximum carbody lateral acceleration (g)	0.75	0.16	0.14
Maximum carbody vertical acceleration (g)	0.90	0.12	0.12
Maximum vertical suspension deflection (%)	95	23	24

Table 63 shows a comparison of the pitch-and-bounce simulation predictions for the baseline and broken spring simulations. All simulation predictions for broken springs **meet** Standard S-2043 criteria in the pitch-and-bounce regime.

Table 63. Simulation Predictions of the Atlas Cask Car with a Broken Spring in Pitch and Bounce

Criterion	Limiting Value	Baseline	Missing Springs
Maximum carbody roll angle (degree)	4.0	0.3	0.3
Maximum wheel L/V	0.80	0.12	0.15
Maximum truck side L/V	0.50	0.09	0.09
Minimum vertical wheel load (%)	25	74	72
Peak-to-peak carbody lateral acceleration (g)	1.30	0.34	0.32
Maximum carbody lateral acceleration (g)	0.75	0.17	0.15
Maximum carbody vertical acceleration (g)	0.90	0.38	0.28
Maximum vertical suspension deflection (%)	95	56	57

Table 64 shows a comparison of the twist-and-roll simulation predictions for the baseline and broken spring simulations. The simulation predictions for the broken springs **meet** Standard S-2043 criteria for the twist-and-roll regime.

Table 64. Simulation Predictions of the Atlas Cask car with a Broken Spring in Twist and Roll

Criterion	Limiting Value	Baseline	Missing Springs
Maximum carbody roll angle (degree)	4.0	1.9	1.9
Maximum wheel L/V	0.80	0.27	0.28
Maximum truck side L/V	0.50	0.17	0.16
Minimum vertical wheel load (%)	25	58	59
Peak-to-peak carbody lateral acceleration (g)	1.30	0.53	0.44
Maximum carbody lateral acceleration (g)	0.75	0.29	0.21
Maximum carbody vertical acceleration (g)	0.90	0.24	0.26
Maximum vertical suspension deflection (%)	95	21	20

8.0 CONCLUSIONS

The FEA simulations and structural test strain measurements both showed that stresses were less than 75 percent of the allowable stress, thereby eliminating the requirement in Standard S-2043, Paragraph 8.1 for the FEA to be refined. When applying the maximum test load, the largest difference between measured and predicted stress was 8.0 ksi on SGBF15. The other measurement at a similar location, SGBF26, was within 4 percent of the predicted stress.

On behalf of the Department of Energy, TTCI is requesting exceptions from the AAR EEC because the post-test simulation predictions of the Atlas car with the production CSM 58 pads did not meet some of the criteria for hunting, curving with single rail perturbation, and curving with various lubrication conditions. The onset of instability in the hunting regime occurred at speeds above 65 mph—beyond the 50-mph limit recommended in AAR circular OT-55 for cars in HLRM service. Although the performance simulated for curving with a single rail perturbation did not meet Standard S-2043 criteria for the carbody roll angle, it did meet the criteria for all other metrics, including those for wheel/rail forces.

Constant curving test results using prototype CSM 70 pads did not meet S-2043 criteria for the maximum wheel L/V ratio or the 95-percent wheel L/V ratio. While constant curving simulation predictions with both the refined model using prototype CSM 70 pads and the production CSM 58 pads met S-2043 criteria, predictions using CSM 58 pads showed a 20 percent reduction in wheel L/V ratios compared to predictions done with CSM 70 pads.

Criteria for all other test regimes were met. Table 65 contains a summary of the simulation predictions for CSM 58 pads and test results.

Table 65. Summary of Dynamic Modeling and Test Results

Standard S-2043 Section	Met/Not Met		
	Preliminary Simulations	Revised Simulations CSM 58 pads	Test Result and Details if Not Met
5.2 Nonstructural Static Tests			
4.2.1/5.2.1 Truck Twist Equalization	Met	Not Simulated	Not Met with CSM 58 pads – **Minimum Test Load:** Wheel load at 50% during 2” drop condition. Wheel load at 24% during 3” drop condition. **Maximum Test Load:** Wheel load at 43% during 2” drop condition. Wheel load at 29% during 3” drop condition.
4.2.2/5.2.2 Carbody Twist Equalization	Met	Not Simulated	Met with CSM 58 pads
4.2.3/5.2.3 Static Curve Stability	Met	Not Simulated	Met with CSM 58 pads
4.2.4/5.2.4 Horizontal Curve Negotiation	Met	Not Simulated	Met with CSM 58 pads
5.4 Structural Tests			
5.4.2 Squeeze (Compressive End) Load	Met	Not Simulated	Met with CSM 58 pads
5.4.3 Coupler Vertical Loads	Met	Not Simulated	Met with CSM 58 pads
5.4.4 Jacking	Met	Not Simulated	Met with CSM 58 pads
5.4.5 Twist	Met	Not Simulated	Met with CSM 58 pads
5.4.6 Impact	Met	Not Simulated	Met with CSM 58 pads

Standard S-2043 Section	Met/Not Met		
	Preliminary Simulations	**Revised Simulations CSM 58 pads**	**Test Result and Details if Not Met**
5.5 Dynamic Tests			
4.3.11.3/5.5.7 Hunting	Met	Not Met At Minimum Test Load: Car unstable at speeds greater than 65 mph with KR wheel profiles Meets with Maximum Test Load	Not Met with CSM 58 pads At Minimum Test Load: Car unstable at speeds greater than 65 mph with KR wheel profiles Meets with Maximum Test Load
4.3.9.6/5.5.8 Twist and Roll	Met	Met	Not tested with CSM 58 pads – Met with CSM 70 pads
5.5.9 Yaw and Sway	Met	Met	Not tested with CSM 58 pads – Met with CSM 70 pads
5.5.10 Dynamic Curving	Not Met Max Test Load Wheel L/V 0.88, Limit=0.8, A-end and B-end lead,	Met	Met with CSM 58 pads – Not met with CSM 70 pads (0.81 Wheel L/V)
4.3.9.7/5.5.11 Pitch and Bounce (Chapter 11)	Met	Met	Not tested with CSM 58 pads – Met with CSM 70 pads
4.3.9.7/5.5.12 Pitch and Bounce (Special)	Met	Not Simulated	Not tested
4.3.10.1/5.5.13 Single Bump Test	Met	Met	Not tested with CSM 58 pads – Met with CSM 70 pads
4.3.11.6/5.5.14 Curve Entry/Exit	Met	Met	Not tested with CSM 58 pads – Met with CSM 70 pads
4.3.10.25.5.15 Curving with Single Rail Perturbation	Not met **Empty with Ballast Load:** Wheel L/V 0.96, Limit=0.8 Truck Side L/V 0.52, Limit=0.5 **Loaded** 5.0-degree roll angle, Limit=4.0	Not met **Minimum Test Load** Carbody roll angle =4.2, limit=4.0 **Maximum Test Load** Carbody roll angle =4.7, limit=4.0	**Minimum Test Load:** Not met with CSM 70 pads (Wheel L/V = 0.88, Truck L/V = 0.50), not tested with CSM 58 pads

Standard S-2043 Section	Met/Not Met		
	Preliminary Simulations	Revised Simulations CSM 58 pads	Test Result and Details if Not Met
4.3.11.4/5.5.16 Standard Chapter 11 Constant Curving	Met	Met	Not tested with CSM 58 pads – Not Met with CSM 70 pads: **Minimum Test Load:** Wheel L/V ratio = 0.86 95% Wheel L/V ratio = 0.66 **Maximum Test Load:** 95% Wheel L/V ratio = 0.63
4.3.11.7/5.5.17 Special Trackwork, No 7 Crossovers	Not Met **Loaded:** Truck side L/V Ratio=0.52, Limit=0.5	Met	Not tested with CSM 58 pads – Met with CSM 70 pads on a No 10 crossover
4.3.11.5 Curving with Various Lubrication Conditions	Not Met **Min Test Load with new profiles:** 95% Wheel L/V = 0.62 (Case 2), Limit=0.6 95% Wheel L/V = 0.66 (Case 4), Limit=0.6 **Min Test Load with worn profiles:** Truck Side L/V = 0.56 (Case 1), 0.62 (Case 2), 0.61 (Case 4), Limit=0.5 95% Wheel L/V = 0.68 (Case 2), 0.61 (Case 4), Limit=0.6 **Max Test Load with worn profiles:** Truck Side L/V = 0.56 (Case 1), 0.62 (Case 2), 0.61 (Case 4), Limit=0.5 95% Wheel L/V = 0.68 (Case 2), 0.61 (Case 4), Limit=0.6	Not Met in following cases **Min Test Load with new profiles:** 95% Wheel L/V = 0.62 (Case 4), Limit=0.6 **Min Test Load with worn profiles:** Truck Side L/V = 0.53 (Case 1), 0.61 (Case 2), 0.58 (Case 4), Limit=0.5 95% Wheel L/V = 0.64 (Case 2), Limit=0.6 **Max Test Load with worn profiles:** Truck Side L/V = 0.52 (Case 1), 0.60 (Case 2), 0.58 (Case 4), Limit=0.5 95% Wheel L/V = 0.66 (Case 2), 0.61 (Case 4), Limit=0.6	Not required
4.3.12 Ride Quality	Met	Not Simulated	Not required
4.3.13 Buff and Draft Curving	Not Met Like car buff load Truck side L/V Ratio=0.51, Limit=0.50,	Met	Not required

Standard S-2043 Section	Met/Not Met		
	Preliminary Simulations	Revised Simulations CSM 58 pads	Test Result and Details if Not Met
4.3.14 Braking Effects on Steering	Met	Not Simulated	Not required
4.3.15 Worn Component Simulations	Not Met Numerous criteria not met in dynamic curving and hunting regimes with several worn components. See reference 2 for details	Not Met in following cases **Hunting stability, maximum lateral acceleration standard deviation:** Worn CCSB low preload: 0.17 Worn primary pads, soft: 0.19 Worn primary pads, stiff: 0.20	Not required

References

1. AAR *Manual of Standards and Recommended Practices*, Car Construction Fundamentals and Details, Performance Specification for Trains Used to Carry High-Level Radioactive Material, Standard S-2043, Effective: 2003; Last Revised: 2017, Association of American Railroads, Washington, D.C.

2. Walker, R., MC Jones, JC Valades-Salazar, R. Joy, M. Miller, and B. Whitsitt, "S-2043 Certification Tests of United States Department of Energy Atlas Railcar Design Project 12-Axle Cask Car." Report No. P-21-037, Transportation Technology Center, Inc., Pueblo, CO, In press.

3. Walker, R. and S. Trevithick, "S-2043 Certification: Preliminary Simulations of Kasgro-Atlas 12-Axle Cask Car." Report No. P-17-021, Transportation Technology Center, Inc., Pueblo, CO, December 2017.

4. Orano Federal Services, September 2019, "DW-20-001 HLRM Atlas Railcar Test Loads Final Document Package", provided to DOE by Transportation Technology Center, Inc., Pueblo, CO.

5. Orano Federal Services, September 2019, "DW-19-013rev1 "HLRM Railcar TTCI Task Order #1; Transmittal of EIR-3022576-001, Revised Assembly Instructions for the DOE Atlas Railcar Test Loads."

6. Koffman, J. L., "Spring Stresses and Deflections". *The Railway Gazette*, January 30, 1959.

TRANSPORTATION TECHNOLOGY CENTER, INC.
A wholly owned subsidiary of the Association of American Railroads

55500 DOT Road • Pueblo, CO 81001
www.aar.com